Modification of cereal and tuber starches using cold plasma technology to improve its structure and functionality

A DISSERTATION SUBMITTED TO THE FACULTY OF THE UNIVERSITY OF MINNESOTA
BY

AKUA YEBOAH OKYERE

IN PARTIAL FULFILLMENT OF THE REQUIREMENTS FOR THE DEGREE OF DOCTOR PHILOSOPY

George A. Annor, Ph.D., Adviser

March 2022

Acknowledgements

I want to express my profound gratitude to my adviser, Dr. George Amponsah Annor, for the opportunity he gave me, to attain this academic milestone. It seemed just like yesterday when Dr. Annor told me about the opportunity to study at the University of Minnesota, Food Science, and Nutrition Department. That was back in 2016, when I was preparing to complete my undergraduate education at the University of Ghana, Legon. Having worked with Dr. Annor on my undergraduate project, he acknowledged my hard work, intellect, and attention to detail and offered me this life-changing opportunity. I remember that call when I was back home in Ghana encouraging me to write the GRE and apply to the Food Science graduate program. I then began my master's in Food Science in 2017 (Fall) and was encouraged by Dr. Annor to convert to a Ph.D. in Fall 2019. I remember Dr. Annor encouraging and telling me I could do it and that he had seen how well I work. Thank you, George, for the life advice, mentorship, and guidance. You have made my Ph.D. dreams a reality.

I would also like to say a big thank you to Dr. Eric Bertoft for proofreading all my research articles. You challenged me to write my papers with sound scientific reasoning and fine-tuned my experiments. The expertise in Starch chemistry and Food Science you brought to the table is much appreciated.

To the other committee members, Dr. Gary A Reineccius, Dr. Len Marquart, and Dr. Kumar Mallikarjunan, thank you for taking the time of your busy schedules to read through my preliminary proposal and final thesis. Thank you for the suggestions and comments.

I would also like to thank Dr. Andreas Blennow for the starch sample as well as Dr. Ted Labuza, Dr. Pam Ismail, Dr. Daniel Gallaher, and Cindy Gallaher for allowing me to use their lab equipment.

Thank you to Dr. Allison Bailey for showing me how to use the light microscope and centrifuge in Dr. Daniel Gallaher's lab. Thank you to Dr. Ali Halalipour (ADM), Dr. Gopinath Tata (University of Minnesota Nuclear Magnetic Resonance Center), Dr. Gail Celio (University of Minnesota Imaging Center), Dr. Bing Luo, Dr. Geoffrey Rojas (Shelburne), and Dr. Javier Garcia Barriocanal at the College of Science & Engineering Characterization facility for your excellent technical assistance. I also want to say a big thank you to Nancy Toedt, Dorit Hafner, Sara Cannon, and Andrew Howe for answering and addressing any concerns I had about the Food Science graduate program.

Thank you to my former lab mates, Ibilola Kougblenou, Juan Mogoginta, Yingxin (Sophie) Zhong, Citra Rahardjo, for helping me settle in the lab. I remember the surprise birthday cake and potluck in Juan's apartment. Thank you again. To my current lab mates Prince G. Boakye- thank you for all the encouragement, advice, and help. You have been an excellent friend and work colleague. To Radhika Bharathi, thank you for being such a bright ray of sunshine. Thank you for all the laughs and for being my workout partner.

I would also like to thank Dr. Sasireka Rajendran for assisting in writing the review article. Thank you to Gabrielle Seliber and Takehiro Murai for helping in data collection.

Now to my family, thank you to my parents- Mr. Jim Y. Okyere and Mrs. Victoria Okyere for all the love and support. Thank you to my siblings, James O. Okyere, Marian Ansa-Otu, Catherine O. Lamptey, and Jemima Okyere, for the emotional and financial support. To my in-law, Ishmael Lamptey, thank you so much for being there through every

step of this journey. For crying and laughing with me and supporting me financially. Thank you to Fred Ansa-Otu and Joshua Addey for their encouragement.

Thank you to my friend and roommate, Sonia Bosire, you have been right by my side through it all, and I am very grateful. Thank you to Vera Micah and Pamela Owusu for listening to me and encouraging me.

In concluding, thank you to every person who contributed to the success of this journey in any shape or form that I may not have mentioned. May the good Lord bless you all!

Dedication

I would like to dedicate this thesis to the Almighty God, Jesus Christ, and the Holy Spirit.

Abstract

Starch is a versatile biopolymer with multiple uses in the food and non-food industries. In the food industry, starch is used as a thickening, binding, gelling, stabilizing, and encapsulating agent amongst others. In the non-food industry, starch can be used as a sizing agent to add strength to paper and textiles, as an adhesive, and used in the manufacture of bioplastics. Starch needs to be modified to enhance its stability, solubility, heat, and shear tolerance for industrial applications. Starch is mostly modified using chemical reagents due to their effectiveness in altering starch physicochemical and functional properties. However, there is increasing concerns about the chemical waste generated during chemical starch modification. There is also an increasing demand for food products with "clean labels". To meet these demands, there is a push to find eco-friendly alternatives such as cold plasma technology. Cold plasma is obtained by applying electrical energy to a gas, which leads to ionization of the gas to produce reactive oxygen and nitrogen species (RONS), ultraviolet radiation, and free radicals. Cold plasma can be applied directly to starches or in the form of plasma-activated water (PAW). In the case of PAW, RONS, ultraviolet radiation, and free radicals are generated in water upon treatment with atmospheric cold plasma. These reactive species can induce changes in the structure and functionality of starches, without generating virtually any waste. The main aim of this research was to modify cereal and tuber starches with a carbon dioxide-argon radio frequency cold plasma for the first time. In addition, plasma-activated water (PAW) at different temperatures was utilized to modify high amylose and waxy starch properties.

In objective one, carbon dioxide-argon radio frequency cold plasma was used to modify waxy starches. A 3 X 3 factorial design with three waxy starches (maize, rice, and

potato) and three treatment levels (no treatment, 0 W and 120 W) was used for the experiment. The starch samples were treated at 0 W (gas treatment) to investigate whether gas treatment alone without ionization could induce changes in the starches. Solid state ^{13}C nuclear magnetic resonance, differential scanning calorimetry, micro-visco-amylograph, wide angle x-ray scattering, scanning electron microscopy and optical light microscopy were used to investigate the effect of cold plasma on waxy starch properties. Starches modified with cold plasma were more stable when subjected to heat and shear. This was indicated by the lower breakdown values obtained for maize (189.0 as compared to 212.8 BU) and rice (24.5 as compared to 32.0 BU) after treatment. The tendency for retrogradation to set in also decreased as indicated by the lower setback and final viscosity values for maize (44 as compared to 65.8 BU; 209.3 as compared to 295.3 BU), rice (48.3 as compared to 89.5 BU, 184.5 as compared to 311.3 BU) and potato (76.5 as compared to 147.3 BU, 386.3 as compared to 516.0 BU) after treatment. However, the morphology of the starches remained unchanged. The crystallinity of waxy potato starch reduced by 2.8% and 5.5% after 0 W and 120 W treatment, respectively, but was unaffected in rice and maize. The ability of starches to form inclusion complexes with iodine were unaffected after plasma or gas treatment. We also, observed V-type single helices in maize and rice starches which could be attributed to the formation of starch-lipid complexes.

In objective two, the effect of radio frequency cold plasma on starch fine structure (unit and internal chain distribution) was determined using the High-Performance Anion Exchange Chromatography (HPAEC), since studies have shown that alterations at the fine structural level impacts starch functionality. Also, the occurrence of cross-linking was investigated using Fourier transform infrared spectroscopy-attenuated total reflectance

(FTIR-ATR). A 3 X 2 X 2 factorial design with three waxy starches (maize, rice, and potato) two starch forms (granular and non-granular) and two treatment levels (no treatment and 120W) was used. Radio frequency plasma resulted in negligible changes at the fine structural level. FTIR-ATR confirmed the ability of cold plasma to induce cross-linking in these starches which explains why these starches were more stable during heat and shear treatment (objective 1). *In vitro* digestibility studies showed that cold plasma treatment increased the amount of slowly digestible starches (5.62%; 10.24%) and resistant starches (0.28%; 85.66%) in non-granular waxy maize and granular waxy potato starches respectively.

In objective 3, plasma-activated water (PAW) at different temperatures was utilized to modify high amylose and waxy starches. A 4 X 4 factorial design with four starches (high amylose maize, high amylose potato, waxy maize, and waxy potato) and four treatment temperatures (no treatment, 25°C, 60°C and 80°C) was used. The X-ray photo electron spectroscopy was used to determine the ability of PAW at different temperatures to induce any changes in the elemental surface composition of these starches. The effect of PAW at different temperatures, on functionality and the thermal profile of starches was also investigated. PAW at 60°C and 80°C increased the solubility and water absorption capacity of the starches. Both treated and untreated starches were mostly made up of carbon and oxygen with trace quantities of nitrogen or silicon. Modification of starches with PAW at 60°C increased the gelatinization temperatures and enthalpies.

Overall, this study demonstrated that radio frequency cold plasma and PAW significantly influenced starch properties. These changes were however not seen at the molecular level as observed in the fine structure analysis.

Table of contents

List of Tables

List of Figures

Chapter 1: Introduction, Rationale, Specific Objectives and Hypothesis

Sections of this chapter have been submitted for publication in Current Research in Food Science Journal.

1.1 Introduction

Starch is the primary energy reserve in plants and is made up of two major polysaccharides: amylose (MW ≈ 10^5-10^6) and amylopectin (MW ≈ 5 x 10^8). Amylose is primarily a linear polysaccharide made of approximately 99% α-(1-4)-D-glucosyl units with < 1% α-(1-6) linkages (Hizukuri et al., 1981). Amylopectin, however, is a highly branched polymer with linear chains of α-(1-4)-D-glucosyl units interconnected with 5% α-(1-6)-linkages (Hizukuri et al., 1983). Native starch typically contains 15-35% amylose and 65-85% amylopectin (Pérez & Bertoft, 2010). Also, there are high amylose and waxy starches with > 35% amylose and < 5% amylose respectively (X. Wu et al., 2006). Amylose retrogrades quickly and forms strong films and tough gels in solution while amylopectin produces weak films and soft gels (Pérez & Bertoft, 2010).

Starch granules are semi-crystalline, consisting of an amorphous part and a crystalline part (Pérez & Bertoft, 2010). The granules have a density of 1.5g/cm^3 which is more significant than water and hence allows easy isolation and purification of starch by gravity sedimentation. The semi-crystalline structure of starch preserves its granular integrity and prevents solubilization of starch at room temperature (Ai & Jane, 2018). Starch is synthesized in granular form at the hilum and can be extracted from seeds, roots, tubers, leaves, pollen, and even algae (Pérez & Bertoft, 2010). Starch granules appear in various shapes such as ellipsoids, spheres, and ovals when viewed under the microscope. The diameter of starch granules can range from 0.1 μm to > 100 μm depending on their

botanical origin (Pérez & Bertoft, 2010). Furthermore, the granules of starch are arranged radially and highly ordered. Thus, when starch is viewed under cross-polarized light in an optical microscope, a “Maltese Cross” structure is observed. This structure is embedded in the crystalline part of starch (Bertoft, 2017). Significant starch sources for commercial applications include maize, potato, cassava, and wheat (Vamadevan & Bertoft, 2015).

It is no surprise that the industrial starch market is projected to be worth 106.64 billion USD by 2022 (Rohan, 2016). This is because starch has multiple applications in both food and non-food industries. Starch is utilized as a gelling, thickening, stabilizing, and flavor encapsulating agent in the baking, brewing, and confectionery industries (Mason, 2009). Non-food uses of starch include adhesives for the manufacture of corrugated paper boards, antifreeze, retarding agents for concrete, and fermentation feedstocks for pharmaceutical products (Glittenberg, 2012). Nonetheless, in its native state, starch is highly unreactive, insoluble, and retrogrades easily. Therefore, starches must be modified to enhance their solubility, textural properties, and heat tolerance for diverse industrial applications (Laovachirasuwan et al., 2010). Starch can be modified using physical, chemical, and biological means. Physical methods can either be thermal (annealing, heat moisture treatment, spray drying, etc.) or non-thermal (pulsed electric field, ultrasonication, high hydrostatic pressure, cold plasma technology, etc.) (Zia-ud-Din et al., 2017) and have proven to be successful in modifying starches. For example, physical processes such as pregelatinizing starches enhance these starches' thickening and water absorption capacity (Hong & Liu, 2018). The biological techniques of starch modification can either be done using genetic engineering to breed specific varieties of starch such as high amylose starches or through enzymatic conversion of these starches to achieve

products like maltodextrins (Bemiller, 1997). Biological methods usually give increased yields and fewer by-products. However, they can be relatively expensive compared to physical methods (Park et al., 2017). Chemical modification techniques are the most widely used and result in the highest efficiency. Chemical methods employed in modifying starches include cationization, acetylation, oxidation and green solvents (Chaiwat et al., 2016; Fan & Picchioni, 2020). There is an increasing concern about the issues of environmental pollution, wastewater treatment, food safety, and the high costs involved in chemical modification methods (Chaiwat et al., 2016). While the use of ionic liquids ("green" solvents) in chemical modification may have less impact on the environment, there are issues such as poor performance in biodegradability, biocompatibility, and sustainability (Dai et al., 2013; Fan & Picchioni, 2020). Hence, physical processes are preferred over chemical methods in altering the structure and functionality of starches.

1.2 Rationale and Significance

It is imperative for scientists to explore sustainable methods to enhance starch properties continuously. These sustainable alternatives help protect the earth and preserve valuable natural resources while improving the quality of life. Also, starch is an important polymer that is readily available, cheap, and versatile in its applications (Bemiller, 1997). As such, this research explores the use of cold plasma technology - a relatively novel non-thermal physical modification technique that has enormous advantages regarding starch modification (Thirumdas, Kadam, et al., 2017a). Cold plasma is a partially ionized gas produced by applying sufficient energy (thermal, electromagnetic, or electric fields, microwave and radio frequencies) to a neutral gas at low or atmospheric pressure (Moreau et al., 2008). Cold plasma can be applied directly or in the form of plasma-activated water

when treating materials (Thirumdas et al., 2018). Cold plasma is employed in areas such as medicine and agriculture. Applications of cold plasma in medicine include wound healing, cancer treatment, tissue regeneration, and blood coagulation (Fridman et al., 2008). In food and agriculture, cold plasma is utilized in the enhancement of seed germination (Thirumdas et al., 2018), microbial inactivation (Moreau et al., 2008), aflatoxin destruction (Scholtz et al., 2015) and more recently, starch modification (Thirumdas, Kadam, et al., 2017a). Some key findings observed after cold plasma modification of starches include a decrease in the cooking time of rice (Thirumdas et al., 2016), reduction in molecular weight (Bie, Pu, et al., 2016), occurrence of cross-links (Zou et al., 2004) and an increase in resistant starches (Trinh, 2018). These authors employed different gas combinations and plasma setups to modify these starches. A comprehensive review of the findings is outlined in the literature review section.

There remains a lot to be discovered on the extent to which cold plasma modifies starch properties (Zhu, 2017). For this modification technique to be adopted by the US Food and Drug Administration (FDA) and the food industries as safe and effective, more in-depth studies, need to be carried out on toxicity, starch functionality, digestibility, and structural changes. Our current research addresses this issue by employing a radio frequency low-pressure system and plasma-activated water to modify the structure and functionality of cereal and tuber starches. To the best of our knowledge, carbon dioxide and argon gas were combined for the first time to modify granular and non-granular waxy starches. We also used plasma-activated water at different temperatures to modify high amylose and waxy starches for the first time. There is a solid push to find innovative ways to balance the natural carbon cycle and decrease carbon dioxide emission, which is a

greenhouse gas. Thus, employing carbon dioxide in starch modification can help lower its amount in the environment and possibly address the climate challenges the world is facing (Snoeckx & Bogaerts, 2017). Thus, the goal of this research is to modify cereal and tuber starches with a carbon dioxide-argon radio frequency cold plasma. In addition, plasma-activated water at different temperatures is utilized to modify the starch properties.

1.3 Hypothesis

It is hypothesized that:

1. Carbon dioxide-argon radio frequency cold plasma will significantly alter the properties of cereal and tuber waxy starches.
2. Carbon dioxide-argon radio frequency cold plasma will alter the unit and internal chain structure and *in vitro* digestibility of waxy starches irrespective of whether they are treated as granular or non-granular starches.
3. Increasing the temperature of plasma-activated water would significantly impact the characteristics of starches.

1.4 Specific Objectives

1. Treat waxy cereal and tuber starches with a carbon dioxide-argon radio frequency cold plasma and investigate its effect on their properties.
2. Study the effects of carbon dioxide-argon radio frequency cold plasma on granular and non-granular waxy starch chain length, and their starch hydrolysis kinetics.
3. Investigate the effects of plasma-activated water temperature on the functionality, structure, thermal and chemical surface analysis of cereal and tuber starches.

Chapter 2: Literature review

Contents of this chapter have been submitted for publication in Current Research in Food Science Journal.

2.1 What is Plasma?

In 1816, Michael Faraday postulated the fourth state of matter which he called radiant matter (Crookes, 1881). William Crookes proved the existence of plasma as ‘‘radiant matter” in a Crookes tube in 1879 (Crookes, 1879). However, the term plasma was introduced by Irving Langmuir in the 1920s as the fourth state of matter. Plasma is a fully or partially ionized gas made up of electrons, ions, free radicals, photons, UV radiation, reactive species, and molecules in their ground or excited states and carries a net neutral charge (S. Pankaj et al., 2018). Plasma can either be naturally occurring or man-made and makes up 99% of the visible matter in the universe. Examples of natural plasmas include the sun, Saint Elmo’s fire, lightning, and the Aurora Borealis and Australis, while examples of man-made plasmas are neon signs, fluorescent lights, and plasma pinches (Snoeckx & Bogaerts, 2017).

2.2 Cold plasma production

Cold plasma is a partially ionized gas produced by applying energy to a gas at low or atmospheric pressure. When the energy is applied, the free electrons naturally present in the gas pick up the energy faster than the ions. Energy is transferred from the accelerated electrons to the heavier gas molecules through elastic and inelastic collisions. As a result of these collisions, the gas goes through several phase reactions-ionization, excitation, and dissociation to produce several reactive species (reactive oxygen species and reactive nitrogen species), new electrons, ions, and free radicals (Milella & Palumbo, 2014).

According to Milella & Palumbo (2014), the electron temperature in cold plasma is relatively high (1-10 eV), while the translational energy of the heavy particles (molecules, ions) is close to room temperature. That is because the electrons have a lighter mass than the heavy particles (Rossi, 2012). Thus, the electrons reach higher kinetic energy faster than the heavy particles. Cold plasma is characterized as being in non-local thermodynamic equilibrium because of this difference in temperature between electrons and heavy particles (Snoeckx & Bogaerts, 2017).

Cold plasma requires a much lower power input, unlike thermal plasmas that need a higher power input (~50MW). Thermal plasmas are generated at high temperatures (4000 K- ≥ 20000K) and pressures (≥ 105Pa) (Moreau et al., 2008). Thermal plasmas are fully ionized gases as all the species (electrons, ions, heavy particles) possess the same temperature. Thermal plasmas are in local thermodynamic equilibrium. The applications of thermal plasmas are diverse, a few of which include extractive metallurgy, fine powder syneresis, and coating technology (Snoeckx & Bogaerts, 2017). However, the extremely high temperatures are not suitable for treating thermally sensitive materials like starches, which is why cold plasma is a more appropriate method for starch modification and other food applications (Liao et al., 2020).

2.3 Generation of cold plasma at low-pressure

2.3.1 Basic Setup

As mentioned earlier, cold plasma can be generated at low or atmospheric pressure. The basic setup of a low-pressure cold plasma system includes a vacuum chamber, a pumping unit that clears unwanted gases from the system, gas feeding tanks, gas controllers, pressure gauges, and electrodes powered by electromagnetic generators using

direct current (DC), alternating current (AC), radio frequencies or microwave frequencies. This low-pressure system can then be controlled by a microcontroller (programmable logic controller, PLC) or a personal computer (Lippens, 2007). According to (Roy Choudhury, 2017), the main advantage of a low-pressure plasma system is that it is easier to control the extent and composition of the critical gas atmosphere from which the plasma is generated, as it is operated in a closed vessel under vacuum. In addition, there is an even distribution of plasma inside the closed vessel (Ebnesajjad, 2014). However, low-pressure plasma systems are not suitable for continuous online processing and can only be conducted in batches. The vacuum equipment required for the plasma setup is expensive (Roy Choudhury, 2017). Basic low-pressure plasma systems used in starch modification as well as other food applications are outlined below:

2.3.2 Glow discharge cold plasma

In a glow discharge, cold plasma is obtained by applying an electric current operating at 100 V or higher through a gas over a pair or a series of electrodes (Figure 2-1). This electric current could either be in the form of an alternating current (AC), a direct current (DC), low frequency (50 Hz), or radio frequency (RF) (40 KHz, 13.56 MHz). The electrons generated in this type of plasma gain sufficient energy through excitation collisions which generate photons responsible for the visible glow (Thornhill, 2007; (Vaideki, 2016).

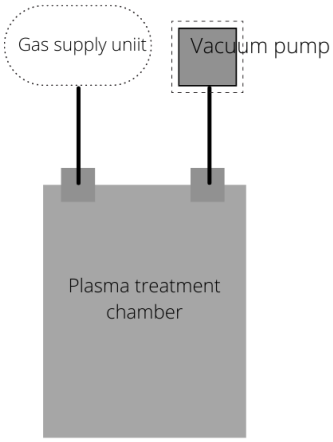

Figure 2-1: Schematic diagram of a low-pressure glow discharge plasma

2.3.3 Radio frequency (RF) discharge cold plasma

Low-pressure radio frequency plasma typically operates in the radio frequency range of 1-100 MHz (Figure 2-2). The power supplied from an electric field can be coupled to the plasma either capacitively (Thirumdas, Trimukhe, et al., 2017b) or inductively (Rossi, 2012). The capacitively coupled RF plasma consists of two parallel electrodes. One of the two electrodes is connected to an RF power supply while the other is grounded (Wilczek et al., 2020). As a result of the electric field created between the two electrodes, the electrons are accelerated and generate secondary electrons and positive ions through inelastic collisions with neutral gas species (Rossi, 2012; Wilczek et al., 2020). The electric current flowing into the coil induces a time-varying magnetic field in the inductively coupled RF plasma. The magnetic field also creates an induction field which causes the acceleration of electrons that produces and sustains the plasma. Inductively coupled RF plasma offers higher treatment efficiency than capacitively coupled RF plasma (Lee, 2018).

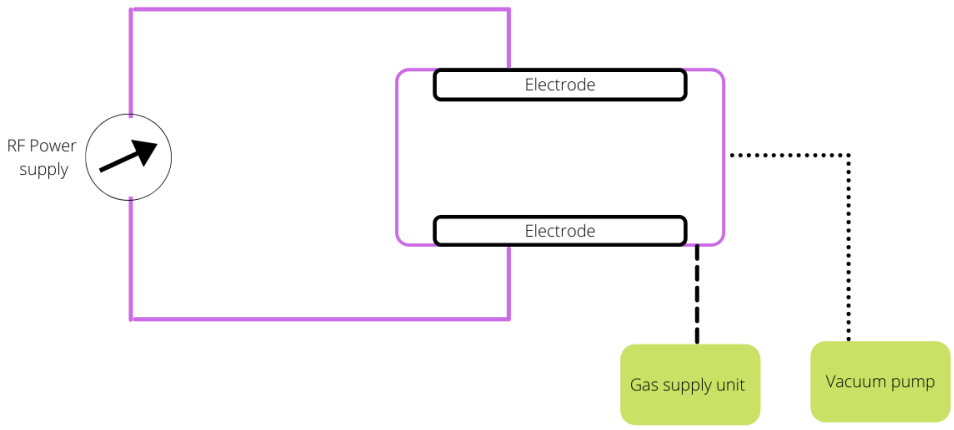

Figure 2-2: Schematic diagram of a low-pressure radio frequency plasma

2.3.4 Microwave discharge cold plasma

A microwave discharge is an electrodeless plasma technique typically operated with an electromagnetic frequency of 2.45GHz (Vaideki, 2016). A magnetron emits electromagnetic waves in a microwave discharge plasma, generating electrical discharges (Laroque et al., 2022). A waveguide directs the electromagnetic waves through a treatment chamber filled with gas electrons in this type of plasma. As a result, the electrons absorb the microwave energy and undergo ionization reactions through inelastic collisions, producing plasma. This type of plasma is more efficient in generating reactive species and has a higher electron density than a radio frequency plasma (Laroque et al., 2022). That is because the collision frequency of electrons is close to the microwave frequency. A microwave discharge plasma can be operated at low or atmospheric pressure (Thomas &

Mittal, 2013). However, it is expensive to operate and not often used in starch modification (I et al., 2004).

2.4 Generation of cold plasma at atmospheric pressure

Plasma types that operate at atmospheric pressure include atmospheric pressure plasma jets, dielectric barrier discharge plasma systems, and corona discharge plasma systems. It could be powered using AC or DC, and these systems are widely operated at a higher voltage (in kV). Atmospheric systems allow continuous type treatment of the product and do not require expensive vacuum equipment (Roy Choudhury, 2017). The most used atmospheric pressure plasma systems are discussed.

2.4.1 Atmospheric Pressure Plasma Jet

According to Niemira (2012), atmospheric pressure plasma jets (APPJ) are cold plasma systems operated at atmospheric pressure. APPJ does not require air-tight vacuum chambers and is easy to build compared to low-pressure plasma systems. Different APPJ has been developed and tested on food systems, including double electrode and end-field jet, based on the type of configurations and excitation mode. APPJ with a double electrode system consists of a plasma generator with two electrodes- one ground electrode and the other connected to the power supply, airflow monitor, and gas inlet (Figure 2-3). The plasma generator usually consists of an outer casing acting as a ground and an inner electrode made from stainless steel, Pyrex tube, or glass. The supplied gas is ionized by applying high voltage ranging from 2.5 kV to 60 kV between these electrodes. The gas is excited from the top and expands to the surrounding air outside the nozzle (Weltmann et al., 2009). The shape of the electrodes could be either rectangle, conical or cylindrical.

Gases used to produce the plasma that proved to have better preservation properties include compressed air, or a combination of argon/nitrogen and oxygen/compressed air (Surowsky et al., 2014). The selection of gas flow rate to attain the required plasma jet length greatly varies based on the design parameters of the APPJ. A single electrode APPJ (End-field jet type) was designed at the Institute of physics (Zagreb, Croatia) and consisted of a Teflon body with a copper wire placed in the capillary tube (Bursać et al., 2016a; Elez Garofulić et al., 2015; Herceg et al., 2016). High voltage is then supplied through the copper wire. Argon was used as the source of plasma. The gas flow rate used in this Single electrode APPJ was 1.5 L/min, which is less than double electrode systems with a gas flow rate of 107 L/min (Iqdiam et al., 2020).

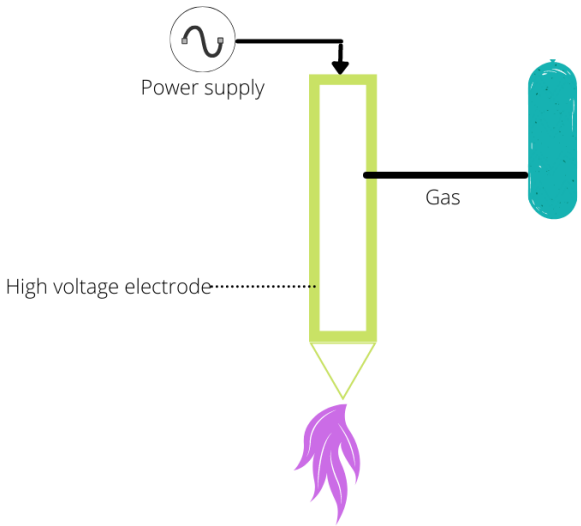

Figure 2-3: Schematic diagram of an Atmospheric pressure plasma jet system

2.4.2 Dielectric Barrier Discharge

Dielectric Barrier Discharge (DBD) plasma consists of electrodes coated with dielectric materials such as plastic, quartz, or ceramic (Figure 2-4). The electrodes are usually placed inside the closed container to prevent the escape of plasma particles, and samples are placed between the electrodes for direct treatment. Besides the coated dielectric materials, the air used in these systems acts as the barrier to the current, preventing the spark formations. These models require high voltage ignition (10 kV) (Chizoba et al., 2017) that could be powered by AC or DC supply. Design parameters like using round-edged electrodes (Moiseev et al., 2014), selection of dielectric materials (Brandenburg, 2018), higher applied voltage is considered to avoid arcing during plasma generation. The gases commonly used in the DBD plasma system include atmospheric air, nitrogen, argon, and helium.

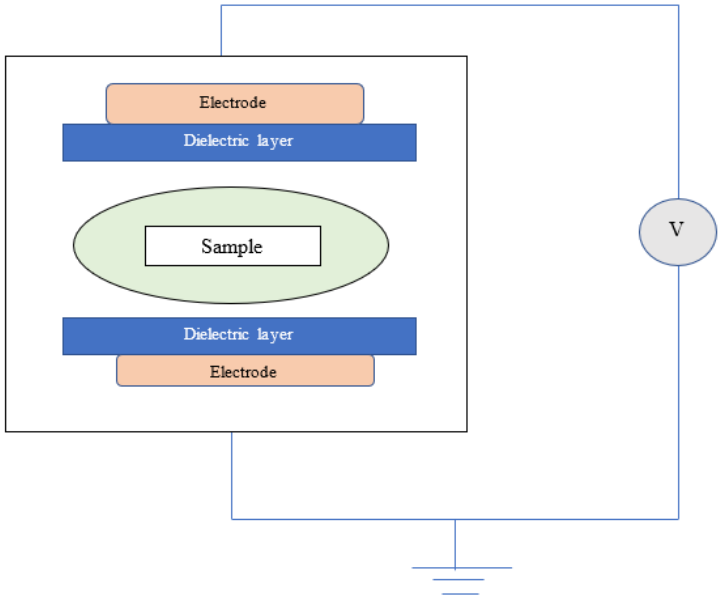

Figure 2-4: Schematic diagram of a Dielectric Barrier Discharge Configuration

2.4.3 Corona Discharge Plasma Systems

Corona discharges are pulsed discharge plasma produced at atmospheric or near atmospheric pressure. When the non-uniform electric field exceeds the breakdown threshold in the limited spatial region, it forms a corona discharge (Raizer & Allen, 1997). Corona discharge plasma setup includes a high voltage supply, electrodes, and sample treatment chambers. The electrodes employed in corona discharges are often asymmetric, like a point and a plane (Turner, 2016). The corona discharge appears as a luminous glow localized around the tip of the electrode (Kim et al., 2009). Based on the type of high voltage applied to the electrodes, corona discharge could be positive (high voltage at the anode) or negative (high voltage at the cathode).

Gases used to produce corona discharge usually include air, nitrogen, argon, a mixture of helium and oxygen, or argon and oxygen (Pignata et al., 2017). The samples are treated either below the electrode or channeled to the treatment chamber through hoses. Corona discharge plasma systems have been configured and tested in many ways, including using an air blower, cold storage system, liquid corona discharge, and cylindrical plasma reactors (Abou-Ghazala et al., 2002; Korachi et al., 2010; Timoshkin et al., 2012).

2.5 Plasma-Activated Water (PAW)

Plasma-Activated Water (PAW) is highly concentrated with chemically reactive oxygen and nitrogen species (RONS). Plasma-activated water is generated by treating water with plasma devices such as the atmospheric pressure plasma (Abuzairi et al., 2018), plasma jet (Adhikari et al., 2019), DBD (Judée et al., 2018), spark or glow discharges (Lu et al., 2017) and corona discharges (Lukes et al., 2008). The composition and concentration

of these species in water depend on the type of gas, applied voltage, treatment time, and whether the plasma source is discharged directly into water or above water's surface (Oh et al., 2016). RONS formed at the gas phase and gas-water interface includes singlet oxygen, atomic oxygen, ozone, excited and atomic nitrogen, hydroxyl radicals, superoxide, hydrogen peroxide, nitrates and nitrites ions, nitric and nitrous acid, as well as peroxynitrous acid (Thirumdas et al., 2018). The formation of these reactive species decreases the pH in the water while increasing the oxidation-reduction potential (ORP) and electrical conductivity (Zhao et al., 2020). The formation of these species makes PAW useful in microbial decontamination (Lin et al., 2020), enhancing plant growth and seed germination (Judée et al., 2018), as well as starch modification (Y. Yan et al., 2020). More details on the mechanism and potential applications of PAW in food are highlighted in Thirumdas et al. (2018).

2.6 Recent applications of cold plasma in food processing

These next few paragraphs focus on the areas where cold plasma technology has been explored in recent times. Cold plasma and PAW are utilized in food decontamination, shelf-life extension, and seed germination (Sarangapani et al., 2018; Thirumdas et al., 2018). Cold plasma is also explored in the modification of food components, including starches, proteins (Mahdavian & Koocheki, 2020; S. Yan et al., 2020; Y.Yan et al., 2019; Bu et al., 2022), food fortification (Aditya et al., 2020), and in treatment of films (Song et al., 2019).

APPJ is used in food processing applications such as treating nuts, fruit juices, spices, and vegetables owing to its ease of access with continuous processing systems

(Amini & Ghoranneviss, 2016; Bursać et al., 2016b; Charoux et al., 2020; Dasan et al., 2017; Elez Garofulić et al., 2015; Go et al., 2019; Grzegorzewski et al., 2011; Iqdiam et al., 2020; Surowsky et al., 2014).

DBD treatment of composite films made of wheat cross-linked starch, and whey protein concentrate showed positive effects on the thermal stability, mechanical and barrier properties of composite films (Song et al., 2019). The plasma treatment of these composite films increased the oxygen-containing groups on the film surface while retaining the internal crystal structure. The grass pea protein isolate's surface electrical charge and solubility were increased by treating it with a DBD system. Cold plasma also positively affected the interfacial and emulsifying properties of the grass pea protein isolate (Mahdavian & Koocheki, 2020).

Cold plasma treatment has been shown to impact the physical properties of fortified food positively. Cold plasma was used to treat noodles fortified with mango flour by Abidin et al. (2018). The noodles treated with cold plasma were less hard and cohesive than the control samples due to increased gluten strength and improved texture with plasma treatment. Aditya et al. (2020) studied the effect of cold plasma on the fortification of coffee powder with calcium from the eggshell. The bulk density of the fortified powder decreased because of surface plasma etching. Plasma treatment enhanced the solubility of calcium in black coffee. Akasapu et al. (2020) used cold plasma to fortify rice with iron. Rice was treated in DBD plasma at 20 kV at different times. The cold plasma treated rice was then fortified with ferrous sulfate (iron). After cooking, rice treated with plasma before fortification showed higher iron bioavailability than the control rice samples. Cold plasma

was used to treat brown rice grains (Park et al., 2020). This cold plasma treated rice was used in the preparation of aqueous tea infusions. The treatment increased the antioxidant activity and total phenolic contents in the brown rice-infused tea without affecting the turbidity.

2.7 Starch modification using cold plasma

As discussed above, it is essential to modify starch to improve its functionality for various applications. Thus, the effect of low and atmospheric pressure plasma systems on various starch properties (molecular, granule morphology, crystallinity, pasting, gelatinization, and rheology) are discussed separately. Details of the operating conditions utilized for starch modification and the effects are summarized in Table 2-1.

Table 2-1: Effect of low and atmospheric pressure plasma systems on starch properties

Starch	Plasma	Operating conditions	Key Findings	Reference
Maize, rice, and potato	Low Pressure Radio-Frequency Plasma (RF)	Power: 120 W Time: 60 min Gas: Carbon dioxide and Argon Gas Flow Rate: 15 and 25 sccm	No effect on shape of the selected starches No change in crystallinity of maize and rice starches Decrease in crystallinity of potato starch Increase in enthalpies of maize, rice, and potato starches	(Okyere et al., 2019)
Potato	Glow plasma	Power: 270 W Time: 30,45, 60 min Gas: Nitrogen, Helium	No change in morphology with Nitrogen glow plasma treatment	(Zhang et al., 2015)

		Operating pressure: 2000 Pa	Decrease in crystallinity, gelatinization temperatures, and enthalpy of gelatinization of potato starch Increase in semi-crystalline lamella in potato	
Cassava	Glow plasma	Power: 270 W Gas: Helium, oxygen Time: 30, 45, 60 min Operating pressure: 2000 Pa	Decrease in crystallinity Increase in semi-crystalline lamella thickness Decrease in enthalpy of gelatinization	(Bie, Li, et al., 2016)
Corn, tapioca	Low Pressure Radio-Frequency Plasma	RF Frequency: 13.56 MHz Power: 40 and 60 W Time: 10 and 20 min Gas: Atmospheric Air	Uneven surfaces and deposits after plasma treatment Decrease in the enthalpies of corn and increase in enthalpies of tapioca starch Increase in water binding capacity	(Banura et al., 2018)
Potato and Corn	Glow plasma	Voltage: 65 kV Time: 30 min Operating pressure: 1.33 Pa Gas: Ethylene	Deposits on starch after plasma treatment	(Lii et al., 2002a)

Rice	Bell Jar type plasma apparatus	RF Frequency: 13.56 MHz Operating pressure: 0.15 mbar Time: 5 and 10 min Power: 40 and 60 W Gas: Atmospheric Air	Formation of fissures / cavities were observed Reduction in the thermal properties Increase in peak viscosity	(Thirumdas, Trimukhe, et al., 2017b)
Kithul palm	Glow discharge plasma	Power: 5 and 15 W Time: 30 and 60 min Pressure: 0.2 mbar Gas: Nitrogen	Formation of fissures after plasma treatment Increase in peak viscosity	(Sudheesh et al., 2019)
Maize films	Capacitively coupled Radio frequency plasma	Gap between electrodes: 3.5 cm Gas: 1-butene	Increase in roughness of the starch films	(Andrade et al., 2005)
Corn starch films	Glow discharge	Frequency: 13.56 MHz Pressure: < 8 Pa Voltage: -100 to -60 V Time: 10, 20 min	Increase in roughness after treatment Appearance of small granules due to plasma coating	(de Albuquerque et al., 2014)
Wheat	Low-pressure radio frequency glow discharge	Power: 20-30 W Pressure: 600 mTorr	Increase in roughness of the starch films No significant change in water vapor permeability	(Sheikhi et al., 2020)

		Gas: Atmospheric air, oxygen Time: 4, 8, and 12 min		
Potato	Oxygen glow	Power: 270 W Time: 30, 45, and 60 min Gas: oxygen	Decrease in the degree of molecular order	(Zhang et al., 2014)
Maize	DBD	Power: 75 W Time: 1, 5, and 10 min Gas: Atmospheric air Dielectric material: quartz	Decrease in relative degree of crystallinity, molecular weight, and viscosity	(Bie, Pu, et al., 2016))
Waxy maize starch and normal maize starch	APPJ	Power: 750 W Frequency: 25 kHz Distance from probe to sample: 14 mm Time: 1-7 min	Etching on the surface of starch granules Increase in water binding capacity Decrease in relative crystallinity	(Zhou et al., 2019)
Potato	APPJ	Power: 750 W Frequency: 25 kHz Distance from probe to sample: 14 mm Time: 1-7 min	Decrease in relative crystallinity without change in crystalline structure	(Y. Yan et al., 2019)
Banana	DBD	Power: 60 – 167 W	Alteration in crystalline structure Increased solubility	(S. Yan et al., 2020)

		Dielectric material used: Quartz	Decreased swelling power	
Corn	APPJ	Power: 400, 600, and 800 W Time: 30 min Dimension of the chamber: 295 mm (diameter), 476 mm (height)	Decrease in peak, trough, and final viscosity No change in swelling power Increase in water soluble indexes Observation of slight fissures without significant change in overall morphology	(T.-Y. Wu et al., 2019)
Maize	APPJ (PAW)	Power: 750 W Frequency 25 kHz Time: 2min	Decreases in swelling power Increases in solubility Increases in resistant starch content Increases in relative crystallinity Increase in gelatinization temperatures in normal maize while a decrease was observed in waxy maize	(Y. Yan et al., 2020)
Corn (Normal, Hylon V, Hylon VII)	Rotatory cylindrical glass reactor (500 mL)	Power: 90 W RF Frequency: 13.56 MHz Gas: HDMSO Flow rate: 0.35 cm^3/min Time: 10 min Agitation: 200 rpm	Formation of fissures and coat deposition on granule surface Increase in absorbance ratios of 1047/1022 cm^{-1} Increases in enthalpy of gelatinization of	(Sifuentes-Nieves et al., 2021)

			high amylose corn starches only	
Corn (Normal, Hylon V, Hylon VII)	Coaxial-DBD	Voltage: 12 kV_{pp} Frequency: 25 kHz Dielectric material: quartz Time: 10 min Gases: Argon/HDMSO	Starch granules covered by a thin coat due to HDMSO polymerization New vibration modes observed in 2965 (CH_3 stretching), 1260 (CH_3 bending in Si-$(CH_3)x$), 840 (Si–C and CH_3 rocking vibrations), and 795 cm^{-1} (Si-O-Si bending vibration) Increase in absorbance ratios of 1047/1022 cm^{-1}	Sifuentes-Nieves et al., 2021
Rice	DBD	Voltage: 40 V Discharge distance: 12 mm Time: 2, 6, 10 min Gas: atmospheric air Input current: 0.8A	Changes in birefringence intensity of granules Increase in amylose content Increase in resistant starch Decreases in relative crystallinity Increase in absorbance ratios of 1047/1022 cm^{-1}	(Sun et al., 2022)
Potato	DBD	Voltage: 50 V Discharge distance: 2 mm Time: 3, 6, 9 min	Maltese cross structure remained unchanged Decrease in intensity of FTIR band at 2871 cm^{-1}	(Guo et al., 2022)

		Input current: 1A	Occurrence of cross-links between starch molecules Decreases in relative crystallinity	
Aria	DBD	Voltage: 7, 10, 14, and 20 kV Discharge distance: 15 mm Time: 15 min Gas: atmospheric air Average pressure: 101 kPa Frequency: 200 Hz	Observation of particle aggregation and fissures in starch granules at 20 kV treatment Decreases in pH values due to formation of acid groups Increase in rapidly digestible starches Increase in amylose content at 20 kV, while a decrease was observed at 14 kV	(Carvalho et al., 2021)
Granular and non-granular waxy maize, rice and potato	Low Pressure Radio-Frequency Plasma	Power: 120 W Time: 60 min Gas: Carbon dioxide and Argon Gas Flow Rate: 25 and 10 sccm	Decreases in short chain length of rice and maize starches (granular and non-granular) Increases in long chain length of rice and maize starches (granular and non-granular) Increases in resistant starches Occurrence of cross-linking in starch chains	(Okyere et al., 2022)

Mango	Novel pin to plate plasma reactor	Voltage: 170 and 230 V Discharge distance: 5 cm Time: 15and 30 min Resonant frequency: 55.51 Hz Discharge frequency: 1.5 kHz Gas: atmospheric air Duty cycle: 90µS	Increases in gel hydration properties Decrease in pH and turbidity Increase in % syneresis Decrease in amylose content Decrease in peak, setback, final and breakdown viscosity	(Kalaivendan et al, 2022)

2.7.1 Effect of low-pressure plasma on starch properties

2.7.1.1 Molecular properties

Low-pressure plasma systems have proven to be effective tools in modifying the molecular properties of starches. A capacitively coupled plasma decreased the degree of rice starch hydrolysis from 91% to 87 % after 60 W treatment for 10 min (Thirumdas, Trimukhe, et al., 2017b). This decrease was due to the cross-linking of rice starch chains, limiting the rate of enzymatic hydrolysis. Solid-state Nuclear Magnetic Resonance (NMR) analysis of waxy starches showed that modification with plasma resulted in an increase in glucose units near α-(1,6)-glycosidic linkages (Okyere et al., 2019). Thus, plasma treatment effectively degraded the polymeric starch chain into its component glucose units.

Furthermore, Zhang et al. (2015) observed a reduction in the number of single and double helices in glow-plasma modified potato starch after solid-state NMR analysis. The authors

concluded that plasma treatment induced the conversion of the starch crystallites into amorphous structures. The amylose content of kithul starch was reduced after plasma modification. That led to a subsequent decrease in the iodine binding capacity of these starches (Sudheesh et al., 2019). The hydrolysis of starch into smaller glucose units limits its ability to bind with iodine (Bailey & Whelan, 1961). Thus, the decrease observed in the iodine binding capacity was due to plasma degrading amylose into glucose units. Banura et al. (2018) and Thirumdas, Trimukhe, et al. (2017b) also reported a decrease in the amylose content of corn and rice starch after plasma modification. The intensity of the H-O-H bending vibration peaks of kithul starch decreased after plasma treatment, as indicated by Fourier Transform Infrared (FTIR) analysis. The authors reported that higher plasma power levels and longer treatment times resulted in the cleavage of hydrogen bonds in starch, thus decreasing the intensity of the H-O-H bending vibration peaks (Sudheesh et al., 2019). Okyere et al. (2022) reported the ability of a radio frequency plasma to induce cross-linking in non-granular waxy maize and rice as well as granular waxy potato and rice starches as shown by Fourier Transform Infrared-Attenuated total reflectance (FTIR-ATR) analysis. The authors also reported minor changes in waxy starches' unit and internal chain structure after RF plasma modification. Gel Permeation Chromatography with Multi-Angle Light Scattering Detection (GPC-MALS) analysis showed that the weight-average molecular weight (Mw) reduced from 4.270 x 107 to 4.716 x 106 g/mol in potato starch after oxygen glow plasma modification. The authors observed a slight decrease in the Mw of corn starch, although it was not as pronounced as that observed in potato starch. Thus, plasma resulted in the depolymerization of these starch chains.

On the other hand, nitrogen and helium glow plasma induced the polymerization of potato starch chains (Zhang et al., 2015). In conclusion, plasma can effectively depolymerize starch granules. Also, plasma can induce cross-linking in starches depending on the treatment conditions.

2.7.1.2 Granule Morphology

Okyere and co-authors (2019) observed no effect on the shapes of maize, rice, and potato starch granules after 120 W of treatment in a radio frequency (RF) plasma for 60 min. Similarly, the morphology of potato starch was not changed after nitrogen glow plasma treatment for 30, 45, and 60 min when observed under a normal and polarized light microscope (Zhang et al., 2015). On the other hand, deposits have been reported in starches after plasma treatment. Banura and co-authors (2018) reported the presence of uneven surfaces and deposits on corn starch granules after treatment in a capacitively coupled RF plasma (60 W, 20 min). This agreed with previous reports by Lii et al. (2002). The authors observed deposits on potato and corn starch after exposure to a glow plasma for 30 min. Also, fissures or cavities were observed in rice starch after treatment in a capacitively coupled RF plasma (60 W, 10min) (Thirumdas, Trimukhe, et al., 2017b). Sudheesh et al. (2019) also observed fissures on kithul starch granules after a low-pressure glow discharge plasma modification. Similarly, fissures were observed in maize starch after hexamethyldisiloxane (HDMSO)-RF plasma treatment (Sifuentes-Nieves et al., 2021).

When the topographic images of starch films were investigated using atomic force microscopy (AFM), an increase was observed in the roughness of these starch films. Andrade et al. (2005) observed an increase in the roughness of corn starch film (plasticized

with glycerol and heated for 90 min) subjected to treatment in a capacitively coupled RF plasma. Comparably, de Albuquerque et al. (2014) reported an increase in protrusions (roughness) after treatment of corn starch film in a glow discharge helium RF plasma operated at -100 V for 10 min. Sheikhi and co-authors (2020) also reported an increase in the roughness of wheat starch film after treatment in a glow discharge plasma. The presence of the fissures, cavities, deposits, and roughness is caused by the etching mechanism of the reactive species generated during modification of starches with cold plasma (Wrobel et al., 1988; S. K. Pankaj et al., 2017; Thirumdas, Kadam, et al., 2017a). The effects of a low-pressure plasma on the morphology of starch depend on the treatment conditions, the plasma type, and the botanical source of starch. Data suggests that a glow discharge plasma treatment can effectively induce fissures on starches.

2.7.1.3 Crystallinity

X-ray diffraction (XRD) analysis to date is the only method for assessing long-range crystalline order in starch (Warren et al., 2016). XRD has shown that the double helices in starch crystallize into A, B, or C allomorphs (Buléon et al., 1998). The A-type and B-type crystal pattern is characteristic of cereal and tuber starches, respectively (Imberty & Pérez, 1989; Popov et al., 2009), while the C-type is usually found in legumes (Buléon et al., 1998). Banura and co-authors (2018) reported negligible changes in the A-type crystal pattern of corn starch after treatment in an RF plasma (60 W, 20 min). Similarly, Okyere et al. (2019) observed no changes in crystallinity after treatment of waxy maize and rice in an RF plasma unit (120 W, 60 min). On the other hand, the relative crystallinity of potato decreased from 38.48% to 33.79% after a helium glow plasma modification for 60 min (Zhang et al., 2015). A carbon dioxide-argon gas RF plasma also

decreased the crystallinity of waxy potato (21.6% to 16.1%) after treatment for 60 min (Okyere et al., 2019). Bie, Li, et al. (2016) also saw a decrease in the crystallinity of cassava starch from 45.78% to 42.68% after oxygen glow plasma modification. Plasma has therefore been shown to cause the reorganization of the double helices into a less perfect crystalline structure. This is because the backbone model of starch allows for flexibility in which the longer chain segments can be reorganized (Vamadevan et al., 2013). Furthermore, the breaking of the hydrogen bonding network in starch during plasma treatment could also be a plausible explanation for the decreases in crystallinity (Bie, Li, et al., 2016). It can be deduced that cold plasma can effectively induce changes in the B and C type crystallinity pattern of starches more than the A-type crystalline pattern.

2.7.1.4 Starch Gelatinization

When starch is heated in water, molecular order is disrupted inside the granules. This results in the swelling of granules, loss of birefringence, native crystallite melting, viscosity development, and solubilization (Jane et al., 1999). The occurrence of this phenomenon is termed starch gelatinization. Several authors have utilized the Differential Scanning Calorimeter (DSC) to study the gelatinization behaviors of starch after cold plasma modification. Zhang et al. (2015) observed a decrease in the gelatinization temperatures and enthalpy of gelatinization (ΔH) of potato after nitrogen and helium glow plasma modification. Bie, Li, et al. (2016) also reported a decrease in the ΔH of cassava starch after oxygen and helium glow plasma modification. In addition, the authors suggested oxygen glow plasma as being more effective in altering the thermal properties of cassava starch. Similarly, Thirumdas, Trimukhe, et al. (2017b) reported a reduction in the thermal properties after modification of rice using an RF plasma (60 W, 10 min).

Banura and co-authors (2018) reported a decrease in corn starch's enthalpies (ΔH) after RF plasma modification.

Interestingly, the enthalpies of tapioca starch increased after RF plasma modification (Banura et al., 2018). Okyere and co-authors (2019) observed a similar increase in ΔH in maize, rice, and potato starches after RF plasma modification. Highly cross-linked starches are characterized by higher gelatinization temperatures and enthalpies due to the stability of starch crystallites (Zou et al., 2004). A degradation in the supramolecular lamellar structure results in a decrease in the gelatinization parameters of starch (Bie, Li, et al., 2016). The ability of cold plasma to induce any changes in the gelatinization properties of starches will essentially be determined by the botanical starch type, gas/ gases employed, power, the pressure of the operating system, and the treatment time.

2.7.1.5 Pasting properties

The pasting properties of starches are influenced by the amylose/amylopectin ratio, the presence of lipids, granule size distribution, and the starch cultivars (Kaur et al., 2007). The Rapid Visco-Analyser (RVA), Brabender Micro-Visco-Amylograph, and Rotational Viscometers are widely used to study the pasting properties of starches (Wiesenborn et al., 1994). Zhang et al. (2015) investigated the pasting properties of potato starch after nitrogen and helium glow plasma modification. Plasma treatment facilitated the swelling of potato granules at a relatively lower temperature. The etching of surface granules during plasma modification would enhance the penetration of the reactive species generated from plasma into the granules. This would result in a destabilizing effect on the starches, thus enhancing swelling and rupture of granules at a lower temperature. Similarly, Thirumdas, Trimukhe,

et al. (2017b) observed a decrease in the pasting temperature of rice after RF plasma modification. Okyere et al. (2019) also reported a reduction in the pasting temperature of waxy potato and rice after RF plasma modification. Peak viscosities reportedly increased in waxy potato (Okyere et al., 2019), rice (Thirumdas, Trimukhe, et al., 2017b), and kithul starch after plasma treatment (Sudheesh et al., 2019). Contrarily decreases were observed in the peak viscosities of potato (Zhang et al., 2015); waxy maize and rice (Okyere et al., 2019). The degradation of the structural bonds would result in starch leaching out of the granules, causing an increase in peak viscosities (Thirumdas, Trimukhe, et al., 2017b). The decreases observed in peak viscosities might be because of the formation of starch lipid complexes induced by plasma treatment. These complexes would restrict the granules from bursting and leaching into the aqueous medium (Eliasson & Ljunger, 1988). The formation of starch lipid complexes would be more likely to occur in cereal starches since they have more lipids than tuber starches (Pérez & Bertoft, 2010). Highly cross-linked starches would also decrease peak viscosities (Thirumdas, Trimukhe, et al., 2017b). The breakdown and final viscosities increased after plasma treatment in rice (Thirumdas, Trimukhe, et al., 2017b) and kithul starch (Sudheesh et al., 2019), whereas they decreased in potato (Zhang et al., 2015); waxy maize and rice (Okyere et al., 2019). Lower breakdown and final viscosities indicate better stability for these starch pastes and a lesser tendency for retrogradation to set in (X.-Z. Han & Hamaker, 2001). In summary, cold plasma decreases the temperature at which these starches paste. However, the effects on the peak, trough, breakdown, setback and final viscosities can differ based on the plasma operating conditions.

2.7.1.6 Rheology

Starch is subjected to varying high temperatures and shear during processing. Hence, it is necessary to measure the rheology to fully understand these starches' deformation and flow behavior (Liu et al., 2009). Plasma treatment (5W-60min, 15W-30min, and 15W-60min) reduced the ability of kithul starch to form strong gels as indicated by the lower G' (magnitude of storage modulus) and G'' (loss modulus) values (Sudheesh et al., 2019). Similarly, Thirumdas, Trimukhe, and co-authors (2017b) reported a decrease in G' and G'' in rice starch after plasma treatment. It can thus be inferred that plasma modification causes molecular degradation, which decreases the onset of retrogradation, resulting in starches that form softer gels.

2.7.2 Effect of atmospheric pressure plasma on starch properties

2.7.2.1 Molecular properties

Analysis of the molecular properties of starches after plasma modification can be employed using techniques such as the High-Performance Anion-Exchange Chromatography (HPAEC), Gel Permeation Chromatography with Multi-Angle Light Scattering Detection (GPC-MALS), High-Performance Size-Exclusion Chromatography coupled with Multi-Angle Laser Light Scattering and Differential Refractometry Detection (HPSEC-MALLS-RI), Fourier Transform Infrared spectroscopy (FTIR), NMR, and X-ray Photoelectron Spectroscopy (XPS) (Zhu, 2017). Guo et al. (2022) observed a decrease in intensity of the FTIR band at 2871 cm^{-1} in potato starch. The authors attributed this decrease to the DBD plasma treatment removing some water molecules from the starch.

Yan et al. (2019) investigated the changes in short-range molecular order of microcrystalline potato starch with the FTIR after APPJ treatment. The authors reported a

decrease in absorbance ratio at 1047/1022 cm^{-1}. A similar reduction was observed in the band ratios of 1047/1022 cm^{-1} in corn starches by Bie, Pu, et al. (2016), Zhou et al. (2019) and in aria starch by Carvalho et al. (2021). On the other hand, S. Yan et al. (2020) observed an increase in absorbance ratio at 1047/1022 cm^{-1}. Sun et al. (2022) also observed an increase in the ratio of absorbance intensity at 1047/1022 cm^{-1}. FTIR bands at 1000, 1022, and 1047 cm^{-1} are sensitive to changes in starch structure (Wilson et al., 1987). The bands at 1000 and 1047 cm^{-1} are much more defined in the crystalline structure of starch, while that of 1022 cm^{-1} is more dominant in the amorphous structure (Warren et al., 2016). Thus, the band ratios at 1022/1000 cm^{-1} and 1047/1022 cm^{-1} are generally accepted as measures of short-range molecular order in starch (Bello-Pérez et al., 2005; Warren et al., 2016). A reduction in the short-range order could be due to the depolymerization of the glycosidic bonds in starch (Zhou et al., 2019). On the other hand, the breakdown and release of amylose from the amorphous regions could reduce the amorphous content and increase the ratio of 1047/1022 cm^{-1} (S. Yan et al., 2020). In addition, cold plasma treatment could induce the formation of short-range double helices and thus, increase the short-range order of the starch (Sun et al., 2022). Furthermore, FTIR has also been used to detect cross-linking in starches. Carvalho et al. (2021) observed an increase in the areas of the C-O-C linkages in aria starch after DBD treatment (10-14 kV). Also, Wongsagonsup et al. (2014) and Deeyai et al. (2013) observed an increase in the relative areas of the C-O-C linkages in starch after plasma treatment. In addition, Wongsagonsup et al. (2014) observed a reduction in relative intensities of the OH- group protons of 50 and 100 W granular and non-granular tapioca starch after plasma treatment. This was due to cross-linking in these starches resulting in the loss of OH groups (Zou et al., 2004). XPS analysis showed an

increase in the O=C–OH bonds in corn starch and a subsequent decrease in the C(C–H), C–O, and O–C–O bonds due to the oxidation of these bonds by plasma reactive species into carboxyl groups (O=C–OH) (Bie, Pu, et al., 2016). Also, Bie, Pu, et al., (2016) reported an increase in the average molecular weight of corn starch after plasma treatment due to plasma depolymerizing the chains. Sun et al. (2022) observed an increase in the molecular weight of amylose in rice starch after DBD plasma treatment. The authors attributed this increase to the polymerization of amylose chains induced by plasma treatment. Kalaivendan et al. (2022) reported an increase in the viscosity average molecular weight (MWv) of mango starches after plasma treatment (170 V). However, increasing the treatment to 230 V reduced the MWv. The authors stated that the lower treatment voltage induced the intermolecular binding of the partially depolymerized starch molecules in the adjacent chains, thereby increasing the MWv. On the contrary, at higher treatment voltage, depolymerization occurs fully inside the starch molecule and thus decreases the MWv. Carvalho et al. (2021) observed a decrease in the amylose content in aria starch after DBD treatment of up to 14 kV. They attributed this decrease to the depolymerization of aria starch into simple sugars. Interestingly, increasing the voltage to 20 kV led to increases in the amylose content. Thus, the higher treatment voltage induced polymerization of the aria starch chains. Atmospheric pressure plasma systems have been shown to depolymerize or induce cross-linking of starches. This depends on several factors such as the treatment time, applied power, pressure, type of gas, and the botanical source of starch.

2.7.2.2 Granule Morphology

Scanning electron micrograph (SEM) images depicted that APPJ plasma treatment resulted in the surface etching of waxy and normal maize starch granules (Zhou et al.,

2019). Similar observations were made by Wu et al. (2019) in corn starch after APPJ treatment. Wu et al. (2018) also observed cavities or fissures in banana starch as treatment intensity increased during corona electrical discharge (CED) plasma modification. DBD modification also caused cracks on the surface of banana starch (S. Yan et al., 2020), red adzuki bean starch (Ge et al., 2021a) and potato starch (Guo et al., 2022). Carvalho et al. (2021) observed the formation of fissures and particle aggregation in aria starch granules after DBD (20 kV) plasma treatment. The highly energetic species produced during plasma generation bombards the starch granule's surface, which induces the volatilization of the starch surface (plasma etching).

On the other hand, APPJ treatment at 400, 600, and 800 W did not alter the Maltese cross structure of corn starch when viewed under a polarized light microscope (Wu et al., 2019). Similarly, Guo et al. (2022) observed no changes in the Maltese cross structure of potato starch after DBD treatment. Atmospheric pressure systems can alter the surface morphology of starches without necessarily altering the highly ordered structure of these starches. Pankaj and co-authors (2017) utilized the AFM to study the surface topography of high voltage atmospheric cold plasma (HVAC) modified films. They observed an increase in surface roughness of these modified films due to plasma etching. The authors reported that rice starch film was more susceptible to surface etching.

2.7.2.3 Crystallinity

The relative crystallinity (RC) of waxy (46.7% to 42.0%) and normal (40.1% to 35.7%) maize starch decreased after APPJ plasma treatment (Zhou et al., 2019). Similarly, the RC of potato starch decreased without a change in the crystalline structure after APPJ treatment (Yan et al., 2019). On the other hand, DBD plasma treatment altered the

crystalline structure of banana starch from C-type to A-type as treatment time increased. The authors also observed a decrease in RC from 21.82% to 17.15% (S. Yan et al., 2020). Guo et al. (2022) observed a decrease in RC of potato starch after DBD plasma treatment without any changes to the B-type crystalline structure. Similarly, Sun et al. (2022) observed a decrease in the RC of rice starch after DBD plasma treatment without any changes to the A-type crystalline structure. The authors attributed this decrease to a disruption in the reorganization of the starch molecules, which could potentially reduce the perfection of the long-range crystalline structure. Depolymerization of starch chains induced by plasma treatment would decrease the relative crystallinity, altering the crystalline structure of starch (Wongsagonsup et al., 2014).

Interestingly, Wu et al. (2018) observed an increase in the RC of banana starch after corona electrical discharge plasma treatment. The authors reported that the reactive species in plasma could induce the de-hydroxylation of the amorphous regions in starch through ether bond formation or condensation reactions. This would cause the starch molecules to rearrange into a perfect crystalline structure. Like low-pressure systems, atmospheric plasma can induce changes in the crystallinity of B and C-type starch more than A-type starches.

2.7.2.4 Starch Gelatinization

Wongsagonsup et al. (2014) observed an increase in ΔH of 50 and 100 W plasma modified granular tapioca starch. However, the gelatinization temperatures did not differ significantly from the untreated samples. Gao et al. (2019) observed an increase in the ΔH of Tartary buckwheat starch and an increase in the gelatinization temperatures of Tartary buckwheat starch, sorghum, and wheat starch. The higher ΔH and temperatures suggest

the presence of longer double helices formed by untwisted ends of the external chains in amylopectin (Vamadevan et al., 2013). Highly cross-linked starches are more resistant to heat and shear damage during thermal treatment (Zou et al., 2004). Contrarily, Wu et al. (2018) reported a decrease in ΔH of banana starch and increased gelatinization temperatures after CED plasma modification. Carvalho et al. (2021) also observed a decrease in gelatinization temperature in aria starch after DBD (14 kV) treatment. Zhou et al. (2019) also observed a decrease in the ΔH of waxy and normal maize starches. Similarly, Guo et al. (2022) observed a decrease in the ΔH after DBD plasma treatment. Depolymerization of starch chains induced by plasma treatment could lead to a reduction in gelatinization temperatures and enthalpies. Regarding starch films, HVAC plasma modified starch films had higher glass transition temperatures than the control films suggesting some degree of cross-linking taking place (Pankaj et al., 2017). Differences observed in the enthalpies and gelatinization temperatures are all based on the type of plasma setups used, the time, gas/gases, power, and pressure employed for starch modification.

2.7.2.5 Pasting properties

The peak viscosity of banana starch decreased from 5242 to 153 cP with an increase in DBD plasma treatment intensity. There was also a decrease in final viscosity, trough viscosity, breakdown, and setback values (S. Yan et al., 2020). Cross-links, Van der Waals forces, and hydrogen bonds between the starch chains were damaged, making it less viscous. Wu et al. (2019) also reported a decrease in corn starch's final viscosity, trough viscosity, and peak viscosity after treating with an atmospheric pressure jet plasma. At a

higher intensity of 800 W, the viscosity significantly reduced to 410 cP, however, there was no change in the pasting temperature of the starch. The trough apparent, high pasting peak, final apparent, and setback viscosities increased after DBD treatment in aria starch when the volage was increased (Carvalho et al., 2021). However, a decrease was observed in the breakdown viscosity, suggesting that DBD treatment enhanced the stability of aria starch to heat and shear. Kalaivendan et al. (2022) observed decreases in mango starch's peak, breakdown, setback, and final viscosity after plasma treatment. The authors attributed the reduction in peak viscosity to the depolymerization of the starch chains. The decrease in breakdown, setback, and final viscosity of mango starch suggests a stabilizing effect of plasma treatment. The pasting properties of starch depend on the variety, plasma types, plasma treatment conditions, and reaction time.

2.7.2.6 Rheology

Modification of starches using atmospheric pressure plasma systems may form stronger or weak gels, depending on the treatment conditions. Guo et al. (2022) observed a decrease in the retrogradation tendency of potato starch gels after DBD plasma treatment. Also, the authors reported a significant increase in the G' and G''. They attributed this increase to the formation of cross-linking in starch molecules induced by plasma treatment. Also, Wongsagonsup et al. (2014) utilized APPJ with argon gas, as an alternative for the chemical modifications of starch. The authors reported that subjecting granular tapioca starch to 50 W plasma treatment led to the formation of stronger gels. This could be attributed to the cross-linking of starch chains. However, increasing the treatment intensity to 100 W weakened the gel structure due to depolymerization. In addition, Bie, Pu, et al.,

(2016) observed a reduction in the viscosity of corn starch after plasma treatment. The active species in plasma induced the cross-linking of side chains, which prevents starch granules from leaching into the solution (Zou et al., 2004).

2.8 Effect of plasma activated water on starch properties

The use of PAW in modifying starches is relatively new; as such, to the best of our knowledge, there is limited information on the effect of PAW on starch properties. The relative crystallinity (RC) of waxy and normal maize starches increased after PAW treatment (Y. Yan et al., 2020). The authors suggested that hydrolysis of the amorphous regions in these starches could have led to the increase observed. Y. Yan and co-authors (2020) observed an increase in ΔH of normal maize starch after PAW modification combined with heat moisture treatment (HMT). The increase in ΔH suggests that PAW modification might have induced the formation of heterogenous crystallites (Alimi & Workneh, 2018). Thus, more energy was required to gelatinize the starches. Waxy and normal maize starches modified with PAW combined with HMT were more resistant to digestion compared to their native counterparts. Thus, PAW combined with HMT induced the formation of cross-links between the side chains of these starches, making it more difficult for the α-amylases to digest these starches (Y. Yan et al., 2020). PAW, therefore, has potential regarding starch modification. However, more research is needed to adopt starch modification method fully.

2.9 Industrial scale up of cold plasma technology for starch modification

Low and atmospheric plasma systems have proven to be effective tools in modifying starch properties. Their ability to modify starches depends on the plasma treatment conditions (power, time, gas/gases, pressure, moisture, humidity) and the

botanical origin of starch. Pressure ranges of 1 to > 2000Pa have been shown to effectively induce changes in the structure and functionality of starches. Treatment times ranging from 2 to 60 min can induce functional and chemical changes. Noble gases like argon and helium ionize more readily than oxygen, carbon dioxide, and air. Hence, they require a much lower energy input (Thirumdas, Kadam, et al., 2017a; Zhu, 2017). However, there is a tradeoff due to their inability to generate reactive oxygen and nitrogen species. Thus, combining a noble gas and carbon dioxide might result in a highly functional modified starch with lower energy expenditure. In addition, combining cold plasma modification with other physical methods of starch modification (Sun et al., 2022) or enzymatic methods of starch modification (Ge et al., 2021b) could also effectively alter the starch properties.

Approval of cold plasma starches to GRAS status by the FDA would require enough scientific literature on its safety, and a consensus among scientific experts that the information provided in literature holds enough credibility to deem it safe. Hence, more studies must be launched into the safety of plasma modified starches. Two of such studies available are shown below; An in vitro study on the effects of atmospheric cold plasma modified wheat grains on beetles (*Tribolium castaneum*) showed that plasma modified wheat did not negatively affect the survival or weight of these insects (Los et al., 2020). In the second study, rats fed with 5000mg/kg or 1000mg/kg/day of cold plasma modified edible films for 14 days did not show any signs of acute toxicity or even death (S. H. Han et al., 2016). In addition, cold plasma modified starches are resistant to digestion due to the formation of cross-links between starch molecules (Zou et al., 2014; Trinh, 2018). These cross-linked starches are stable and resistant to α-amylase digestion in the small intestine (Yeh & Yeh, 1993). Also, cold plasma modified starches can potentially be labeled without

the modified starch label once enough data is obtained on its toxicity and safety. As such, the starch industry must explore the utilization of cold plasma for starch modification based on sufficient literature. A major limitation to the industrial scale-up of this technology could be the construction and design of expensive vacuum equipment. However, the industry can combat this by using atmospheric cold plasma systems that do not require a vacuum unit. In addition, different authors employ different treatment modes for starch modification. Comparative studies optimizing the best treatment conditions for the various botanical starches would ideally hasten the industrial scale-up of this green technology. Cold plasma is successfully being employed in the medical industry (wound healing, cancer treatment), textile (finishing, printing), electronics and semiconductor industry (coating and etching) and can thus be implemented in the food industry.

2.10 Conclusion

Starch modification using cold plasma technology, which includes plasma-activated water, has proven to be an emerging alternative for chemical modifications. The atmospheric plasma systems have the flexibility of being used for continuous operations and production of PAW. In comparison, the low-pressure systems ensure an even distribution of plasma during modification since it is operated inside a closed vessel. Both low and atmospheric pressure plasma systems produce cross-linked starches that are more resistant to digestion. In addition, starches modified with cold plasma have good water absorption capacity and are more stable during thermal processing. The modifications in the starch properties depend on the type of gas used for plasma generation, plasma operating conditions (including power, time, pressure), and the source from which starch is obtained. We can conclude that cold plasma could be perfected and scaled up for

commercial applications of starch modifications. Atmospheric pressure plasma systems might be more cost-effective for scaling up since they don't require an expensive vacuum system and offer the flexibility for continuous operations.

Chapter 3: Modification of cereal and tuber waxy starches with radio frequency cold plasma and its effects on waxy starch properties

Contents for this chapter have been published in Carbohydrate polymers, Volume 223, 115075 (Okyere et al., 2019) https://doi.org/10.1016/j.carbpol.2019.115075 and are being reproduced here with permission from the editor (Copyright © Elsevier).

3.1 Overview

The use of carbon dioxide-argon gas radio frequency cold plasma in modifying waxy rice, maize and potato was explored in this paper. Treatment with plasma at 120 W or 0 W (carbon dioxide-argon gas mixture only) resulted in significant increases in the enthalpy of gelatinization of all three waxy starches. Treatment with plasma or gas resulted in a significant increase in the resistant starch content of maize and potato with rice increasing only after gas treatment. Significant decreases were observed in the setback and final viscosities after 120 W treatment in all starches. Plasma and gas treatment resulted in a 5.5% and 2.8% decrease in crystallinity of potato but not rice and maize starch. NMR results showed the presence of V-type single helices in mostly maize and rice starches. Carbon dioxide-argon radio frequency cold plasma served as a useful tool in modifying the properties of all three waxy starches.

Keywords: Cold plasma, starch modification, radio frequency, carbon dioxide-argon

3.2 Introduction

Starch is a polymeric carbohydrate molecule harnessed for food and non-food use. It is the main energy reserve for most green plants and exists as semi-crystalline granules. Amylose and amylopectin are the two major polyglucans that constitute the starch granule. Both are made of chains of α-(1,4)-linked D-glucose units, interconnected through α-(1,6)-glycoside linkages, contributing to branches in the polymer (Vamadevan & Bertoft, 2015).

Starch in its native form has several drawbacks which limits their use in various applications. These drawbacks are mostly due to their unreactive nature, insolubility, retrogradation tendencies and inability to withstand high temperatures and shear during processing (Jayakody & Hoover, 2008). In order to overcome these challenges starch is modified by various means, including the use of chemicals and enzymes as well as physical processes in order to meet the huge market demands for starches with unique properties (Kaur et al., 2012). Physical methods of starch modification such as cold plasma technology, is currently being employed because it is considered a green technology devoid of the use of chemicals (Thirumdas, Kadam, et al., 2017a). Plasma, which is known as the fourth state of matter, is generated when energy (electric, magnetic, thermal, microwave or radiofrequency) is applied to a gas, resulting in the production of active species such as electrons, ions, free radicals and large numbers of unionized neutral molecules (Thirumdas, Kadam, et al., 2017a). Plasma is basically divided into high temperature plasma and low temperature plasma. In high temperature plasma all species involved in the plasma reaction are in thermal equilibrium, this is however not the case for low temperature plasma (Bogaerts et al., 2002). Plasma chemistry is dependent on the type and composition of gases fed into the plasma unit, humidity, applied power and treatment time (Misra et al.,

2016). The type of gases used may lead to the introduction of hydroxyls, ketones, aldehydes, esters and free radicals as in the case of carbon dioxide and argon gas plasmas (Desmet et al., 2009). Cold plasma has been applied in areas such as the inactivation of microbes (Moreau et al., 2008), and enzymatic inactivation (Misra et al., 2016).

With regards to starch modification, a low-pressure glow plasma treatment generated using air caused a decrease in molecular weight and radius of gyration of starches (Lii et al., 2002b). (Wongsagonsup et al., 2014) also reported a reduction in molecular weight upon treatment of starch with a jet atmospheric argon plasma. (Thirumdas et al., 2016) reported a decrease in cooking time of rice and an increase in the rate at which amylose molecules leach during cooking after treatment with a low-pressure radio frequency cold plasma generated using air. Plasma treatment may either alter or have no effect on gelatinization temperatures and the enthalpy (ΔH) when measured by differential scanning calorimetry. (Bie, Li, et al., 2016) reported a decrease in enthalpy and an increase in the temperature of gelatinization upon treatment of starches with an oxygen and helium glow plasma. However, Wongsagonsup et al. (2014) reported a decrease in gelatinization temperature. Cold plasma treatment has therefore been proven as an effective way of modifying starches. To the best of our knowledge, there is limited information with regard to the effect of a radio frequency cold plasma generated using a carbon dioxide-argon gas mixture on the properties of waxy starches. We hypothesize that radio frequency cold plasma will significantly alter the properties of cereal and tuber waxy starches. In this present study the morphological, pasting and thermal properties, iodine binding, resistant starch, starch damage, crystallinity, and changes in short range molecular order of waxy

rice, maize and potato as affected by a carbon dioxide-argon radio frequency cold plasma treatment was investigated.

3.3 Materials and Methods

3.3.1 Materials

Waxy maize and waxy potato starch used for the experiment were obtained from Ingredion Incorporated (Bridgewater, NJ, USA). Waxy rice was obtained from Remy Industries (Belgium). Potassium iodide and iodine were obtained from Sigma Aldrich (St. Louis, MO, USA). CO_2 and Ar gases were obtained from Matheson, Eagan, Minnesota. All chemicals used for the experiments were of analytical grade.

3.3.2 Plasma apparatus and treatment

The plasma unit connected to a vacuum pump, chilling unit, and a radio frequency power (RF) supply with a frequency of 13.56 MHz (Plasma Etch Industries, Carson City, Nevada, USA) was used. CO_2 and Ar gases were used for plasma generation each at a flow rate of 25 standard cubic centimeters per minute (sccm) and 15 sccm respectively. An RF power of 120 W and 0 W was supplied to the sample. Native starches were used as control samples. The 0 W power was used to investigate the effects of just the carbon dioxide and the argon gas. The 120 W was used to enhance dissociation of CO_2 into carbon monoxide and oxygen in the RF plasma unit based on methods previously reported by (Spencer & Gallimore, 2011). About 15 g of starch was spread evenly on a glass petri dish and placed inside the plasma chamber based on methods previously described by (Thirumdas, Trimukhe, et al., 2017b). Once the vacuum setpoint of 0.6 cubic feet per minute was reached treatment of the starches were done for 30 min, stirred, and retreated for another 30 min. The vacuum setpoint was used as recommended by the manufacturer of the plasma

unit. The treated samples were stored in snap cap vials and kept in a desiccator at room temperature until further analysis.

3.3.3 Thermal properties

Gelatinization onset, peak, and conclusion temperature and enthalpy (ΔH) parameters were determined using the differential scanning calorimeter (DSC) from Mettler Toledo (Ohio, USA) using methods described by (Bertoft et al., 2016) with modifications. This was done by heating one part (4 mg) starch in three parts (12 mg) deionized water in a hermetically sealed DSC pan from 25°C to 105°C at a heating rate of 5°C/min. Starches were equilibrated to room temperature for approximately 30 minutes prior to testing. The starches were then tested against an empty pan used as a reference. The results were analyzed using the STARe thermal analysis software. Samples were analyzed in duplicates.

3.3.4 Pasting properties

Pasting properties of starches were studied using the Micro-Visco-Amylograph (MVAG) (Brabender® GmbH & Co KG, Duisburg, Germany) operated at 250 rpm using methods described by (Hagenimana & Ding, 2005) with modifications. Starch slurry (5 g, db), dispersed in 100 mL of deionized water, was directly placed into a stainless-steel measuring bowl, and then heated from 30 to 95°C, held for 20 min at 95°C, and cooled to 50°C. Heating and cooling rates were 3°C/min. The parameters were defined by (Limpisut & Jindal, 2002) as breakdown, the drop in viscosity at the end of cooking with reference to the peak viscosity; setback, the rise or fall in viscosity at the end of the cooling cycle; peak viscosity, maximum viscosity and final viscosity, viscosity at the end of the cooking and cooling cycle. Viscosity was measured in BU.

3.3.5 Starch granule morphology and iodine binding of waxy starch components

3.3.5.1 Scanning electron microscopy (SEM)

Scanning electron micrographs were obtained with the Hitachi S3500N variable pressure microscope (Tokyo, Japan). Samples were added to a double-sided adhesive tape mounted on an aluminum stub and coated under vacuum with a thin film of gold. An accelerating voltage of 5.0 -10.0 kV was used (Thirumdas, Trimukhe, et al., 2017b).

3.3.5.2 Light microscopy

A thin layer of starch grains suspended in potassium iodine solution was observed under the Olympus BX40 light microscope (Melville, NY, USA) connected to a digital camera (Olympus DP11-N) and a monitor (Sony PVM-14N5U; Tokyo, Japan). Images were acquired with the Olympus CellSens Dimension software (Melville, NY, USA). Polarized light images were acquired with the same imaging system using a polarized light filter (Goldstein et al., 2017).

3.3.5.3 Iodine binding of waxy starch components

Iodine affinity of starch granules was determined by dissolving (~2 mg) of waxy starch in (100 µL) 90% DMSO with subsequent heating in a hot water bath (80°C) for 5 min. The samples were stirred slowly at room temperature (25°C) overnight. They were then diluted with 1900 µL warm water. The carbohydrate content was determined by pipetting 1 mL of starch solution followed by the addition of phenol–sulfuric acid reagent (DuBois et al., 1956). The λ_{max} of the starch–iodine complex of the samples (1 mL) was determined with the WPA Spectrawave S800 diode array spectrophotometer (Biochrom Ltd., Cambridge, U.K.) after the addition of 100 µL of 0.01 M I_2/0.1 M KI. The peak value

(PV) was calculated as the absorbance at λ_{max} divided by the carbohydrate content and reflects the relative iodine affinity (Bertoft et al., 2016).

3.3.6 Wide Angle X-ray Scattering (WAXS)

X-ray diffraction (WAXS) patterns of the untreated and treated starch samples were analyzed using a Bruker D8 Advance X-ray diffractometer (Bruker AXS, Germany) equipped with a Cu Kα radiation source λ = 1.5406 Å, operating at 40 kV and 40 mA. The relative intensities were recorded in a scattering angle range (2θ) of 5.0–40.0 with a scintillation counter at a scanning speed of 0.02º min^{-1}. The relative crystallinity (RC) was expressed as a percentage and was calculated from the crystalline (I_c) and amorphous areas (I_a) obtained in each diffraction pattern using the equation: RC (%) = $I_c/(I_a+I_c)$ x 100 (Goldstein et al., 2017).

3.3.7 ^{13}C CP MAS NMR

Solid-state ^{13}C CP MAS NMR experiments were carried out using a Bruker Advance III 700 MHz spectrometer (Karlsruhe, Germany) equipped with a 3.2 mm triple resonance based on methods described by (Zhang et al., 2015) with modifications. Approximately 30 mg of the sample was packed into the MAS rotor and spun at 12 kHz spinning rate. All the spectra were acquired at a temperature of 298 K using a recycle delay of 3 s and number of scans for each sample was set to 1000. The peaks obtained were integrated using the Bruker's Topspin™ software (Karlsruhe, Germany). Figures of NMR spectra are shown in the appendices data section for reference (Figure A1).

3.3.8 Starch damage and resistant starch assays

Measurement of starch damage and resistant starch in treated and untreated granules was analyzed following the assay procedure by Megazyme International Ireland (Bray, Co. Wicklow, Ireland) (AACC Method 76-31.01; AOAC Method 2002.02).

3.3.9 Statistical analysis

All results were statistically analyzed by one-way ANOVA with Statgraphics Centurion XVI, version 16.1.0 (Stat Point, Warrenton, VA, U.S.A.). Duncan's multiple range test was used to determine statistical significance between means at a p-value of < 0.05.

3.4 Results and discussion

The waxy starch samples were treated at a radio frequency power (RF) of 120 W with the native starches as controls. The samples were also exposed to the carbon dioxide-argon gas mixture under vacuum in the plasma unit without RF (0 W). The 0 W samples will be referred to as gas treated waxy maize, rice, or potato starch (GTWMS, GTWRS, or GTWPS) respectively.

3.4.1 Scanning electron microscopy (SEM)

Cavities or pores could be seen in both treated and untreated waxy rice, maize, and potato starch samples (Figure 3-1). These cavities are thought to be caused by the drying of kernels (Whistler & Turner, 1955), a result of the starch purification process (Hall & Sayre, 1971), or a result of the isolation and preparation techniques used for electron microscopy (Sujka & Jamroz, 2007). However, Fannon et al., (1992) suggested that these cavities were created as a result of enzymatic hydrolysis, which gives the enzyme molecules access to the interior of starch granules. (Huber & BeMiller, 2000) suggested that pores in waxy starch could be formed by the crystallization of amylopectin molecules leading to shrinkage of the starch matrix as the granule grows and develops. Plasma or gas treatment did not result in any visible changes in any of the three waxy starches when observed under the scanning electron microscope.

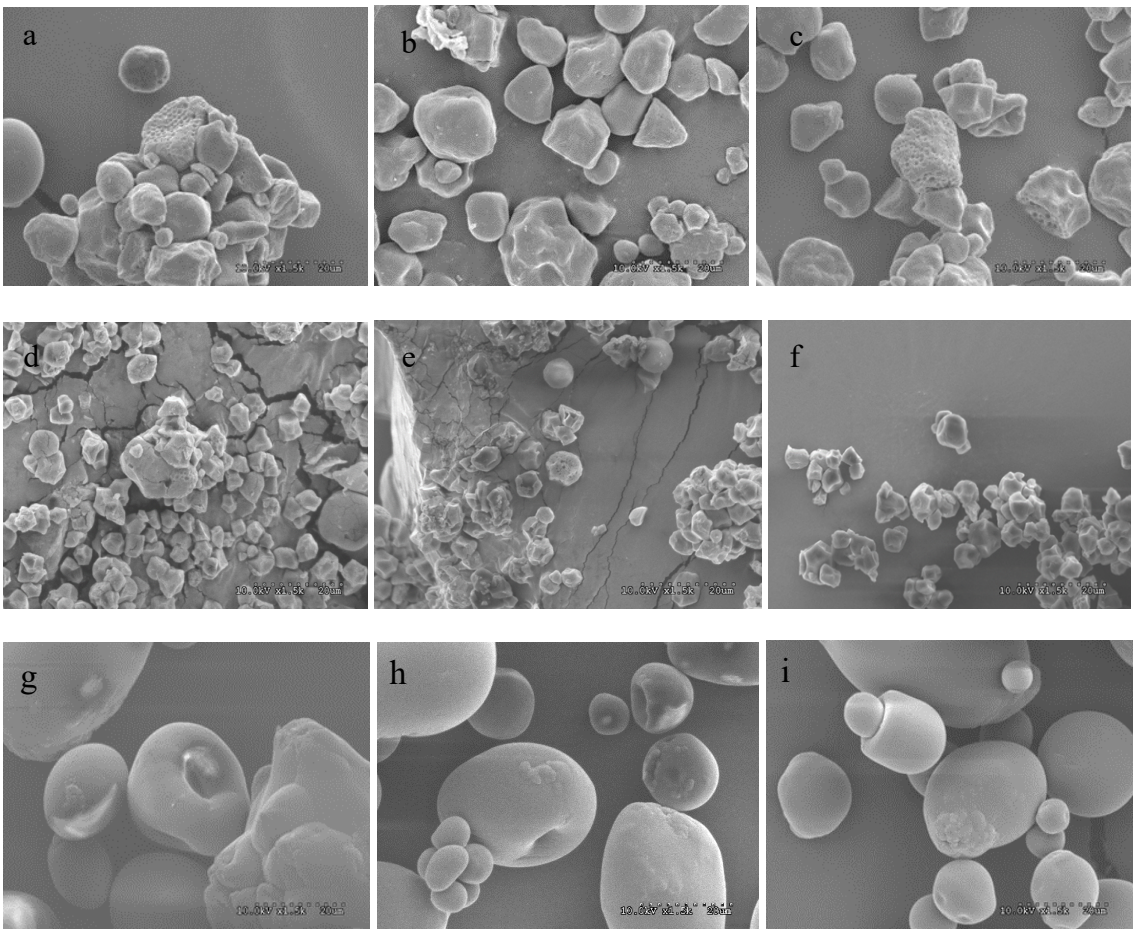

Figure 3-1: Scanning electron microscopy images of plasma treated and non-plasma treated waxy starch samples

Plasma Treated Waxy Maize Starch (a), Gas Treated Waxy Maize Starch (b), Waxy Maize Starch (c), Plasma Treated Waxy Rice Starch (d), Gas Treated Waxy Rice Starch (e), Waxy Rice Starch (f), Plasma Treated Waxy Potato Starch (g), Gas Treated Waxy Potato Starch (h), Waxy Potato Starch (i).

3.4.2 Light microscopy and iodine binding of waxy starches

Maize and rice starches typically have angular or polyhedral shapes whilst potato starch has an oval shape (Figure 3-2). It is well known that rice granules are smaller than those of maize, whereas potato granules are comparatively large (Waterschoot et al., 2015). Waxy starch granules typically turn red to blue-purple when stained with iodine (Figure 3-2) (Bailey & Whelan, 1961). Starch samples used in this study behaved similarly even after plasma or gas treatment when observed under the light microscope (Figure 3-2). This was in accordance with (Bie, Li, et al., 2016) and Zhang et al. (2015), who reported no changes in granule morphology after plasma treatment.

According to Jackson (2003), as polarized light passes across a region of high molecular order it bends, and this leads to birefringence (Figure 3-3) observed in native starches. Birefringence is therefore indicative of the crystalline structure in starch granules (BeMiller & Whistler, 2009). Plasma and gas treatment did not cause any visible changes in the Maltese cross pattern of any of the three waxy starches.

Iodine is well-known to form inclusion complexes with both amylose and amylopectin (Bailey & Whelan, 1961). The iodine-amylose complex results in an intense blue color with absorption maxima at wavelengths (λ_{max}) > 600 nm, whilst that of amylopectin leads to a faint red to blue-purple color with λ_{max} < 600 nm. The λ_{max} values for all three waxy starches were typical of amylopectin and ranged from 535.5 to 557.5 nm, with waxy potato starch having the highest values (Table 3-1). This is because waxy potato has longer chain segments than rice and maize (Hizukuri, 1985). There were no statistical differences in the λ_{max} values of treated and untreated waxy rice and maize starch, but a significant increase could be observed in potato after plasma treatment (554.5-557.5).

The increase observed in waxy potato could have resulted from removal of branches resulting in longer internal chain lengths that reacted with iodine (Chauhan & Seetharaman, 2013).

The peak value (PV) is an indirect quantitative indicator of the amount of chain segments in amylopectin that can bind with iodine for λ_{max} values < 575 nm (Bailey & Whelan, 1961). PV for the amylopectin samples ranged from 0.37 to 1.0 (Table 3-1). Plasma treatment did not significantly affect the peak values of waxy maize, but it increased significantly in potato (0.84-1.00) and rice (0.37-0.48). The increased PV values may be a result of plasma treatment removing some branches in amylopectin, which could result in longer internal chain segments reacting with iodine (Chauhan & Seetharaman, 2013). A significant increase was seen in waxy rice (0.37-0.59) also after the simple gas treatment without RF possibly due to the reason stated above, whilst instead a decrease was observed in potato (0.84-0.62). This decrease of PV observed after gas treatment may be a result of depolymerization of the amylopectin molecule into shorter chain fragments (Duan & Kasper, 2011).

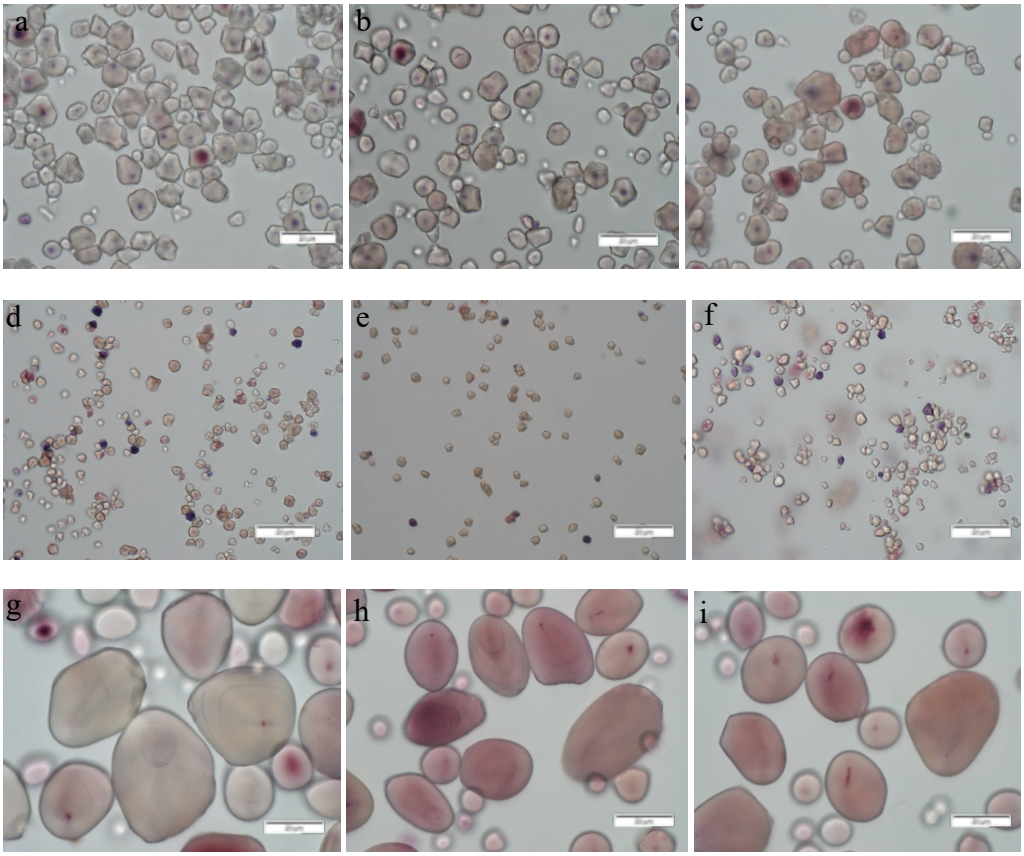

—— Scale 20 µm

Figure 3-2: Light microscopy images of plasma treated, and non-plasma treated waxy starch samples suspended in potassium iodine solution

Plasma Treated Waxy Maize Starch (a), Gas Treated Waxy Maize Starch (b), Waxy Maize Starch (c), Plasma Treated Waxy Rice Starch (d), Gas Treated Waxy Rice Starch (e), Waxy Rice Starch (f), Plasma Treated Waxy Potato Starch (g), Gas Treated Waxy Potato Starch (h), Waxy Potato Starch (i).

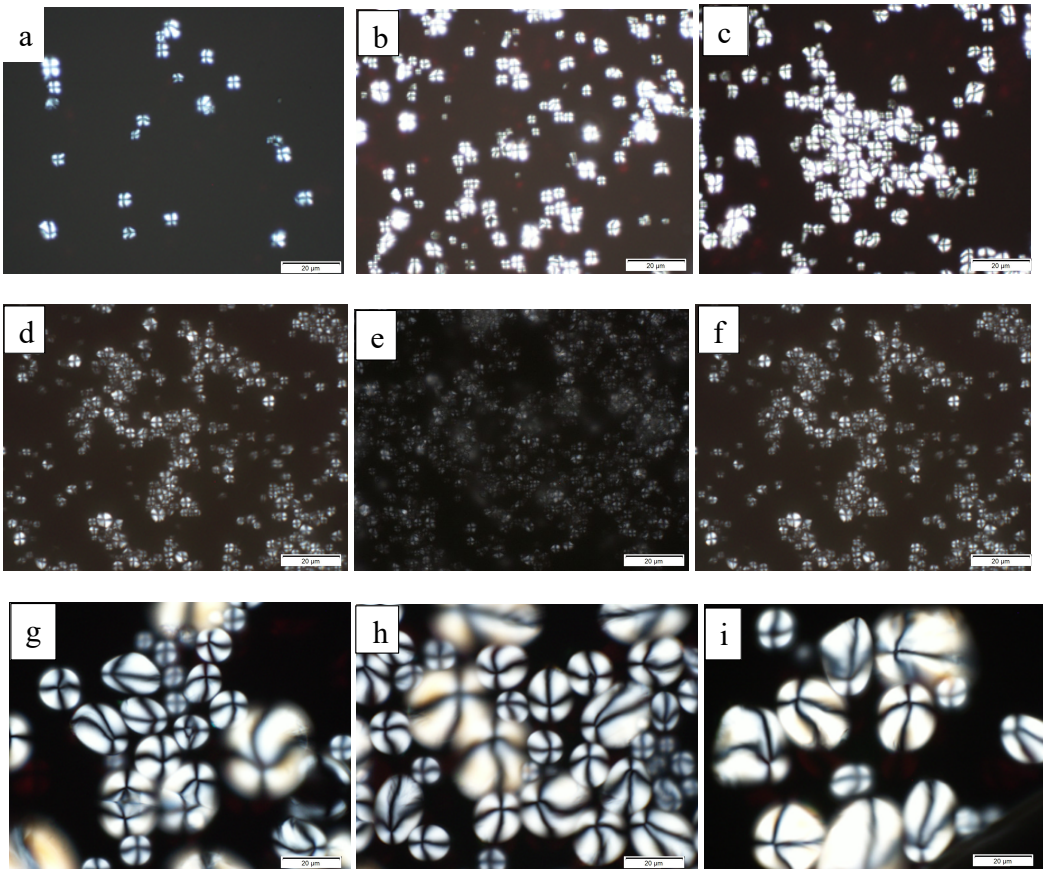

——— Scale 20 µm

Figure 3-3: Polarized light microscopy images of plasma treated and non-plasma treated waxy starch samples

Plasma Treated Waxy Maize Starch (a), Gas Treated Waxy Maize Starch (b), Waxy Maize Starch (c), Plasma Treated Waxy Rice Starch (d), Gas Treated Waxy Rice Starch (e), Waxy Rice Starch (f), Plasma Treated Waxy Potato Starch (g), Gas Treated Waxy Potato Starch (h), Waxy Potato Starch (i).

Table 3-1: Iodine affinity values of plasma treated and untreated waxy starch samples

Sample	λ_{max} of amylopectin (nm)	Peak value
PTWMS	536.5[a]	0.52[a]
GTWMS	541.5[a]	0.59[a]
WMS	535.5[a]	0.43[a]
PTWRS	537.5[a]	0.48[ab]
GTWRS	540.5[a]	0.59[b]
WRS	541.5[a]	0.37[a]
PTWPS	557.5[b]	1.00[c]
GTWPS	553.5[a]	0.62[a]
WPS	554.5[a]	0.84[b]

[a] Means with different superscript letters shows significant differences (p-value < 0.05) between treated and untreated waxy starches of the same type; PTWMS: Plasma Treated Waxy Maize Starch, GTWMS: Gas Treated Waxy Maize Starch, WMS: Waxy Maize Starch, PTWRS: Plasma Treated Waxy Rice Starch, GTWRS: Gas Treated Waxy Rice Starch, WRS: Waxy Rice Starch, PTWPS: Plasma Treated Waxy Potato Starch, GTWPS: Gas Treated Waxy Potato Starch, WPS: Waxy Potato Starch.

3.4.3 Pasting properties

Plasma and gas treatment resulted in significant decreases in the pasting temperature of waxy rice and potato (Table 3-2). This was however not the case for maize. Thus, it appears that plasma and gas treatment enhanced the ability of the waxy rice and potato starch granules to swell at a relatively lower temperature suggesting a destabilizing effect on their structure (Zhang et al, 2015). Sample peak viscosities significantly

decreased after 120 W of plasma treatment in maize (from 406.3 to 354.3 BU) and rice (from 253.8 to 160.8 BU) but increased in potato (from 906.8 to 942.3 BU). The decrease in peak viscosities might be a result of starch-lipid complexes (Eliasson & Ljunger, 1988). There is evidence to suggest the formation of complexes between amylopectin and lipids. Eliasson & Ljunger, (1988) suggested the outer branches of the amylopectin molecule could assist in the formation of a helical inclusion complex with the acyl chains of a suitable lipid. An atmospheric cold plasma-dielectric barrier was shown to induce lipid oxidation in dairy and beef fat (Sarangapani et al., 2017). Thus, plasma could have resulted in the oxidation of lipids in waxy rice and maize leading to the formation of free fatty acids that could have formed complexes with the starch granules, decreasing the peak viscosity. Noteworthy, the simple gas treatment had the same effect as the plasma treatment in potato starch, but it exhibited no effect in the cereal starches. During swelling, starch components leach out of the granules and dissolve in the medium (Gallant et al., 1997) resulting in an increase in peak viscosity (Thirumdas, Trimukhe, et al., 2017b). During plasma treatment the highly energetic species may have bombarded potato more efficiently thus penetrating the granules and causing amylopectin to leach more during pasting. In addition, potato starch granules are known to swell considerably more than cereal starches (Vamadevan & Bertoft, 2015), which might further enhance the effect. The breakdown viscosity is an indication of the stability of the starch paste (Saunders et al., 2011). A lower breakdown value shows better stability after gelatinization. Plasma treatment resulted in lower breakdown values for maize (189 as compared to 212 BU) and rice (24.5 as compared to 32.0 BU). Potato starch, however, showed less stability after plasma treatment (632.5 as compared to 538.0 BU). Interestingly, for potato starch, but not for the cereal starches, gas

treatment also destabilized the paste (578.5 as compared to 538.0 BU). Thus, a higher degree of cross-linking seems to have taken place in the cereal starches, making these starches more stable (Zou et al., 2004). The presence of more water molecules in the hexagonal unit cell of potato could easily be converted to free radicals during plasma and gas treatment, which will lead to degradation of the starch structures resulting in less stability during shear and heat treatment (Zhang, et al., 2015). Significant decreases in the setback and final viscosities were observed in all starch pastes after plasma treatment, whereas gas treatment exhibited no effect in any of the samples. Thus, only plasma treatment enhanced the ability of all three waxy starches to withstand retrogradation, which is desirable in cases where staling needs to be prevented (Zhang et al., 2015).

3.4.4 Thermal properties

Plasma treatment mostly enhanced the susceptibility of all three starches to thermal treatment as shown by the slightly lower gelatinization onset temperatures (T_o), whereas only potato starch possessed a significant decrease in the peak temperature (T_p) (Table 3-3). A significant decrease was observed in T_o and T_p in potato also after gas treatment. The conclusion temperature (T_c) remained unchanged in all samples with the exception of maize, which significantly decreased after gas treatment but increased after plasma treatment. Decreases observed in the gelatinization temperatures might have been as a result of depolymerization after plasma treatment (Zhang et al., 2015). Increases were observed in the enthalpy of gelatinization of all three waxy starches after gas and plasma treatment. This may be a result of active molecular species from plasma and the gases inducing cross-linking of amylopectin side chains (Zou et al., 2004), which could have a stabilizing effect on the starch crystallites. The higher enthalpies also seem to suggest the

presence of longer double helices, perhaps formed by organizing untwisted ends of the external chains of the amylopectin (Vamadevan, Bertoft, Soldatov, et al., 2013).

Table 3-2: Pasting properties of plasma treated and untreated waxy starches

Sample	Pasting Temp (°C)	Peak Viscosity (BU)	Breakdown Viscosity (BU)	Setback Viscosity (BU)	Final Viscosity (BU)
PTWMS	70.5[a]	354.3[a]	189.0[a]	44.0[a]	209.3[a]
GTWMS	70.5[a]	403.0[b]	214.5[b]	62.8[b]	251.3[b]
WMS	70.1[a]	406.3[b]	212.8[b]	65.8[b]	295.3[b]
PTWRS	66.9[a]	160.8[a]	24.5[a]	48.3[a]	184.5[a]
GTWRS	67.0[a]	254.8[b]	30.8[ab]	84.3[b]	308.3[b]
WRS	67.5[b]	253.8[b]	32.0[b]	89.5[b]	311.3[b]
PTWPS	64.5[a]	942.3[b]	632.5[c]	76.5[a]	386.3[a]
GTWPS	64.5[a]	948.3[b]	578.8[b]	137.8[b]	507.3[b]
WPS	66.0[b]	906.8[a]	538.0[a]	147.3[b]	516.0[b]

[a] Means with different superscript letters show significant differences (p-value < 0.05) between treated and untreated waxy starches of the same type; PTWMS: Plasma Treated Waxy Maize Starch, GTWMS: Gas Treated Waxy Maize Starch, WMS: Waxy Maize Starch, PTWRS: Plasma Treated Waxy Rice Starch, GTWRS: Gas Treated Waxy Rice Starch, WRS: Waxy Rice Starch, PTWPS: Plasma Treated Waxy Potato Starch, GTWPS: Gas Treated Waxy Potato Starch, WPS: Waxy Potato Starch**,** BU: Brabender Units.

Table 3-3: Thermal properties of plasma treated and untreated waxy starch samples

Sample	T_o (°C)	T_p (°C)	T_c (°C)	ΔH (J/g)
PTWMS	64.5[a]	70.8[a]	78.7[c]	12.0[c]
GTWMS	65.1[ab]	71.0[a]	73.0[a]	9.6[b]
WMS	65.2[b]	71.0[a]	77.6[b]	8.7[a]
PTWRS	60.5[a]	67.4[a]	75.2[a]	9.2[c]
GTWRS	61.1[b]	67.6[a]	74.5[a]	7.6[b]
WRS	61.0[b]	67.6[a]	74.7[a]	6.9[a]
PTWPS	61.7[a]	66.8[a]	72.6[a]	14.4[c]
GTWPS	62.6[b]	67.5[b]	73.0[ab]	13.9[b]
WPS	63.9[c]	68.6[c]	73.6[b]	13.3[a]

[a] Means with different superscript letters show significant differences (p-value < 0.05) between treated and untreated waxy starches of the same type; PTWMS: Plasma Treated Waxy Maize Starch, GTWMS: Gas Treated Waxy Maize Starch, WMS: Waxy Maize Starch, PTWRS: Plasma Treated Waxy Rice Starch, GTWRS: Gas Treated Waxy Rice Starch, WRS: Waxy Rice Starch, PTWPS: Plasma Treated Waxy Potato Starch, GTWPS: Gas Treated Waxy Potato Starch, WPS: Waxy Potato Starch.

T_o: onset temperature, T_p: peak temperature, T_c: conclusion temperature, ΔH: enthalpy of gelatinization

3.4.5 Wide angle X-ray scattering

X-ray diffractograms for waxy maize and rice starch showed high intense reflections at 2θ values of 15, 17, 18 and 23 typical of the A-type patterns, whilst that of waxy potato showed strong signals at 15, 17, 22 and 24 typical of the B-type patterns (Figure 3-4). Previous reports by (Varatharajan et al., 2011) also confirmed that waxy potato exhibits a B-type pattern. Decreases were seen in the peak intensities for waxy potato after plasma treatment, which reflects decreases in crystallinity. The percent

crystallinity for PTWPS was 16.1% as compared to 21.6% for WPS. Treatment with gas also resulted in a 2.8% decrease in crystallinity. Visible changes could be observed in the X-ray diffractogram of waxy potato only. Thus, it seems plasma and gas treatment could have resulted in the reorganization of the double helices in potato into a less perfect crystalline structure. This change would be possible because the proposed backbone model of starches allows for flexibility in which the longer chain segments in potato can move freely as opposed to the constricted cluster model (Vamadevan, Bertoft, & Seetharaman, 2013). However, the diffraction peaks associated with the A-type pattern in waxy maize and rice starch were unaffected after either plasma or gas treatment. (Banura et al., 2018) also reported that a low-pressure radio frequency cold plasma did not affect the A-type pattern of crystallinity in maize and cassava starch. Moisture content of starches is known to be very important when it comes to crystallinity of starches. This is because starches with more water molecules seem to be more susceptible to molecular degradation by secondary electrons formed after plasma generation. The consequent breakdown of water molecules results in the formation of active hydroxyl radicals, which could lead to decreases in crystallinity (Thirumdas, Kadam, et al., 2017a). Potato starch has its double helices packed in a hexagonal unit cell with 36 water molecules (Imberty & Pérez, 1989) whilst maize and rice have their double helices packed into a monoclinic unit cell with 8 water molecules (Popov et al., 2009). This might account for the possible decreases in crystallinity observed in waxy potato as compared to maize and rice after plasma treatment.

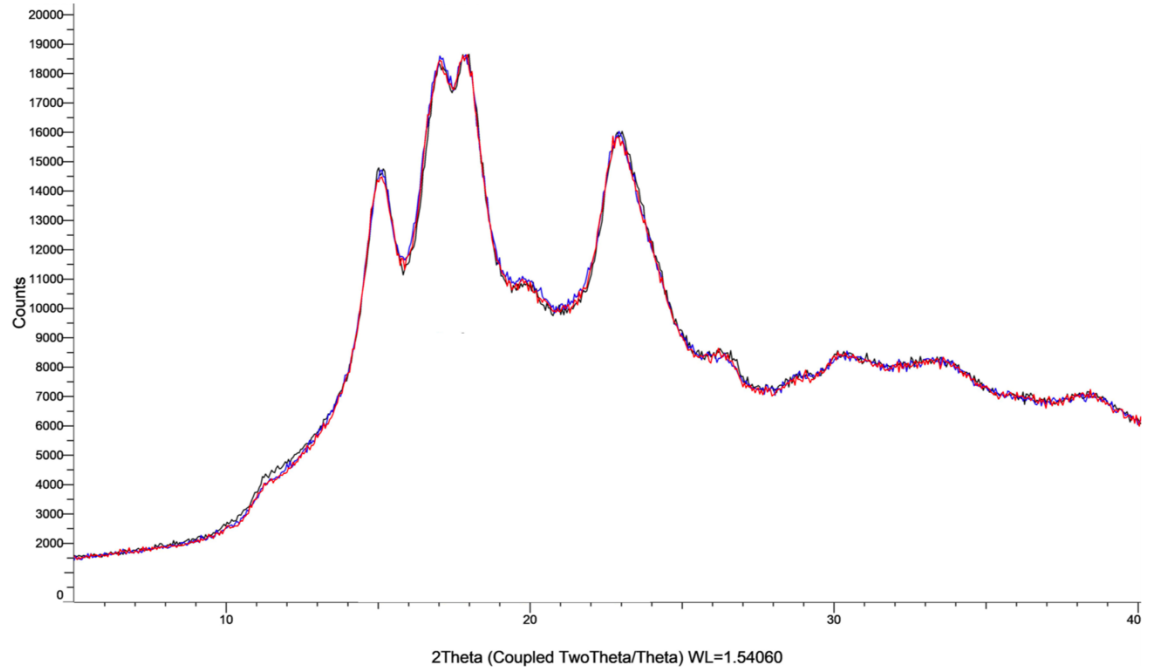
Counts
2Theta (Coupled TwoTheta/Theta) WL=1.54060

b

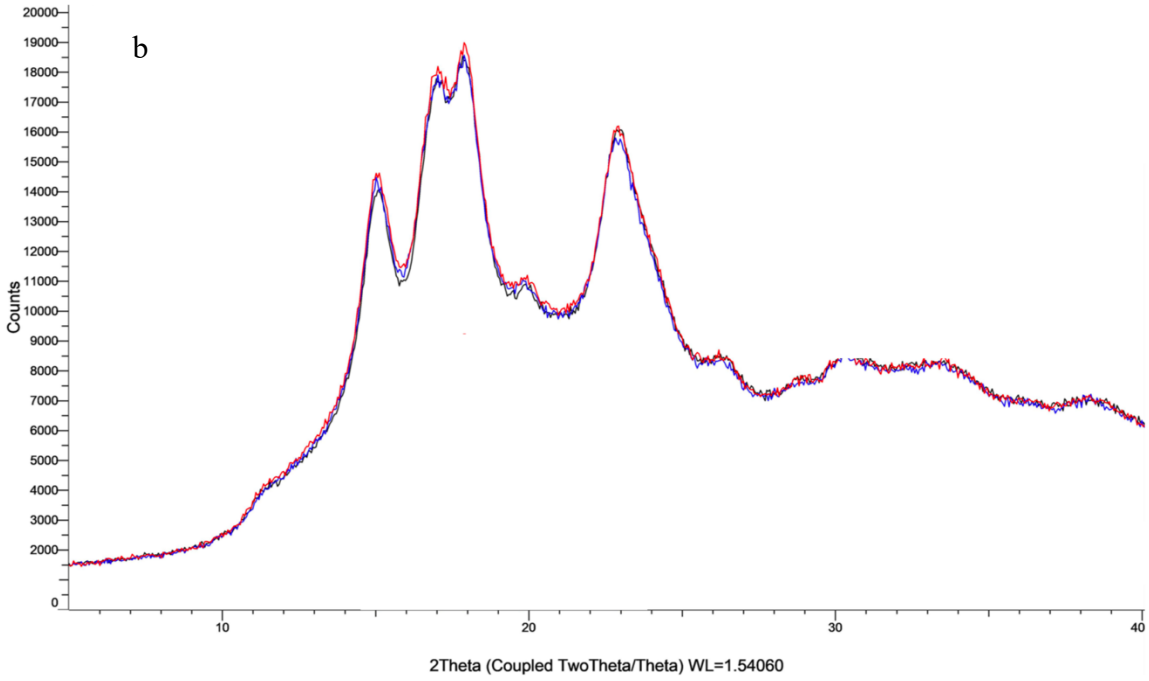
Counts
2Theta (Coupled TwoTheta/Theta) WL=1.54060

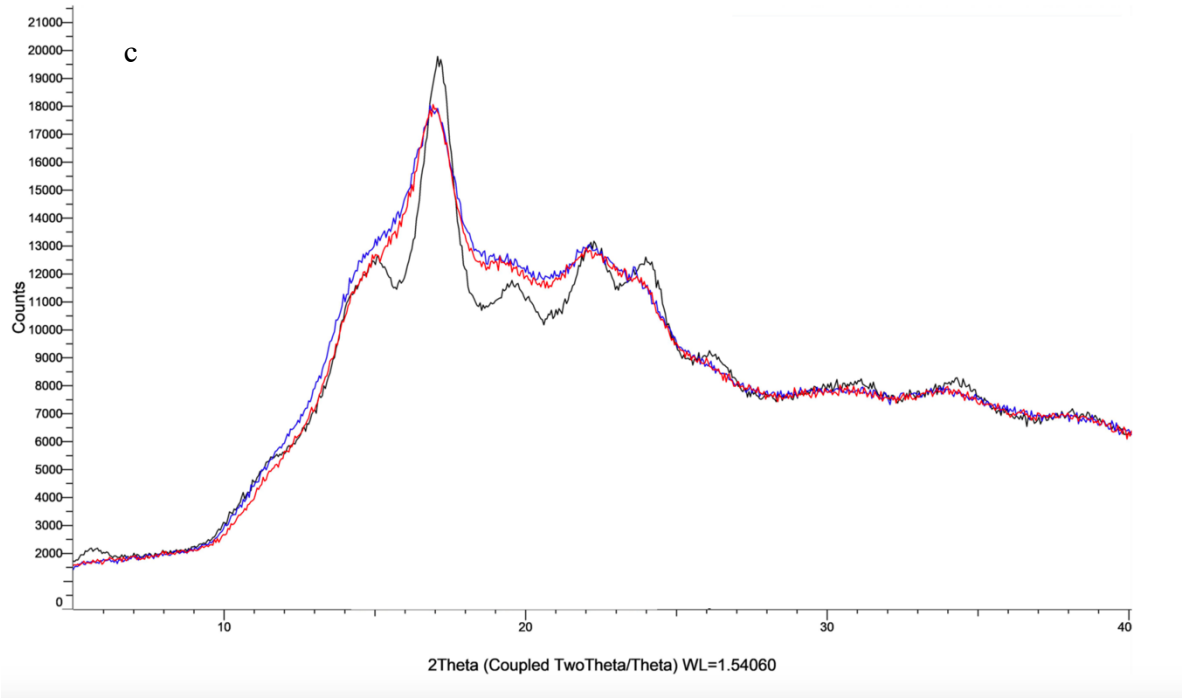

Figure 3-4: X-ray diffraction patterns for plasma treated and untreated waxy starch samples

Waxy maize starch samples (a), Waxy rice starch samples (b) , Waxy potato starch samples (c), [1] Color identification (Black = untreated starch samples, Blue =Gas treated samples, Red = Plasma treated samples).

3.4.6 Solid-state CP/MAS ^{13}C NMR

The solid-state CP/MAS ^{13}C NMR was used to understand the changes in molecular organization at shorter-distance scales (Table 3-4). Signal intensities obtained at C1 (90-110 ppm) and C4 (82-86 ppm) were integrated and the areas under each peak was calculated relative to the intensity at peaks C2, 3 and 5 (69-78 ppm). The A-type cereal starches are characterized by a twofold symmetry and results in three inequivalent residues per turn (Mihhalevski et al., 2012) which is confirmed by the distinct three peak pattern in the C1 region whilst the B-type potato starch has a threefold symmetry with respect to adjacent double helices resulting in two inequivalent residues per turn and is confirmed by

the two peak pattern in the C1 region (Gidley & Bociek, 1985). The areas of peaks around 96.4-97.7 ppm observed in all three starches are indicative of glucose units near α-(1,6)-glycoside linkages located within branched regions (Mihhalevski et al., 2012) and were seen to increase after plasma and gas treatment. Peaks at around 101.1 and 103 ppm are characteristic of V-type single helices (Tan et al., 2007) and increased in maize and rice after treatment but were hardly visible in potato. The absence of these peaks in potato is possibly due to its low lipid content in comparison to cereal starches (Singh et al., 2009) since starch lipid-complexes are known to form V-type single helices (Debet & Gidley, 2006). Peaks at 104.2 to 105.3 ppm, which were only present for potato, have been associated with the junction zones of the double helices in amylopectin and increases in their areas were noted after both gas and plasma treatment. The area of the intensities at C4 increased after plasma and gas treatment in maize and potato but decreased in rice. Tan et al. (2007) suggested that peaks in this area also reflect the presence of single helices. We suggest that peaks around 106-108 ppm, which were only visible in the cereal starches, might possibly be a result of cross-linked side chains, which then would explain the better stability shown by these starches in the pasting profile in comparison to potato starch. It is important to state that we did not detect V helices in our XRD diffractograms. Previous reports by (Gessler et al., 1999) have stated that the XRD is less sensitive to detect V helices because the segments of the amylopectin/amylose chain adopting the V-form are too short to be detected by XRD, which requires more helical turns to yield measurable diffraction intensities. Thus, as reported by Tan et al. (2007), NMR is more suited for detecting V-helices.

Table 3-4: Positions and areas of integrated peaks from solid-state CP/MAS 13C NMR of plasma treated and untreated waxy starch granules

Sample name	C1		C4	
	Peak (ppm)	Area (%)	Peak (ppm)	Area (%)
PTWMS	96.4	1.5	86.1	7.1
	101.6	14.6		
	108.2	8.3		
GTWMS	96.9	1.7	86.1	7.4
	102.6	12.8		
	107.7	8.6		
WMS	97.5	1.4	85.7	6.5
	101.5	10.1		
	107.5	5.7		
PTWRS	97.2	2.2	86.2	5.8
	101.8	13.4		
	107.2	8.8		
GTWRS	96.5	1.3	86.5	5.8
	101.1	11.3		
	106.7	11.3		
WRS	97.2	0.9	85.4	6.4
	101.1	9.6		

	107.1	7.4		
PTWPS	97.2	3.2	86.2	8.2
	104.5	21.3		
GTWPS	97.8	4.0	87.1	7.4
	105.3	19.5		
WPS	96.9	0.83	85.7	6.9
	104.2	6.5		

C1, carbon one NMR peak of starch; C4, carbon four NMR peak of starch; PTWMS: Plasma Treated Waxy Maize Starch, GTWMS: Gas Treated Waxy Maize Starch, WMS: Waxy Maize Starch, PTWRS: Plasma Treated Waxy Rice Starch, GTWRS: Gas Treated Waxy Rice Starch, WRS: Waxy Rice Starch, PTWPS: Plasma Treated Waxy Potato Starch, GTWPS: Gas Treated Waxy Potato Starch, WPS: Waxy Potato Starch.

3.4.7 Starch damage and resistant starch determination

The extent of starch damage in all three waxy starches (Table 3-5) ranged from 0.74-5.33% before plasma or gas treatment. The starch damage enhanced after 120 W of plasma treatment in potato (1.09 as compared to 0.74) and maize (2.33 as compared to 2.20) and after gas treatment in rice (5.56 as compared to 5.33). The level of starch damage directly affects the intake of water by starch granules (Gibson et al., 1992). Thus, an increase in damaged granules may result in a higher water absorption capacity of starch granules. Plasma treatment has been shown to cause structural damage to starch granules (Thirumdas, Trimukhe, et al., 2017b) due to the production of the highly energetic species, which bombards starch granules (Wang et al., 2012).

The RS values ranged from 0.12 to 44.31% for all three untreated waxy starches (Table 3-5). The highest RS portion was seen in potato, and this is because potato has a relatively higher concentration of phosphate groups in comparison to maize and rice. The presence of these phosphate groups makes waxy potato resistant to amylase digestion (Kanazawa et al., 2008). There were significant increases in the RS portion of all three waxy starches, with the exception of 120 W plasma treatment in rice starch. Increases in the RS portion may have been due to cross-linking induced by treatment with plasma. The highly energetic electrons produced after plasma treatment could have resulted in the excitation of argon and oxygen (Ar^*, O^*) and induce the polarization of O-H bonds of some hydroxyl groups. The energy transformed by Ar^* or O^* during collision would then result in the loss of OH groups from two different glucosyl units, causing them to cross-link by an ether linkage (starch-O-starch) (Zou et al., 2004)(Rombo et al., 2004) have reported that starches can become indigestible via the formation of ether linkages. Yeh and Yeh (1993) reported that α-amylases cannot digest cross-linked starches because this mechanism stabilizes starch granules. Interestingly, the simple treatment with carbon dioxide-argon gas increased the RS even more than plasma treatment and had also a strong effect on the rice starch. (Trinh, 2018) found similar increases in RS of both raw and cooked cassava starch after treatment with a dielectric barrier discharge plasma generated using argon gas. The author attributed these increases to the cross-linking induced by plasma treatment.

Table 3-5: Starch damage and resistant starch values of plasma treated and untreated waxy starch samples

Sample	% Starch damage	% Resistant Starch
PTWMS	2.33[b]	1.21[b]
GTWMS	2.19[a]	1.73[c]
WMS	2.20[a]	0.84[a]
PTWRS	5.43[ab]	0.18[a]
GTWRS	5.56[b]	1.33[b]
WRS	5.33[a]	0.12[a]
PTWPS	1.09[c]	66.48[b]
GTWPS	0.78[b]	69.18[c]
WPS	0.74[a]	44.31[a]

[a] Means with different superscript letters show significant differences (p-value < 0.05) between treated and untreated waxy starches of the same type; PTWMS: Plasma Treated Waxy Maize Starch, GTWMS: Gas Treated Waxy Maize Starch, WMS: Waxy Maize Starch, PTWRS: Plasma Treated Waxy Rice Starch, GTWRS: Gas Treated Waxy Rice Starch, WRS: Waxy Rice Starch**,** PTWPS: Plasma Treated Waxy Potato Starch, GTWPS: Gas Treated Waxy Potato Starch, WPS: Waxy Potato Starch.

3.5 Conclusion

Carbon dioxide-argon radio frequency cold plasma enhanced the ability of all three waxy starches to withstand retrogradation as shown by the lower setback and final viscosities, a characteristic that can be utilized to prevent staling in bread. Higher enthalpies were observed after DSC analysis in all three starches. There was a decrease in crystallinity in waxy potato, but not rice and maize, as shown by WAXS. The NMR results showed the possible formation of V-type single helices as indicated by increases in peak areas at 101.1

and 103 ppm in the cereal starches. Significant increases seen in the resistant starch portion in potato and maize after plasma treatment and after gas treatment in rice was desirable for human health. Cereal and tuber starches can be effectively modified by RF cold plasma and could serve as replacement for chemical methods of modification in industry. The extent of modification is however dependent on the botanical source as plasma and gas treatment affect starches from different botanical sources differently.

3.6 Funding

This research did not receive any specific grant from funding agencies in the public, commercial, or non-profit sectors.

3.7 Acknowledgements

We appreciate the help given by Dr. Gopinath Tata at the Minnesota NMR Center, Dr. Gail Celio at the University of Minnesota imaging center as well as Gabrielle Seliber at the college of biological sciences.

3.8 Conflict of interest

The authors declare no conflict of interest

Chapter 4: Structural characterization and enzymatic hydrolysis of radio frequency cold plasma treated starches

Contents for this chapter have been published in Journal of Food Science, Food Chemistry section (Okyere et al., 2022) (https://doi.org/10.1111/1750-3841.16037) and are being reproduced here with permission from the editor (Copyright © Wiley).

4.1 Overview

The effect of carbon dioxide-argon radio frequency cold plasma treatment on the *in vitro* digestion and structural characteristics of granular and non-granular waxy maize, potato, and rice starches was investigated in this study. The effect on the fine structure of waxy potato was very minimal after plasma treatment irrespective of their granular or non-granular form. The short chain length (SCL) of waxy maize and rice (granular and non-granular) starches was reduced leading to subsequent increases in the long chain length (LCL). *In vitro* digestibility studies showed that cold plasma treatment enhanced ($p < 0.05$) the amount of slowly digestible starches (5.62%; 10.24%) and resistant starches (0.28%; 85.66%) in non-granular waxy maize (WMS NG) and granular waxy potato starches (WPS G) respectively. The amount of rapidly digestible starches increased in granular waxy maize starch (WMS G) (85.08%) but was unaffected in non-granular waxy rice (WRS NG), WPS G and non-granular waxy potato starches after plasma treatment. FTIR-ATR data confirmed the ability of cold plasma to induce cross-linking in waxy starches specifically in WMS NG, WRS G, WRS NG and WPS G. Overall, the unit and internal chain structure of the waxy starches were mostly unaffected by radio frequency plasma treatment. Cross-linking served as the dominant mechanism by which plasma altered the structure and digestibility of these starches.

Keywords: radio frequency cold plasma, cross-linking, granular and non-granular waxy starches, resistant starches

4.2 Practical Application

Cold plasma technology has been suggested as a green technique for starch modification. More research is however needed to facilitate the industrial scale up of this technology. In this study, we utilized a carbon dioxide-argon radio frequency cold plasma to modify waxy maize, rice, and potato starches. Cold plasma treatment resulted in starches that were resistant to digestion and were highly cross-linked. The cross-linking would give the starches the ability to possibly withstand the high temperatures and shear that can be applied during industrial processing.

4.3 Introduction

Starch is a biopolymer synthesized in the granular form irrespective of whether it is waxy, high amylose or normal starch. It is made up of two major polysaccharides: amylose and amylopectin. Amylose is mostly a linear polysaccharide with chains made of α-(1-4)-D-glucosyl units. Amylopectin (waxy starch) on the other hand, is an extensively branched starch polymer with linear chains of α-(1-4)-D-glucosyl units interconnected with α-(1-6)-branches (Hizukuri et al., 1981); (Hizukuri et al., 1983).

Amylopectin is further classified into short chains and long chains with a degree of polymerization (DP) < 36 and > 36, respectively (Hizukuri, 1986). The short chains form double helices, which make up the crystalline lamellae in starch granules (Imberty et al., 1991). The crystallites formed by the double helices can be characterized by X-ray diffraction as A-type (tightly packed double helices with fewer water molecules) or B-type (less tightly packed double helices with more water molecules) (Imberty et al., 1991). In some instances, for example, in peas and legumes, a mixed pattern called C-type is observed (Buléon et al., 1998). The long chains form the backbone on which the short chains are anchored (Bertoft, 2017). Furthermore, the chains of amylopectin can also be classified as external and internal. The external chains extend from the outermost branch of a chain to its non-reducing end, while the internal chains are the chain segments between the branches (Manners, 1989). The chains of amylopectin were initially grouped into unsubstituted A-chains, substituted B-chains, and the single C-chain to which the sole reducing end group is attached (Peat et al., 1952). All A-chains are external chains while the B-chains have one external segment, and the remaining segments are internal (Manners, 1989). The unit and internal chain profile of amylopectin can be analyzed by hydrolyzing

the α-(1-6)-branches with the debranching enzymes isoamylase and pullulanase (Pérez & Bertoft, 2010). Analysis of amylopectin internal chains requires removal of the external chain segments with β-amylase prior to debranching with isoamylase and pullulanase. β-Amylase reduces all A-chains into maltose and maltotriose and the external segments of the B-chains into glucose and maltose producing the β-limit dextrin (Bertoft, 1989).

Starch has a variety of applications in both food and non-food industries. It can be utilized as a flavor encapsulating agent in brewing industries (Mason, 2009), and as an adhesive for the manufacture of corrugated paper boards (Glittenberg, 2012). However, native starch is unreactive and insoluble limiting its use in industry. Starch needs to be modified to enhance its solubility, textural properties, and heat tolerance for diverse processing applications (Laovachirasuwan et al., 2010). In addition, modifying starches can potentially decrease the rate of digestion and slow down the release of glucose into the bloodstream which helps in the control of type 2 diabetes (Frost & Dornhorst, 2000; Gao et al., 2019).

Starch can be modified using physical, chemical, and enzymatic means. Physical methods can be thermal or non-thermal and include methods such as annealing, heat moisture treatment, pulsed electric field and cold plasma. Chemical and enzymatic methods include etherification and α-amylase hydrolysis, respectively (Bemiller, 1997; Chen et al., 2018; Zia-ud-Din et al., 2017). Gelatinization of starches is also one method of altering the physical form of starch to obtain non-granular starch (Ratnayake & Jackson, 2006). When starches are heated in water above 60°C (gelatinized), several structural changes take place which include the loss of birefringence, native crystallite melting, granules swell several times their initial size, and starch solubilization (Jane et al., 1999; Tester & Morrison,

1990). Freeze dried non-granular starches have higher water binding capacity and solubility compared to granular starches (Puspitowati & Driscoll, 2007; Krystyjan et al., 2017). Another relatively novel method of starch modification is plasma technology. In plasma technology, either thermal or non-thermal plasmas can be generated. Plasma is generated when energy (thermal, electrical, magnetic, radio or microwave frequencies) is applied to a gas (air, carbon dioxide, oxygen, argon, nitrogen, helium), resulting in the formation of several reactive species (electrons, ions, free radicals) (Conrads & Schmidt, 2000). Thermal plasmas are generated at high temperatures and pressures and involve a high power input. Contrarily, non-thermal plasmas (cold plasma) require lower pressures and temperatures with less power input (Moreau et al., 2008). Cold plasma is an eco-friendly non-thermal process devoid of chemical waste generation. Cold plasma unlike thermal plasmas is suitable for modifying thermally sensitive biopolymers such as starch (Thirumdas, Kadam, et al., 2017a).

Studies have been published on the molecular and structural changes of starch after cold plasma modification to enhance the industrial scale up of this green technology. This is because the molecular weight size of starches is important for its end user applications. Starches (maltodextrins) with lower degree of polymerization are utilized in gluten free breads to increase baked volume (Casper & Atwell, 2014). Also starches with high molecular weight and amylose content produce thermoplastic films with high tensile strength (Lopez-Rubio et al., 2008).

In regard to the effect of cold plasma treatment on the molecular properties of starches, Bie, Pu, et al. (2016) reported a decrease in the weight-average molecular weight of corn starch (19.34×10^6 to 0.98×10^6 g/mol) after a 10 min dielectric barrier discharge

(DBD) air plasma treatment. Oxygen glow plasma treatment (60 min) was shown to decrease the weight-average molecular weight of potato starch from 4.270×10^7 to 4.716×10^6 g/mol (Zhang et al., 2014). However, Zhang et al. (2015) reported an increase in the weight-average molecular weight of potato starch from 6.11×10^7 to 10.42×10^7 g/mol after nitrogen and helium glow plasma treatment for 60 min. Gao et al. (2019) reported an increase in the number of short chains after DBD plasma treatment in tartary buckwheat starch, sorghum starch, quinoa starch and wheat starch. Nonetheless, to the best of our knowledge, there is scarcity of information on the effect of radio frequency cold plasma on the unit and internal chain structure of amylopectin. Understanding the effect of cold plasma technology on the unit and internal structure of amylopectin is important since studies have shown that it influences the functional and thermal properties of starches (Bertoft et al., 2016; Han & Hamaker, 2001; Jane & Chen 1992; Kohyama et al., 2004). In this present study, the effect of carbon dioxide-argon radio frequency cold plasma on the unit and internal chain structure of granular and non-granular waxy starches is reported. FTIR-ATR was utilized to characterize the functional structures of the modified starch. The effect of plasma on i*n vitro* starch digestibility was investigated as well. It is important to point out that the physical structure and functional properties of the granular starches were analyzed previously, and plasma was shown to effectively modify the granular starches (Okyere et al., 2019). We are following up that work with an analysis of the fine structure of both granular and non-granular starches to fully understand the effect of plasma treatment on starches. It is our hypothesis that the carbon dioxide-argon radio frequency

cold plasma will alter the unit and internal chain structure and *in vitro* digestibility of waxy starches irrespective of whether they are treated as granular or non-granular starches.

4.4 Materials and Methods

4.4.1 Materials

The waxy rice starch used for the experiment was obtained from Remy Industries (Leuven, Belgium). Waxy maize and potato starches were purchased from Ingredion Incorporated (Bridgewater, NJ, USA). CO_2 and Ar gases were obtained from Matheson (Eagan, MN, USA). The following enzymes were purchased from Neogen Megazyme (Lansing, Michigan, USA): *Pseudomonas* sp. isoamylase (EC 3.2.1.68; specific activity 240 U/mg), *Klebsiella planticola* pullulanase (EC 3.2.1.41; specific activity 30 U/mg), barley β-amylase (EC 3.2.1.2; specific activity 435 U/mg); pancreatic α-amylase (EC 3.2.1.1; specific activity 75 U/mg) and amyloglucosidase (EC 3.2.1.3; specific activity 36 U/mg). All chemicals used in the experiments were of analytical grade.

4.2.1 Preparation of non-granular waxy starches

Waxy starches (15 g) were suspended in 100 mL of double-distilled water in a stainless-steel bowl. The starch slurry was heated from 30°C to 95°C and held at 95°C for ca. 5 min using the Micro Visco Amylograph (MVAG) (Brabender® GmbH & Co KG, Duisburg, Germany) operated at 250 rpm with a heating rate of 3°C/min. The samples were transferred immediately into 50 mL falcon tubes and frozen at -20°C. The non-granular waxy starches (solubilized starches) were then lyophilized and crushed into a powder with a mortar and pestle.

4.4.2 Plasma apparatus and treatment

Treatment of granular and non-granular waxy starches in the radio frequency (RF) plasma unit was based on methods previously reported by Okyere et al. (2019) with some modifications. Briefly granular and non-granular waxy starches were treated in the RF (13.56 MHz) plasma unit (Plasma Etch Industries, Carson City, Nevada, USA) connected to a vacuum pump and chilling unit. CO_2 and Ar gases were supplied for plasma generation each at a flow rate of 25 and 10 standard cubic centimeters per minute (sccm), respectively. An RF power of 120 W was supplied to the sample to enhance dissociation of CO_2 into carbon monoxide and oxygen in the RF plasma unit based on methods previously reported by Spencer & Gallimore, (2011). Untreated waxy starches (granular and non-granular) were used as control samples. Approximately 15 g of starch was spread evenly on a glass petri dish and placed inside the plasma chamber based on methods previously described by Thirumdas, Trimukhe, et al. (2017b). Once the vacuum setpoint of 0.6 cubic feet per minute was reached, treatment of the starches was done for 30 min, stirred, and retreated for another 30 min. The vacuum setpoint was chosen based on recommendations of the manufacturer of the plasma unit. All treated samples were stored in snap cap vials and kept in a desiccator at room temperature until further analysis.

4.4.3 Production of β-limit dextrins for internal chain profile analysis

Approximately 100 mg of plasma treated, and untreated waxy starches (granular and non-granular) were dissolved in 3 mL of 90% dimethylsulphoxide by stirring in a boiling water bath for 10 min, after which the samples were left to stir overnight at room temperature. The samples were diluted with 32.7 mL (~70°C) warm water before the addition of 0.33 volumes of 0.01 M sodium acetate buffer, pH 6.0, and a volume of β-

amylase corresponding to 4 U/mg of the substrate was added and left to stir overnight. The mixture was inactivated by boiling for 5 min and filtered using a tangential filtration system (Pall Corporation, NY, USA). The β-limit dextrins were frozen and lyophilized for further analysis (Bertoft, 2004).

4.4.4 Analysis of unit chain distributions of granular and non-granular waxy starches and their β-limit dextrins

Waxy starches or their β-limit dextrins (2.0 mg) were dissolved in 50 μL of 90% DMSO and stirred gently overnight at room temperature. The solution was diluted with warm water (400 μL, ~80°C), followed by the addition of 50 μL of 0.01 M sodium acetate buffer, pH 5.5. Isoamylase (1 μL) and pullulanase M1 (1 μL) corresponding to 0.5 U and 0.65 U, respectively, were added to the mixture and stirred gently overnight at room temperature. After debranching, the enzymes were inactivated by boiling for ca. 5 min. The volume of the mixture was adjusted to obtain a final concentration of 1 mg/mL and filtered through a 0.45 μm nylon filter into 2 mL vials. The filtered samples (25 μL) were analyzed with the DIONEX ICS-5000^{+} HPAEC system (Dionex Corporation, Sunnyvale, CA, USA) equipped with a pulsed amperometric detector, CarboPac PA-100 ion-exchange column (4 × 250 mm), and a similar guard column (4 × 50 mm). The samples were then eluted with a flow rate of 1 mL/min. The two eluents used were 150 mM sodium hydroxide (A) and 150 mM sodium hydroxide containing 500 mM sodium acetate (B). An elution gradient was made by mixing eluent B into eluent A as follows: 0–9 min, 15–36% B; 9–18 min, 36–45% B; 18–110 min, 45–100% B; 100–112 min, 100–15% B; and 112–130 min, 15% B. The system was stabilized by elution at 15% B for 60 min between runs

(Annor et al., 2014a). The areas under the chromatograms were corrected to carbohydrate concentration following the method of Koch et al. (1998).

4.4.5 In vitro digestion analysis of starch

The *in vitro* digestibility of the waxy starches (granular and non-granular) was measured using the modified Englyst et al. (1992) method using the kit provided by Neogen Megazyme (Lansing, Michigan, USA). The amount of rapidly digestible starch (RDS), slowly digestible starch (SDS), total digestible starch (TDS), and resistant starch (RS) were obtained after incubation of the starches with a purified mixture of pancreatic α-amylase and amyloglucosidase enzymes. The amount of RDS was measured at 20 min while that of SDS was measured at 120 min. TDS refers to the starch that was hydrolyzed within the 4 h incubation period while RS refers to the unhydrolyzed fraction of the starch after 4 h of incubation with the enzyme. The *in vitro* starch digestibility results were expressed on a dry weight basis.

4.4.6 Fourier transform infrared spectroscopy-attenuated total reflectance measurement (FTIR-ATR)

The Attenuated Total Reflection (ATR) measurements was done using a Nicolet iS50 FTIR (Thermo Fisher Scientific, MN, USA) equipped with a Deuterated Triglycine Sulfate Attenuated Total Reflection (DGTS ATR) detector by spreading a thin layer of starch onto the diamond crystal and applying pressure using the pressure tower. A total of 64 scans were recorded with a spectral resolution of 4 cm^{-1} within a spectral range of 4000 to 650 cm^{-1}. The Spectra was collected using the OMNIC software. All the samples were recorded against a background spectrum (which is a spectrum without a starch sample in place). The spectra were baseline corrected and normalized using the Min/Max method

(Pu et al., 2011) after which the intensities of the bands at 930 and 1150 cm^{-1} were computed using the OPUS 7.0 software.

4.4.7 Cross polarized light microscopy

A thin layer of granular and non-granular waxy starch suspended in water was viewed under the Olympus BX40 light microscope (Melville, NY, USA) connected to a digital camera (Olympus DP26) and a monitor (Dell Precision T3600; Texas, USA). The images were acquired with Olympus CellSens Dimension Software (Melville, NY, USA) by using a polarized light filter (Goldstein et al., 2017).

4.4.8 Statistical analysis

All results were statistically analyzed by one-way ANOVA with Statgraphics Centurion XVI, version 16.1.0 (Stat Point, Warrenton, VA, U.S.A.). Duncan's multiple range test was used to determine statistical significance between means at a p-value of < 0.05.

4.5 Results and Discussion

4.5.1 Polarized light microscopy

Normal light waves typically vibrate in all directions. However, light can be made to vibrate in a single plane by using a polarized light filter (McMahon, 2004). When native granular starch is viewed under polarized light microscopy a ‘Maltese cross’ structure is typically observed (Figure 4-1) (French, 1972). This ‘Maltese cross’ structure shows radial organization and suggest a high degree of order inside the native starch granules, which represents the crystalline part of the granules (Bertoft, 2017). We observed no ‘Maltese cross’ structures in the non-granular waxy starches prior to plasma treatment showing that the crystalline domains had been converted to amorphous starches after cooking in the Micro Visco Amylograph.

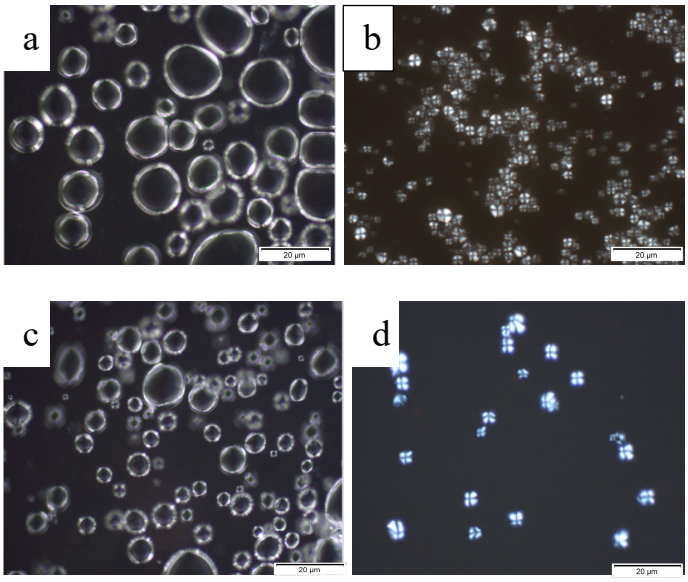

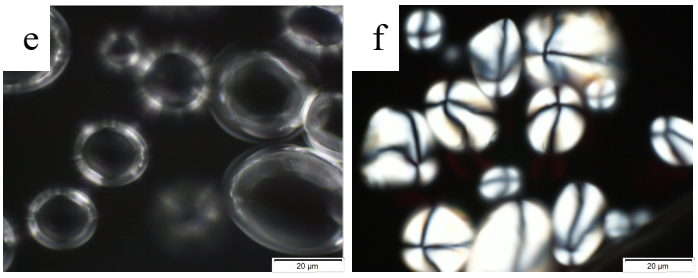

Figure 4-1: Polarized light microscopy images of granular and non-granular waxy starch samples

Non-granular waxy maize starch (a), granular waxy maize starch (b), non- granular waxy rice starch (c), granular waxy rice starch (d), non-granular waxy potato starch (e), granular waxy potato starch (f).

4.5.2 Chain length profiles

The unit chain length profiles of plasma treated, and untreated granular and non-granular starches are presented in Figure 2. Chains longer than DP 55 were not resolved as peaks, hence, the chains from DP > 55 were estimated by continuously dividing the chromatograms into equal areas for each chain length (Bertoft, 2004). The results seem to suggest that plasma treatment affected the unit chain length profiles of the non-granular starches (Figure 4-2a-c) more than the granular starches (Figure 4-2d-f) although this was not significant. This is because the non-granular starches are disordered during pasting (Tester & Morrison, 1990) and highly porous after freeze drying (Puspitowati & Driscoll, 2007). Hence it is easier for the reactive species in plasma to penetrate and alter the unit chain length profiles in comparison to the granular starches (Thirumdas, Kadam, et al., 2017a). The peak DP of the short chains was at DP 14 for both treated and untreated waxy maize starches (Figure 4-2a,d). In addition, the relative carbohydrate concentration (weight

%) at the peak DP 14 reduced after plasma treatment in both the non-granular and granular waxy maize starches (Figure 4-2a,d). Subsequently, we observed an increase in the carbohydrate concentration of the long chains from DP ≥ 64 in PTWMS NG and DP ≥ 130 in PTWMS G albeit not significant. Similarly, plasma treatment resulted in a reduction in the carbohydrate concentration of the peak DP 12 of non-granular and granular waxy rice starch (Figure 4-2b,e). This led to the increase in the carbohydrate concentration of long chains from DP ≥ 62 in PTWRS NG and DP ≥ 80 in PTWRS G. The profiles suggested that plasma treatment resulted in polymerization of the long chains which explains the decreases observed in the carbohydrate concentration at the peak DP of the short chains (Zou et al., 2004). Plasma treatment had hardly any detectable effect on the unit chain composition of neither non-granular nor granular WPS (Figure 4-2c,f).

In general, the internal chain length profiles of the treated and untreated waxy starches had two sub-groups of short B-chains, which is characteristic of starches from different botanical sources (Bertoft et al., 2008) (Figure 4-3a-f). The minor group, typically referred to as the "fingerprint" B-chains (B_{fp}), has a DP ranging from 4-7 when measured in amylopectin β-limit dextrins (Bertoft, 2004). The remaining short B-chains, referred to as BS_{major}, possessed a peak at DP 11 for all the cereal and tuber starches. The long B-chains had peak DPs between 34 and 36 for both plasma treated and untreated waxy starches. Figure 4-3a-f indicates that the internal chain profiles of all the waxy starches were minimally influenced by plasma treatment. However, the internal chain profile of the long B-chains of WPS NG was slightly higher after plasma treatment, which gives an indication of plasma inducing polymerization of the chains.

We reported previously in Okyere et al. (2019), the possibility of longer internal chain segments reacting with iodine resulting in increased peak values (λ_{max}) observed in plasma treated granular waxy potato starch (PTWPS G) and plasma treated granular waxy rice starch (PTWRS G). In this present study, we observed a slight increase, albeit not significant, in the internal chain length (ICL) of PTWPS G and PTWRS G (Table B1), which could react with the iodine and thus increase the peak values as stated previously. The data for the average chain lengths and relative molar amounts of the different chain categories are presented in the appendices (Table B1 and B2). We observed no significant differences in these parameters.

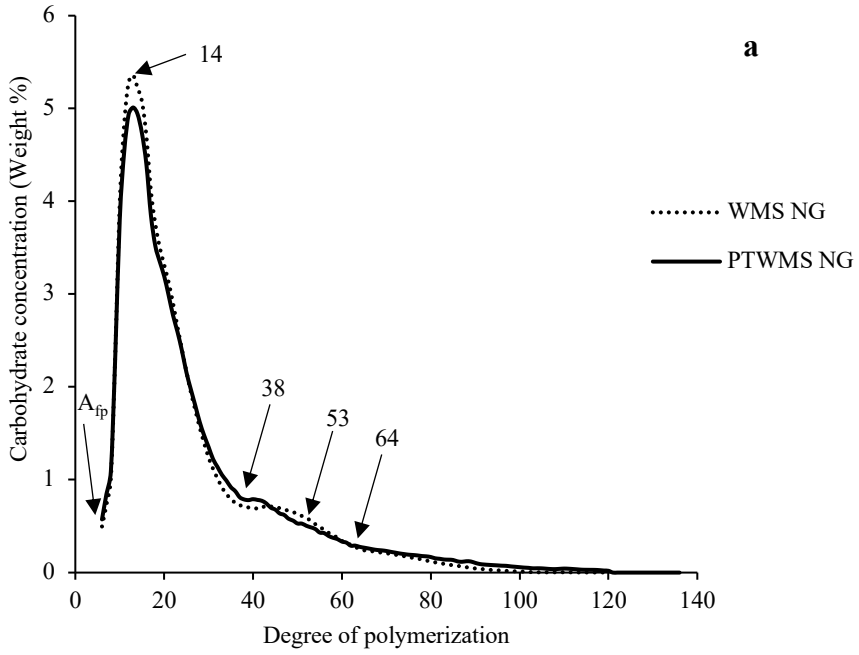

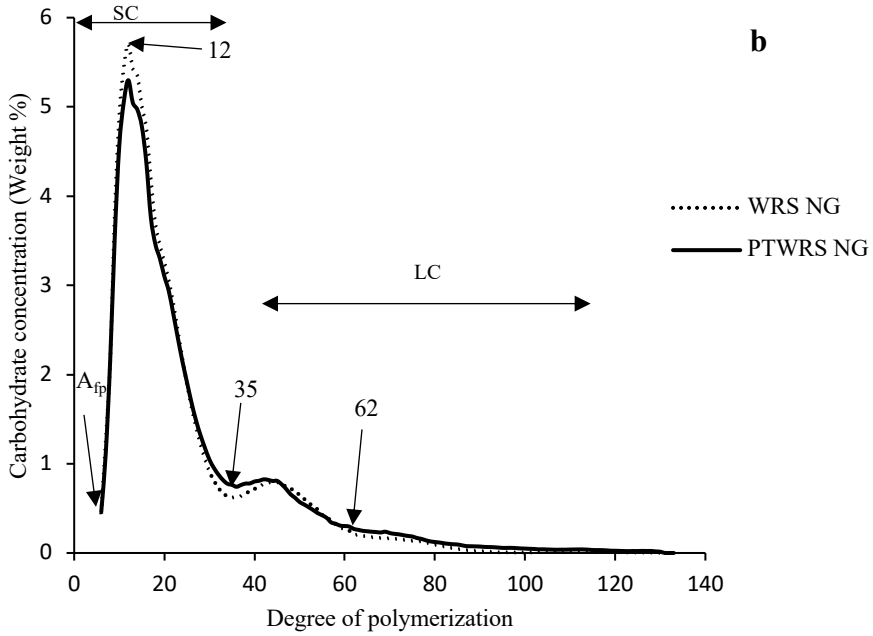
b
SC
12
LC
35
62
A_{fp}
WRS NG
PTWRS NG
Carbohydrate concentration (Weight %)
Degree of polymerization
0
1
2
3
4
5
6
0
20
40
60
80
100
120
140

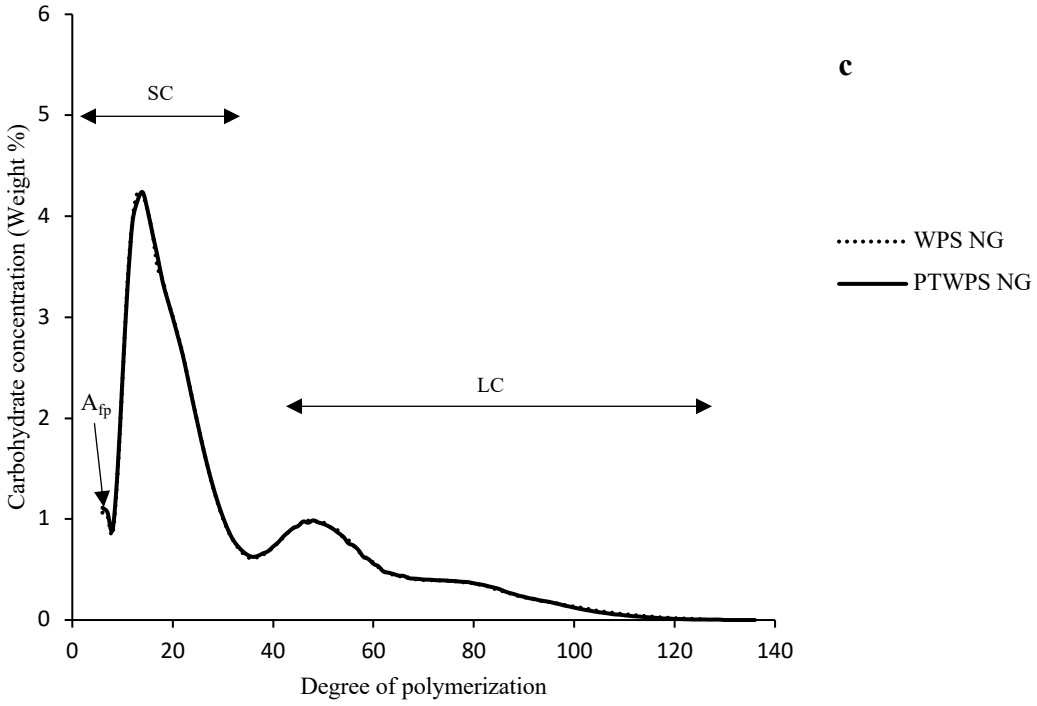
c
SC
LC
A_{fp}
WPS NG
PTWPS NG
Carbohydrate concentration (Weight %)
Degree of polymerization
0
1
2
3
4
5
6
0
20
40
60
80
100
120
140

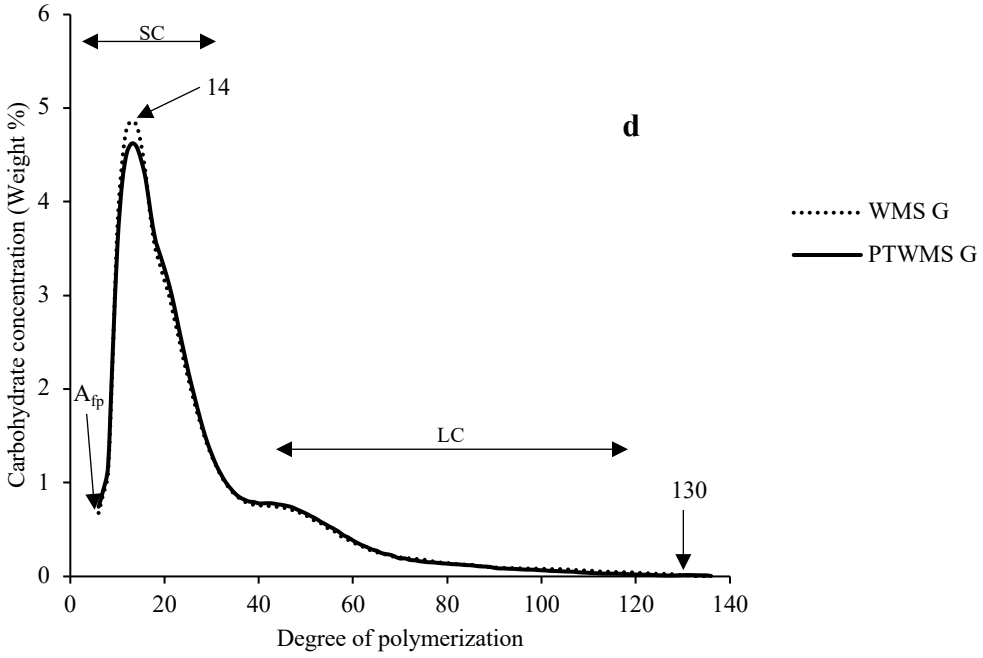
SC
14
d
WMS G
PTWMS G
Carbohydrate concentration (Weight %)
A_{fp}
LC
130
Degree of polymerization

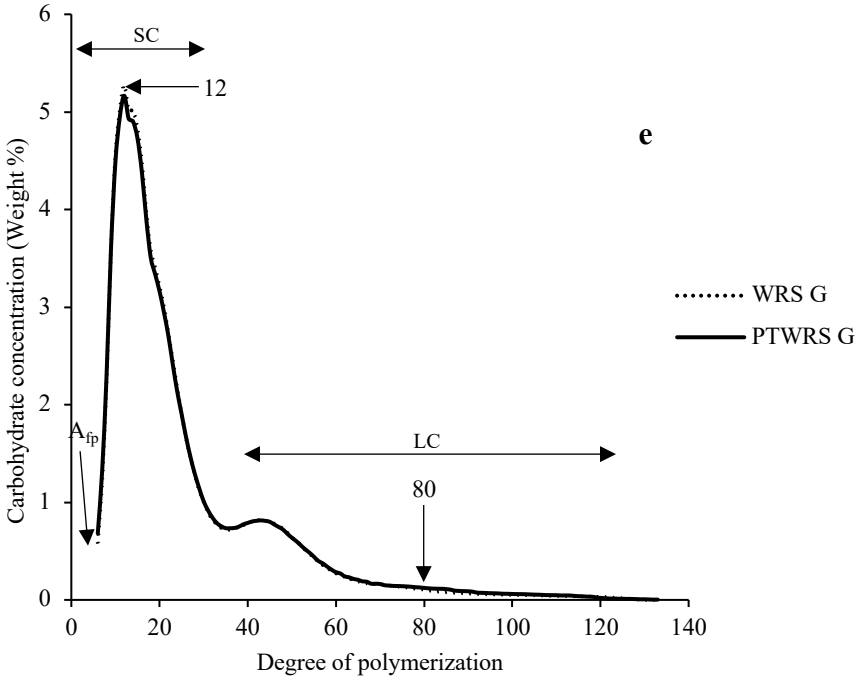
SC
12
e
WRS G
PTWRS G
Carbohydrate concentration (Weight %)
A_{fp}
LC
80
Degree of polymerization

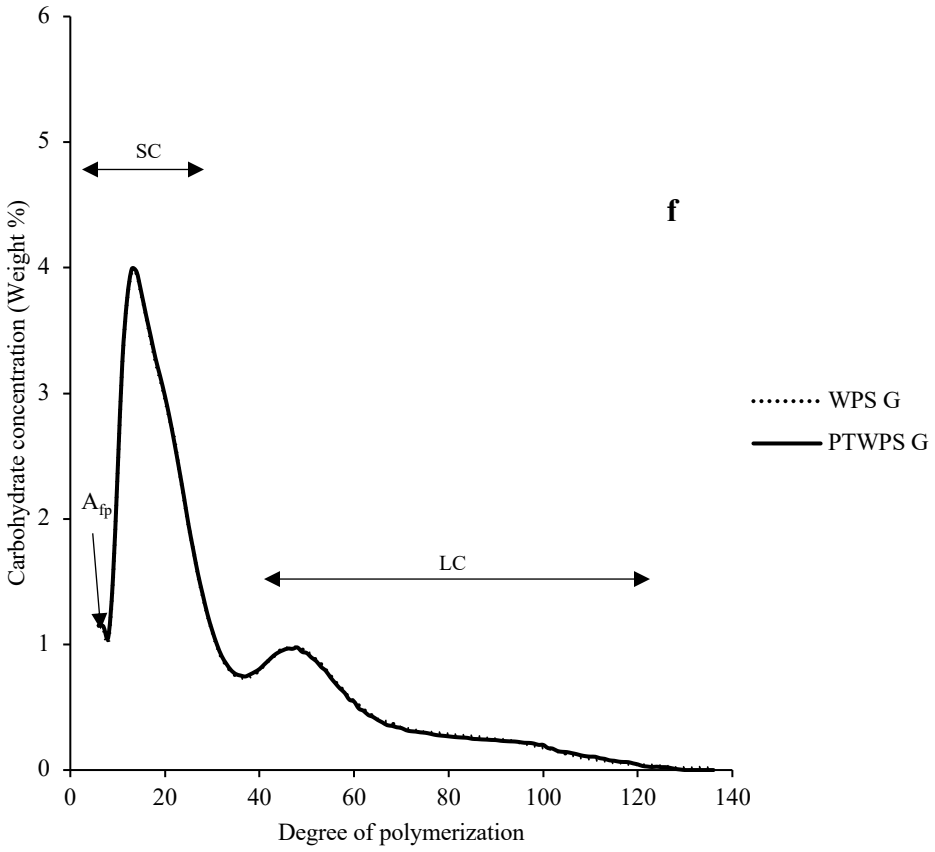

Figure 4-2: The unit chain profiles of debranched granular and non-granular waxy starches

Arrows indicate degree of polymerization. a = WMS NG: Waxy Maize Starch Non-Granular, PTWMS NG: Plasma Treated Waxy Maize Starch Non-Granular; b = WRS NG: Waxy Rice Starch Non-Granular, PTWRS NG: Plasma Treated Waxy Rice Starch Non-Granular; c = WPS NG: Waxy Potato Starch Non-Granular, PTWPS NG: Plasma Treated Waxy Potato Starch Non-Granular; d =WMS G: Waxy Maize Starch Granular, PTWMS G: Plasma Treated Waxy Maize Starch Granular; e = WRS G: Waxy Rice Starch Granular , PTWRS G: Plasma Treated Waxy Rice Starch Granular; f = WPS G: Waxy Potato Starch Granular, PTWPS G: Plasma Treated Waxy Potato Starch Granular. SC = Short Chains, LC = Long Chains; A_{fp} = "fingerprint" A-chains

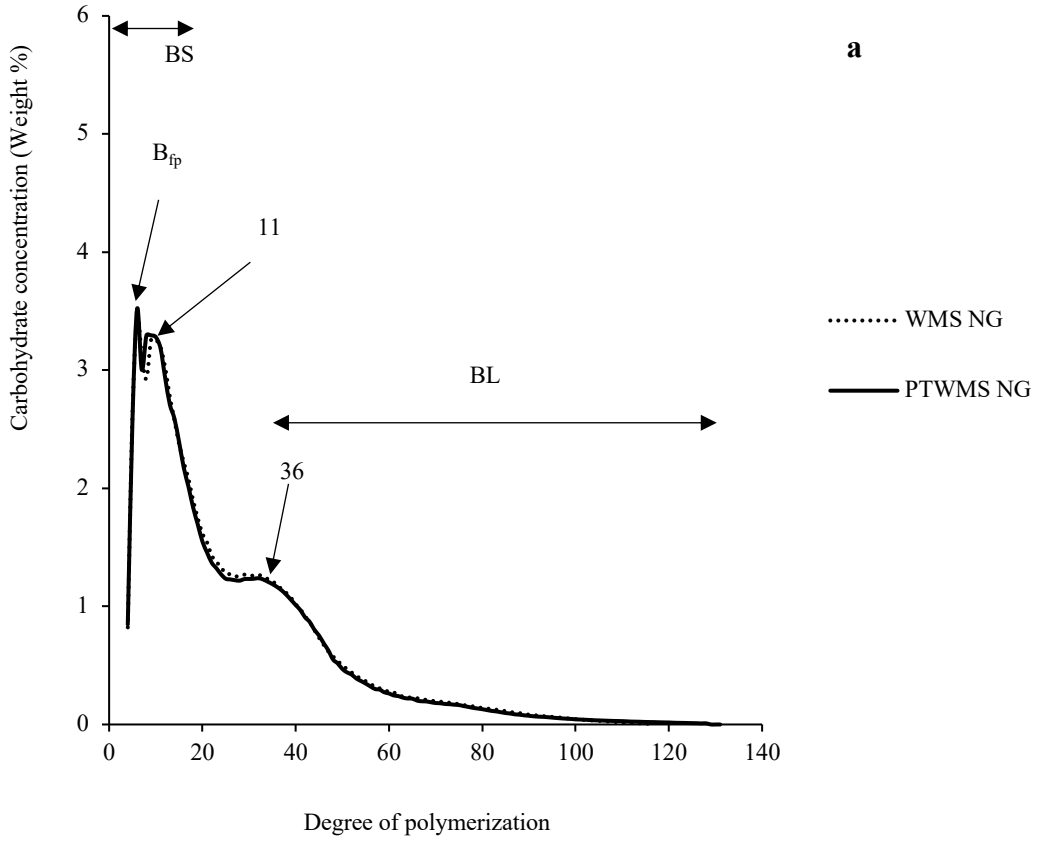
a
BS
B_{fp}
11
BL
36
WMS NG
PTWMS NG
Carbohydrate concentration (Weight %)
Degree of polymerization
0
1
2
3
4
5
6
0
20
40
60
80
100
120
140

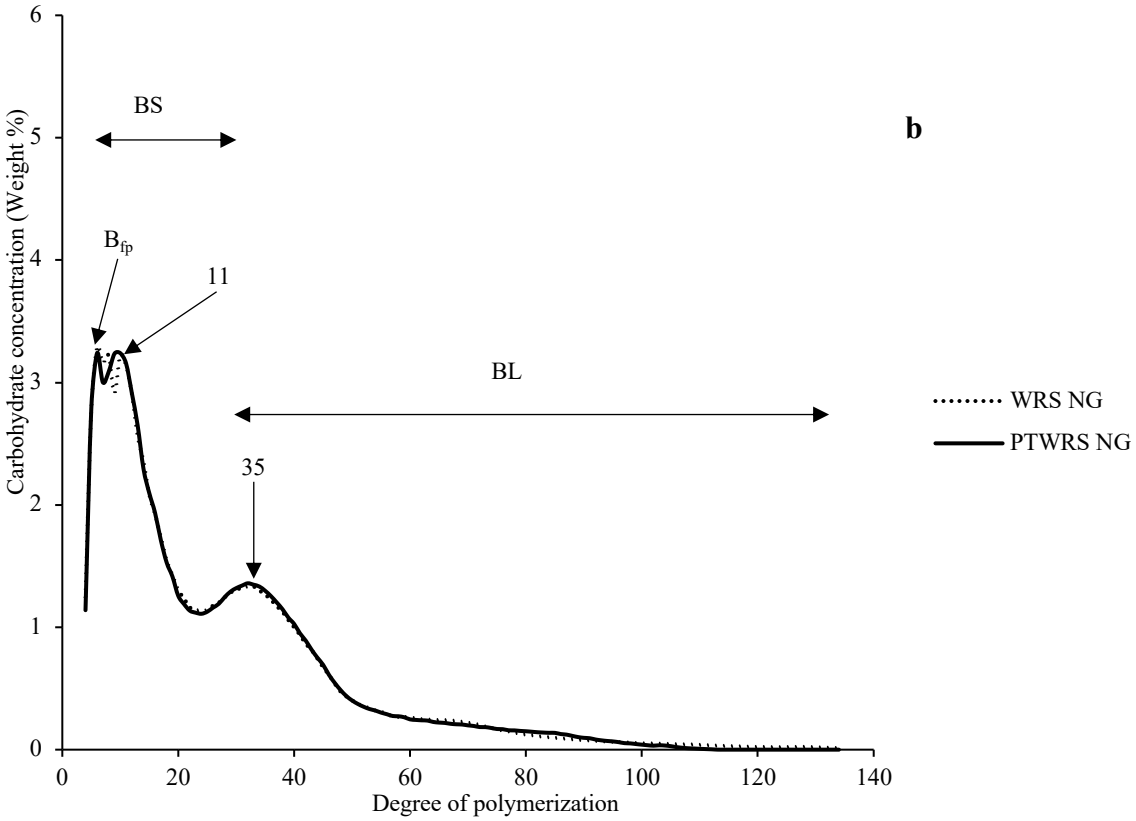
b
BS
BL
B_{fp}
11
35
Carbohydrate concentration (Weight %)
Degree of polymerization
WRS NG
PTWRS NG
0
1
2
3
4
5
6
0
20
40
60
80
100
120
140

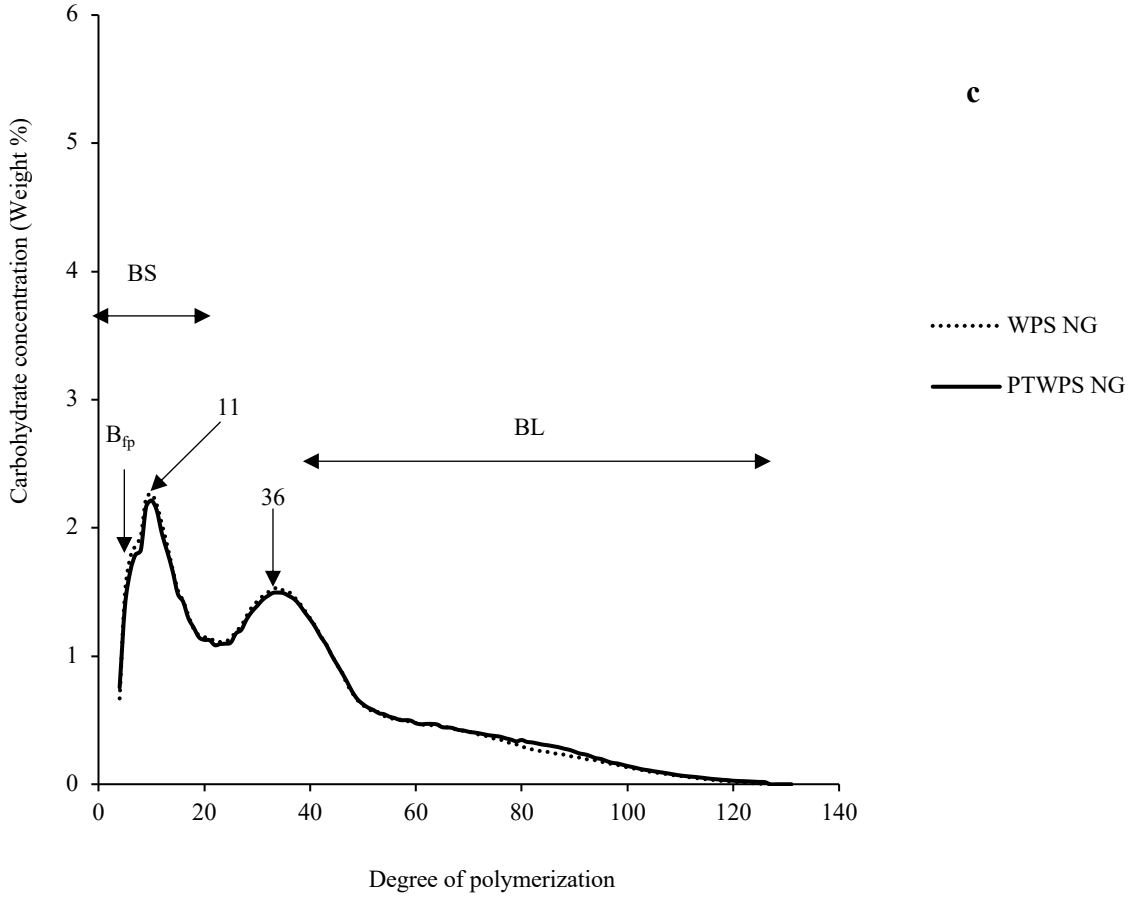
c
Carbohydrate concentration (Weight %)
Degree of polymerization
BS
BL
B_{fp}
11
36
WPS NG
PTWPS NG
0
1
2
3
4
5
6
0
20
40
60
80
100
120
140

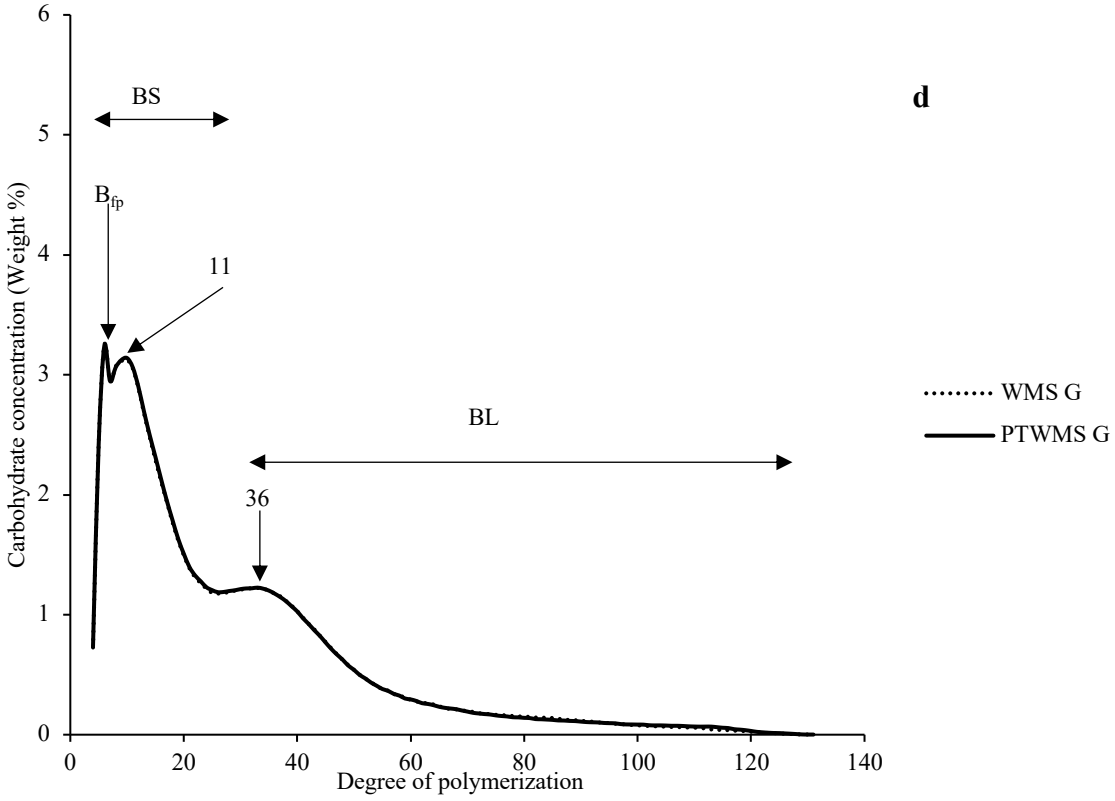
d
BS
B_{fp}
11
BL
36
Carbohydrate concentration (Weight %)
Degree of polymerization
WMS G
PTWMS G
0
1
2
3
4
5
6
0
20
40
60
80
100
120
140

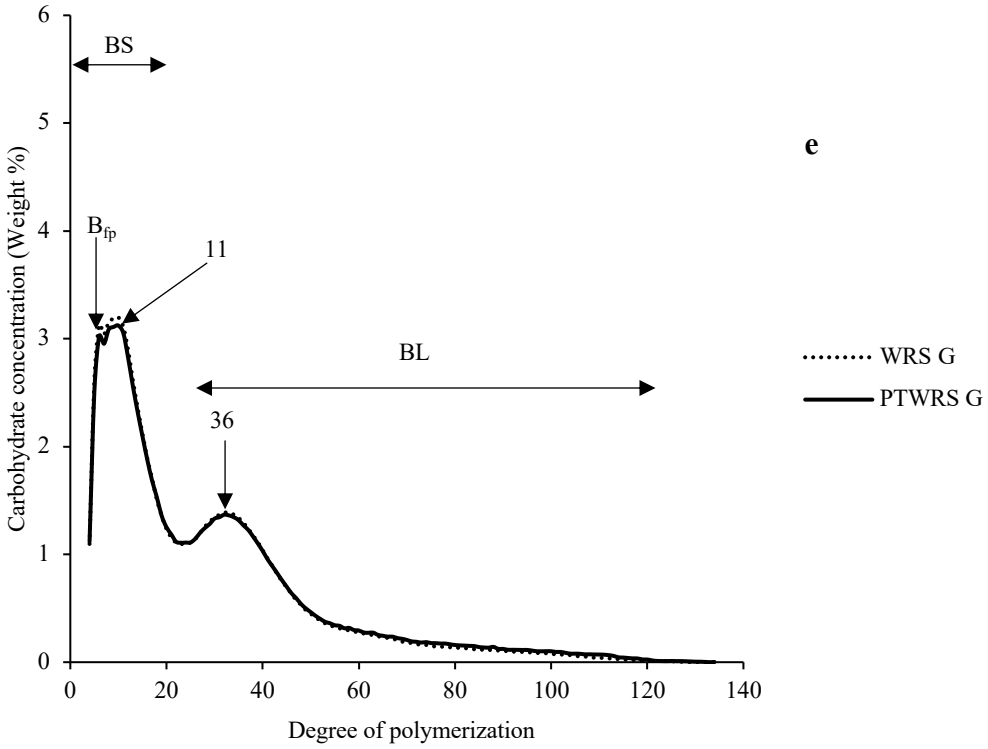
BS
B_{fp}
11
BL
36
Carbohydrate concentration (Weight %)
Degree of polymerization
0
1
2
3
4
5
6
0
20
40
60
80
100
120
140
e
WRS G
PTWRS G

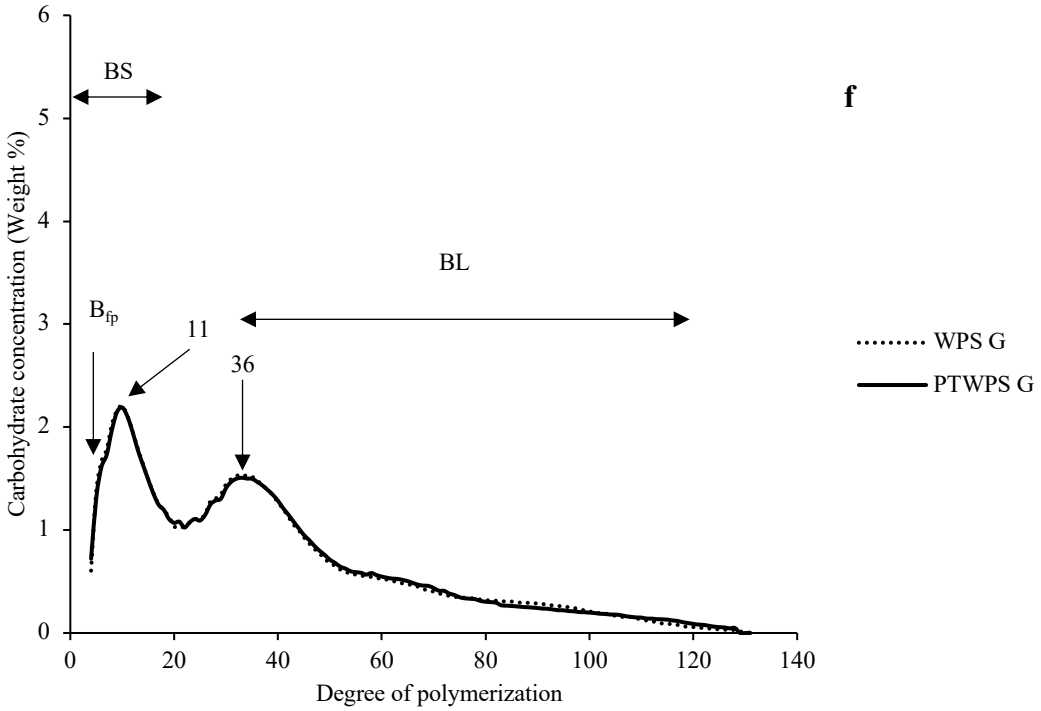

Figure 4-3: The chain profiles of debranched β-limit dextrins of granular and non-granular waxy starches

Arrows indicate degree of polymerization. a = WMS NG: Waxy Maize Starch Non-Granular, PTWMS NG: Plasma Treated Waxy Maize Starch Non-Granular; b = WRS NG: Waxy Rice Starch Non-Granular, PTWRS NG: Plasma Treated Waxy Rice Starch Non-Granular; c = WPS NG: Waxy Potato Starch Non-Granular, PTWPS NG: Plasma Treated Waxy Potato Starch Non-Granular; d =WMS G: Waxy Maize Starch Granular, PTWMS G: Plasma Treated Waxy Maize Starch Granular; e = WRS G: Waxy Rice Starch Granular , PTWRS G: Plasma Treated Waxy Rice Starch Granular; f = WPS G: Waxy Potato Starch Granular, PTWPS G: Plasma Treated Waxy Potato Starch Granular. Short B-chains (BS) are subdivided into "fingerprint" B-chains (B_{fp}) and a major group (BS_{major}).

4.5.3 In vitro digestion of granular and non-granular waxy starches

The results of the *in vitro* starch digestibility are shown in Table 4-1. Plasma treatment led to an increase ($p < 0.05$) in the amount of RDS in WMS G (85.08%). This led to a subsequent decrease ($p < 0.05$) in the amount of SDS (18.10%) and RS (1.35%). However, the amount of TDS (95.47%) was somewhat reduced although this was not significant ($p < 0.05$). Similarly, there were no differences ($p < 0.05$) in the amount of TDS in WMS NG, WRS NG and WPS NG after plasma treatment. Plasma treatment has been shown to induce etching and volatilization of starches (Moreau et al., 2008; Morent et al., 2011). This facilitates the movement of enzymes into the starch (Thirumdas, Kadam, et al., 2017a), thus, making it possible for the enzymes to hydrolyze WMS G more rapidly after plasma treatment. The amount of RDS in WMS NG slightly increased, however, this was not significant. Likewise, there were no differences ($p < 0.05$) in the amount of RDS in WRS NG, WPS G and WPS NG after plasma treatment. We observed that plasma treatment significantly enhanced the content of SDS (5.62%) and RS (0.28%) in WMS NG. Similar observations were made in the SDS (10.24%) and RS (85.66%) of PTWPS G. In the case of non-granular waxy rice, we observed an increase ($p < 0.05$) in the amount of SDS (5.51%) after plasma treatment. Plasma treatment has also been shown to induce cross-linking of the starch chains by forming C-O-C ether linkages (Zou et al., 2004; Okyere et al., 2019). This makes the starches more stable and prevents α-amylases from digesting them (Yeh & Yeh, 1993). The occurrence of cross-linking in the starches after plasma treatment was confirmed by the FTIR data (Table 4-2). Foods high in slowly digestible starches and resistant starches are important in maintaining a healthy weight and in the control of type 2 diabetes as it delays gastric emptying and slows the release of

glucose into the blood stream (Frost & Dornhorst, 2000; Giri et al., 2017). It was interesting to note that WPS G had the highest amount of RS due to the high concentration of phosphate groups which makes the starch resistant to amylase digestion (Kanazawa et al., 2008). Also, granular potato starch has a non-penetrable surface due to the lack of pores on the surface contributing to its high RS content (Chen et al., 2019). Contrarily, boiling potato has been shown to reduce the phosphate groups in potato (Bethke & Jansky, 2008). This accounts for the low amount of RS in non-granular waxy potato.

In general, the ratio of SDS:TDS was much higher in both granular and non-granular plasma treated starches with the exception of WMS G. Thus, plasma is an effective means of slowing down the rate of digestion by inducing cross-linked networks in these starches (Zou et al., 2004). Also prior to plasma treatment, the non-granular starches have higher RDS than the granular starches. This is because cooking starches makes it easily digestible due to the disruption of the highly ordered native granular starch during gelatinization (Tamura et al., 2016). This makes it easy for α-amylases to digest cooked starches (non-granular starch) (Guo et al., 2018). Interestingly, the results show that plasma treatment can effectively slow down the digestion of the non-granular starches. This could be due to the fact that gelatinizing starch during cooking opens the molecular chains (Kumar & Khatkar, 2017). These open chains could possibly cross-link during plasma treatment thus slowing down the rate of digestion (Zou et al., 2004). Overall, the results showed that plasma treatment influenced the rate of digestion of granular and non-granular waxy starches.

Table 4-1: RDS, SDS, TDS and RS values of treated and untreated starches

Sample	% RDS	% SDS	% TDS	% RS	% (SDS:TDS)
WMS G	61.55 ± 1.19^{a}	32.10 ± 0.62^{b}	96.02 ± 0.11^{a}	1.76 ± 0.02^{b}	33.43
PTWMS G	85.08 ± 0.25^{b}	18.10 ± 0.26^{a}	95.47 ± 0.24^{a}	1.35 ± 0.05^{a}	18.96
WMS NG	91.93 ± 0.33^{a}	2.34 ± 0.38^{a}	99.92 ± 0.43^{a}	0.21 ± 0.02^{a}	2.34
PTWMS NG	93.06 ± 0.60^{a}	5.62 ± 0.01^{b}	99.19 ± 0.00^{a}	0.28 ± 0.00^{b}	5.67
WRS G	98.79 ± 0.20^{b}	2.32 ± 0.26^{a}	97.57 ± 0.09^{b}	0.87 ± 0.00^{a}	2.38
PTWRS G	95.15 ± 0.56^{a}	3.37 ± 0.20^{b}	96.30 ± 0.39^{a}	0.93 ± 0.02^{a}	3.50
WRS NG	98.97 ± 0.00^{a}	4.31 ± 0.08^{a}	98.19 ± 0.35^{a}	0.12 ± 0.01^{a}	4.39
PTWRS NG	97.44 ± 0.92^{a}	5.51 ± 0.24^{b}	98.25 ± 1.00^{a}	0.10 ± 0.00^{a}	5.61
WPS G	2.40 ± 0.29^{a}	6.44 ± 0.31^{a}	13.77 ± 0.04^{a}	83.77 ± 0.10^{a}	46.77
PTWPS G	3.08 ± 0.02^{a}	10.24 ± 0.00^{b}	15.78 ± 0.01^{b}	85.66 ± 0.66^{b}	64.89
WPS NG	98.68 ± 0.44^{a}	4.68 ± 0.08^{a}	96.20 ± 0.76^{a}	0.63 ± 0.05^{a}	4.86
PTWPS NG	97.55 ± 0.33^{a}	5.58 ± 0.39^{a}	95.11 ± 0.53^{a}	0.77 ± 0.01^{a}	5.87

Means with different superscript letters show significant differences (p-value < 0.05) between treated and untreated granular and non-granular waxy starches of the same type and form.

WMS G: Waxy Maize Starch Granular, PTWMS G: Plasma Treated Waxy Maize Starch Granular, WMS NG: Waxy Maize Starch Non-Granular, PTWMS NG: Plasma Treated Waxy Maize Starch Non-Granular, WRS G: Waxy Rice Starch Granular , PTWRS G: Plasma Treated Waxy Rice Starch Granular, WRS NG: Waxy Rice Starch Non-Granular, PTWRS NG: Plasma Treated Waxy Rice Starch Non-Granular, WPS G: Waxy Potato Starch Granular, PTWPS G: Plasma Treated Waxy Potato Starch Granular, WPS NG: Waxy Potato Starch Non-Granular, PTWPS NG: Plasma Treated Waxy Potato Starch Non-Granular.

RDS-Rapidly Digestible Starch, SDS-Slowly Digestible Starch, TDS- Total Digestible Starch and RS-Resistant Starch

4.5.4 Fourier transform infrared spectroscopy-attenuated total reflectance measurement

The FTIR-ATR spectra of all the starch samples were characterized by absorption bands at 930-961 cm^{-1}, 1021-1094 cm^{-1} and 1149-1162 cm^{-1} which corresponds to the C-O-C skeletal mode of glycosidic linkage, C-O-H bending, and C-O-C asymmetric stretching of the glycosidic bond, respectively (Deeyai et al., 2013; Warren et al., 2016) (Figure 4-4). The bands at 1640-1670 cm^{-1} have been attributed to tightly bound water in starch mainly due to its hygroscopic nature, while the bands at 2900-3000 cm^{-1} and 3000-3600 cm^{-1} corresponds to the CH, CH_2 stretching region and O-H stretching region, respectively (Abdullah et al., 2018; Deeyai et al., 2013; Kizil et al., 2002; Pozo et al., 2018). There are reports of carbon dioxide gas plasmas incorporating hydroxyl functional groups in starches (Thirumdas et al., 2017a) and this phenomenon was observed in WMS NG (Figure 4-4a), WRS NG (Figure 4-4b) and WRS G (Figure 4-4e) after plasma treatment in the present study. This is because the absorption bands at the O-H stretching region was relatively higher in these aforementioned samples after treatment. We observed increases in the relative intensities of the C-O-C linkages in WMS NG, WRS G, WRS NG and WPS G after plasma treatment (Table 4-2), thus confirming that plasma treatment induced the formation of cross-linking of the side chains of these starches. Plasma induced cross-linking has been shown to generate C-O-C linkages (Zou et al., 2004).

We observed previously (Okyere et al., 2019) a lower breakdown value in plasma treated granular waxy rice starch (PTWRS G) during pasting. This suggests some degree of cross-linking taking place in the granular waxy rice starch after plasma treatment, which was confirmed in the FTIR results obtained. We also observed (Okyere et al., 2019) higher

enthalpies of gelatinization in granular waxy rice starch (WRS G) and granular waxy potato starch (WPS G) after plasma treatment, suggesting that these starches were cross-linked and thus much energy was required during thermal treatment to gelatinize the starches. We observed the occurrence of these cross-links in the FTIR data in the present investigation.

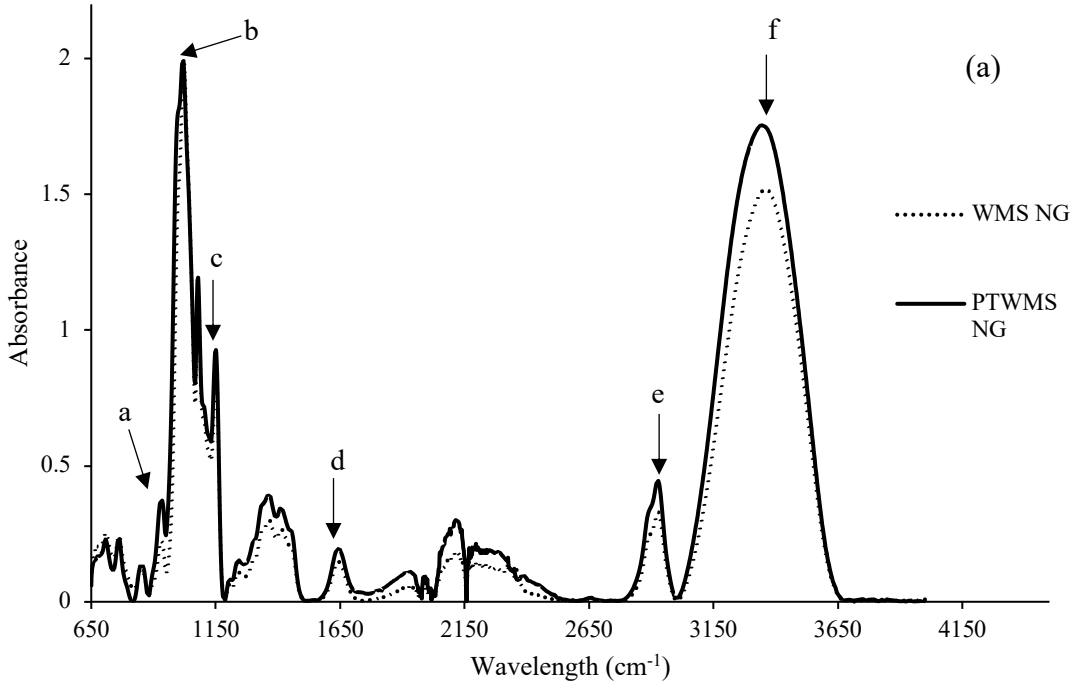

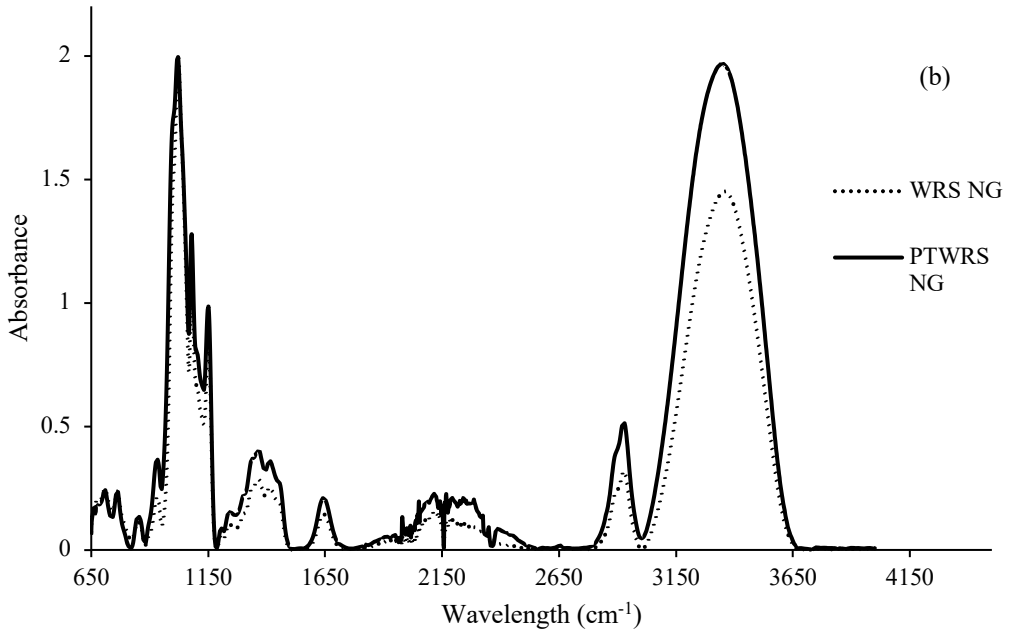
(b)
WRS NG
PTWRS NG
Absorbance
Wavelength (cm-1)
0
0.5
1
1.5
2
650
1150
1650
2150
2650
3150
3650
4150

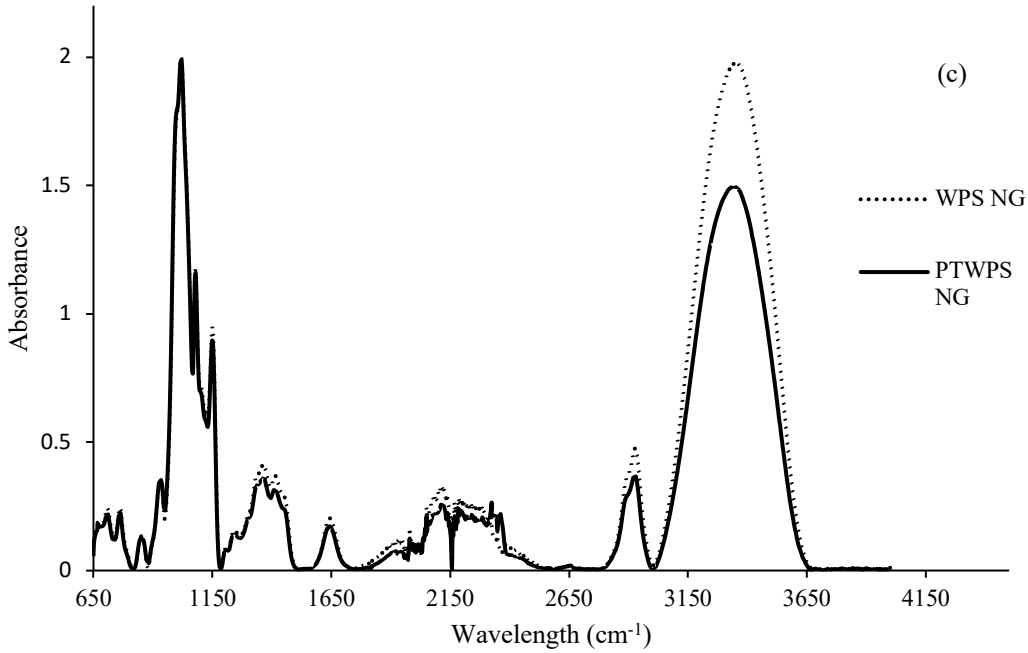
(c)
WPS NG
PTWPS NG
Absorbance
Wavelength (cm-1)
0
0.5
1
1.5
2
650
1150
1650
2150
2650
3150
3650
4150

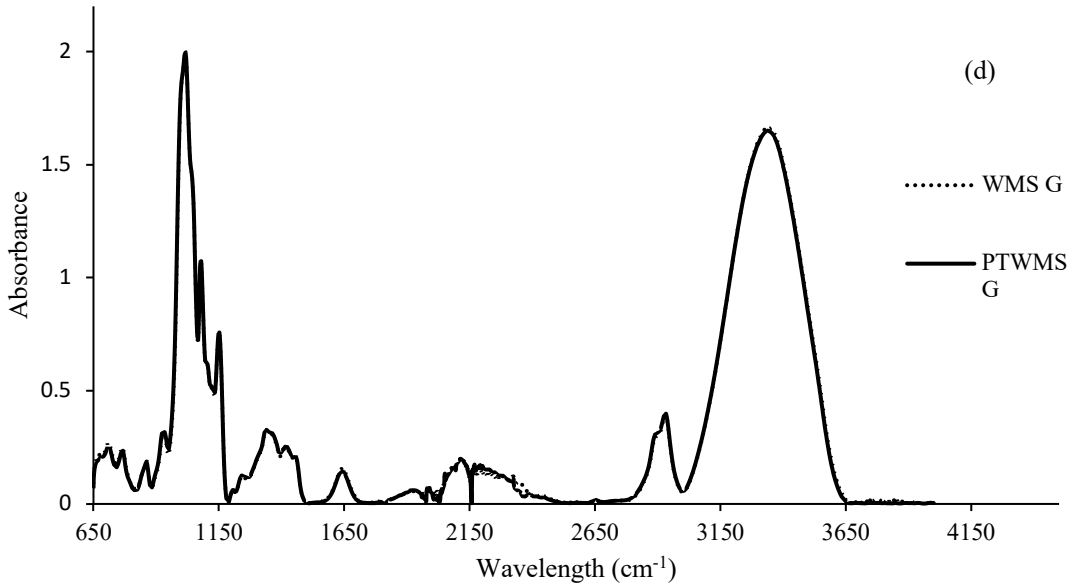
(d)
WMS G
PTWMS G
Absorbance
Wavelength (cm-1)
0
0.5
1
1.5
2
650
1150
1650
2150
2650
3150
3650
4150

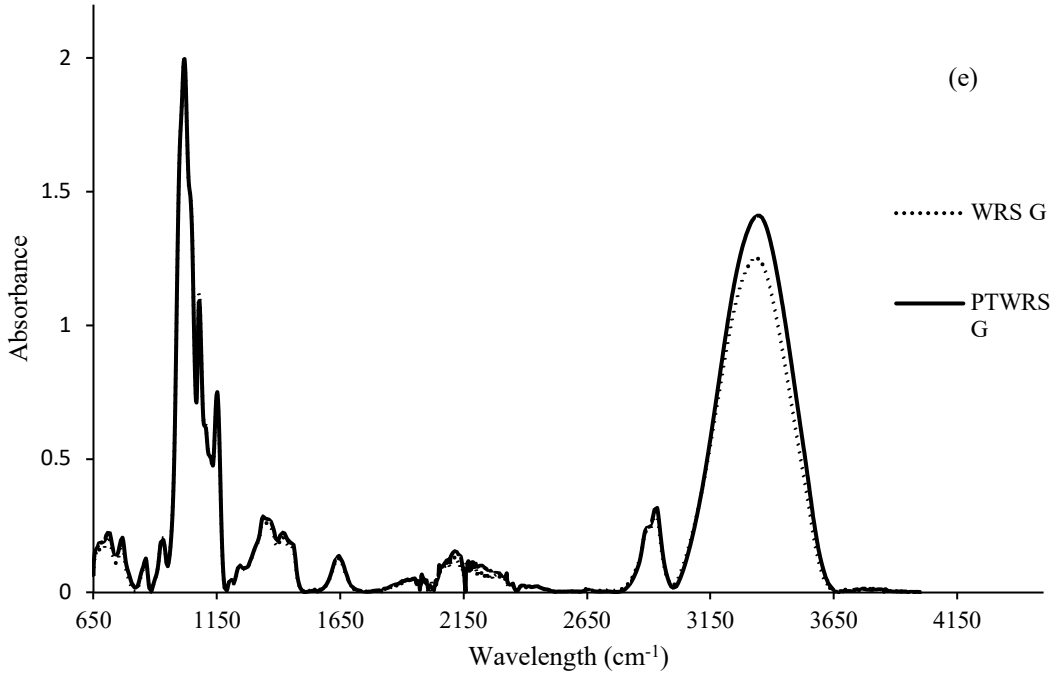
(e)
WRS G
PTWRS G
Absorbance
Wavelength (cm-1)
0
0.5
1
1.5
2
650
1150
1650
2150
2650
3150
3650
4150

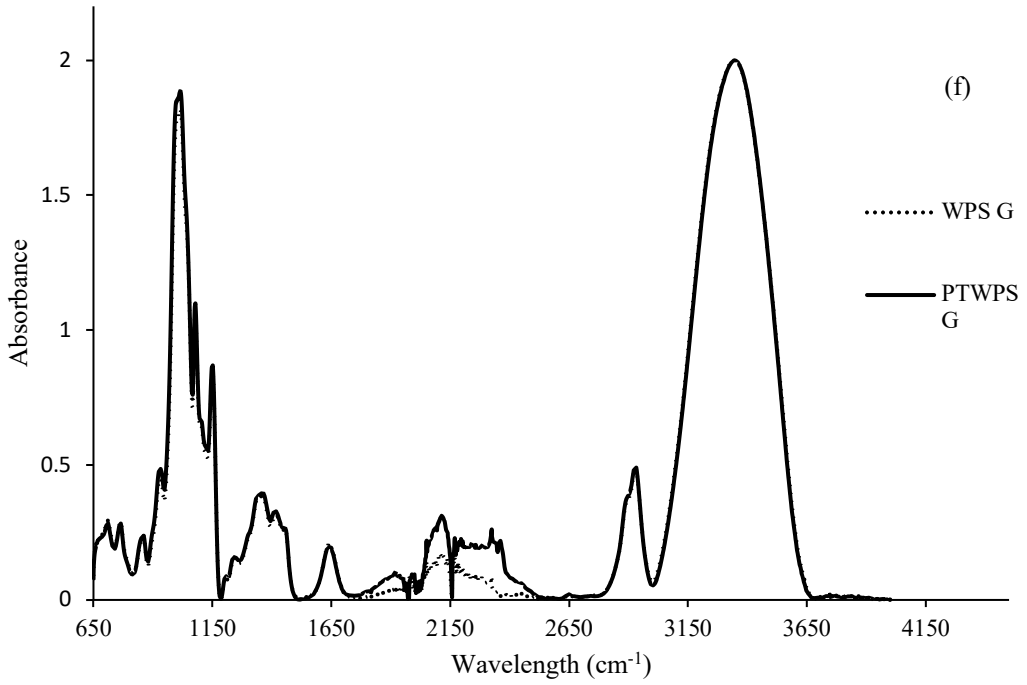

Figure 4-4: The FTIR-ATR spectra of granular and non-granular waxy starches

(a) = WMS NG: Waxy Maize Starch Non-Granular, PTWMS NG: Plasma Treated Waxy Maize Starch Non-Granular; (b) = WRS NG: Waxy Rice Starch Non-Granular, PTWRS NG: Plasma Treated Waxy Rice Starch Non-Granular; (c) = WPS NG: Waxy Potato Starch Non-Granular, PTWPS NG: Plasma Treated Waxy Potato Starch Non-Granular; (d) =WMS G: Waxy Maize Starch Granular, PTWMS G: Plasma Treated Waxy Maize Starch Granular; (e) = WRS G: Waxy Rice Starch Granular , PTWRS G: Plasma Treated Waxy Rice Starch Granular; (f) = WPS G: Waxy Potato Starch Granular, PTWPS G: Plasma Treated Waxy Potato Starch Granular

Labels in Figure 4A apply to all other FTIR spectra

a = C-O-C skeletal mode of glycosidic linkage, b = C-O-H bending, c = C-O-C asymmetric stretching glycosidic bond, d = tightly bound water in starch, e= CH, CH_2 stretching region and f= O-H stretching region

Table 4-2: Relative Intensities of C-O-C Glycosidic Linkages after FTIR-ATR Analysis

Sample	Relative Intensities of C-O-C Glycosidic Linkages	
	930cm^{-1}	1150cm^{-1}
WMS G	0.115	0.31
PTWMS G	0.115	0.293
WMS NG	0.141	0.342
PTWMS NG	0.167	0.354
WRS G	0.133	0.281
PTWRS G	0.136	0.303
WRS NG	0.137	0.361
PTWRS NG	0.159	0.376
WPS G	0.116	0.334
PTWPS G	0.121	0.356
WPS NG	0.175	0.383
PTWPS NG	0.162	0.369

WMS G: Waxy Maize Starch Granular, PTWMS G: Plasma Treated Waxy Maize Starch Granular, WMS NG: Waxy Maize Starch Non-Granular, PTWMS NG: Plasma Treated Waxy Maize Starch Non-Granular, WRS G: Waxy Rice Starch Granular , PTWRS G: Plasma Treated Waxy Rice Starch Granular, WRS NG: Waxy Rice Starch Non-Granular, PTWRS NG: Plasma Treated Waxy Rice Starch Non-Granular, WPS G: Waxy Potato Starch Granular, PTWPS G: Plasma Treated Waxy Potato Starch Granular, WPS NG: Waxy Potato Starch Non-Granular, PTWPS NG: Plasma Treated Waxy Potato Starch Non-Granular.

4.6 Conclusions

The effects of plasma treatment on the unit chain and internal chain profile were mostly negligible. The relative amount of short chains of waxy maize and rice (granular and non-granular) starches was reduced, which resulted in slight increases in the long chains. Starches modified with plasma are beneficial in slowing down the release of glucose in the blood stream. This is because plasma enhanced the amount of slowly digestible starches and resistant starches in WPS G, WMS NG and WRS NG. FTIR-ATR data showed that plasma induced cross-linking of WMS NG, WRS G, WRS NG and WPS G. Thus, it appears that cross-linking of the amylopectin side chains, which results in the formation of ether linkages, is the major mechanism by which carbon dioxide- argon radio frequency plasma modified the waxy starches utilized in this study.

4.7 Funding

This research did not receive any specific grant from funding agencies in the public, commercial, or non-profit sectors.

4.8 Acknowledgements

The authors are grateful to Gabrielle Seliber (College of Biological Sciences, University of Minnesota), and Juan Mogoginta (Department of Food Science and Nutrition, University of Minnesota) for their excellent technical assistance. Parts of this work was also carried out in the Characterization Facility, University of Minnesota, which receives partial support from NSF through the MRSEC program with the help of Dr. Bing Luo.

4.9 Conflict of interest

The authors declare no conflict of interest.

Chapter 5: Temperature of plasma-activated water and its effect on the thermal and chemical surface properties of cereal and tuber starches.

5.1 Overview

To investigate plasma-activated water (PAW) treatment effects on starch properties, high amylose and waxy starches from maize and potato were incubated with PAW at different temperatures (25°C, 60°C and 80°C). Starches incubated at 60°C increased ($p < 0.05$) the gelatinization parameters except the enthalpy of gelatinization of waxy potato starch. Starch swelling power significantly decreased while the water absorption capacity and solubility increased when incubated at 80°C. X-ray photoelectron spectroscopy (XPS) analysis showed the oxidation of C-C/C-H and C-O into carboxyl groups in waxy and high amylose maize starches incubated with PAW at 60°C and 80°C, respectively. Evidence of cross-linking was observed in waxy maize and high amylose potato incubated with PAW at 80°C and 25°C, respectively. Overall, the results indicated temperature is an important factor in the modification of cereals and tuber starches with PAW.

Keywords: Plasma-activated water, temperature, XPS analysis, thermal properties, hydration properties

5.2 Introduction

Starch is an important biopolymer utilized in diverse food applications due to its thickening, binding, gelling, stabilizing and encapsulating abilities (Bemiller, 1997). Native starches typically exist in granular form and are made up of a linear molecule (amylose) and a highly branched molecule (amylopectin). The former consists of α-(1,4) glycosidic bonds with 1% α-(1,6) branched points, while the latter has α-(1,4) glycosidic bonds interconnected through 5% α-(1,6) linkages (Hizukuri et al., 1981; Hizukuri et al., 1983; Pérez & Bertoft, 2010). Normal starches typically contain 20-35% amylose and 65-80% amylopectin. There are, however, high amylose and waxy starches with > 35% amylose and < 5% amylose, respectively (X. Wu et al., 2006). High amylose and waxy starches have unique abilities; High amylose starch is inherently resistant to digestion (RS2) and forms strong cohesive gels while the waxy starches have better paste clarity, forms soft sticky gels and are inherently non-resistant to digestion (Li et al., 2019). Resistant starch type 2 (RS2) refers to raw starch granules mostly B-type crystalline starches that are resistant to enzyme digestion (Li et al., 2019).

Starch is modified to improve its functionality and stability for industrial processing due to its inert, insoluble, and retrogradation tendencies (Laovachirasuwan et al., 2010). Starch can be modified by chemical, enzymatic and physical means (Bemiller, 1997). Chemical methods are well known and give the highest efficiency; however, the drawback is in the high cost of chemicals and waste generation (Thirumdas, Kadam, et al., 2017a). Enzymatic methods can also be expensive and require extreme care to avoid contamination during modification (Park et al., 2017). The current trend is to explore eco-friendly physical methods of starch modification, and plasma-activated water (PAW) falls into this category

(Thirumdas et al., 2018). Plasma-activated water is a chemically reactive water obtained using atmospheric plasma devices to generate reactive species directly inside water, or above the surface of water over a period of time. Reactive oxygen and nitrogen species such as atomic oxygen, hydroxyl radicals, ozone, hydrogen peroxide, nitric oxide, nitrates, nitrites, and peroxynitrites are generated in the gas-water interface when air is used as the discharge gas (Lukes et al., 2014). The pH of plasma-activated water is low (acidic) while the oxidative-reductive potential and electrical conductivity are high as result of the reactive species generated in the gas-water interface. This makes PAW suitable for hindering microbial growth, enhancing seed germination, and in our case starch modification (Thirumdas et al., 2018).

PAW is relatively easy to produce and less expensive compared to chemical and enzymatic methods of starch modification (Thirumdas et al., 2018). Hence it is necessary for scientists to fully explore this alternative method for modifying starches. To the best of our knowledge, there remains to date limited knowledge on the effect of PAW on high amylose and waxy cereal and tuber starches. Yan et al. (2020) utilized plasma-activated water and heat moisture treatment (PAW-HMT) to modify waxy and normal maize starches. They observed an increase in resistant starches and solubility and a decrease in swelling power of PAW-HMT modified starches. However, more research is still needed on the effect of PAW on starch properties since it has promising prospects in terms of modifying starches in an eco-friendly way.

In this study, we used the X-ray photo electron spectroscopy, Fourier transform infrared spectroscopy with attenuated total reflectance, and differential scanning calorimetry to determine the effects of PAW temperature on the properties of high amylose

and waxy cereal and tuber starches for the first time. This study is important in expanding our knowledge on how the temperature of PAW alters the surface chemistry, thermal, and functional properties of starches. It is hypothesized that increasing the temperature of PAW would significantly impact the characteristics of starches, and as such, PAW can be adopted as an alternative means of starch modification.

5.3 Materials and methods

5.3.1 Materials

Waxy maize (AMIOCA) and potato (ELIANE 100) starches and high amylose maize (HYLON V) starch used for the experiment were obtained from Ingredion Incorporated (Bridgewater, NJ, USA). High amylose potato (44% amylose) was obtained from Andreas Blennow, Ph.D., Department of Plant and Environmental Sciences, University of Copenhagen, Denmark. The atmospheric pressure plasma jet (APPJ) operating at 120 V was obtained from Enercon Industries (Menomonee Falls, Wisconsin, USA). Chemicals used in this study were of analytical grade.

5.3.2 Plasma-activated water production and starch modification

5.3.2.1 Generating plasma-activated water

Deionized water (200 mL) was treated with an APPJ for 30 min with constant stirring. Air at 80 pound-force per square inch (psi) was used as the discharge gas. This was repeated to obtain 4 L of plasma-activated water. The distance between the APPJ probe and the surface of the water was 10 cm. The pH, oxidative-reductive potential (ORP), and conductivity were measured using the SURE TEST® pH/EC/TDS/mV LAB METER (Greentrees Hydroponics, California, USA). PAW was used within a week to ensure its potency wouldn't decline. The measured parameters are presented in Table 5-1.

5.3.2.2 Treatment of starches with plasma-activated water

Approximately 1.5 g of starch was treated with plasma-activated water (100 mL) for 12 hours at three different temperatures (25°C, 60°C and 80°C). The starch slurries were constantly shaken at 200 rpm during treatment. The slurries were centrifuged at 2000 *g* (10 min), after which the supernatant was carefully discarded. The pellets were washed with deionized water and centrifuged at 2000 *g* (10 min). This was repeated thrice after which the remaining pellet was reconstituted in water, frozen and lyophilized. The treated starches were kept in snap cap vials in a desiccator until further analysis. Native starches were used as control.

5.3.3 Amylose content determination

Determination of the amylose content in the high amylose potato starch was done based on methods described by Chrastil (1987). Starch samples (10 – 20 mg) were suspended in 85% methanol and incubated at 60°C for 30 min with occasional mixing to extract all lipids. The samples were centrifuged at 1500 rpm for 5 min after which the supernatant was discarded. The lipid extraction was repeated. Samples were solubilized for 30 min at 100°C in 6 mL of urea-DMSO (0.6M urea in 90% DMSO). Subsequently, 0.1 mL of the solubilized sample was transferred into 5 mL of 0.5% trichloroacetic acid in a separate test tube. The solutions were mixed, after which 0.05 mL of 0.01N I_2-KI solution (1.27 g I_2/L + 3 g KI/L) was added and vortexed immediately and left to stand at 25°C. The blue color formed was read at 620 nm after 30 min against water (blank). Hylon VII corn starch was used as our standard amylose sample.

The amylose content was determined based on the formula

A x 45.8 = mg of amylose per L in cuvette, (1)

where A is the absorbance of the sample.

5.3.4 Fourier transform infrared spectroscopy-attenuated total reflectance (FTIR-ATR) measurement of treated and untreated starches

The FTIR-ATR measurements were done using a Nicolet iS50 FTIR (Thermo Fisher Scientific, MN, USA) equipped with a Deuterated Triglycine Sulfate Attenuated Total Reflection (DGTS ATR) detector by spreading a thin layer of starch onto the diamond crystal and applying pressure using the pressure tower. A total of 64 scans were recorded with a spectral resolution of 4 cm^{-1} within a spectral range of 4000 to 650 cm^{-1}. The spectra were collected using the OMNIC software. All the samples were recorded against a background spectrum (which is a spectrum without a starch sample in place). The spectra were baseline corrected and normalized using the Min/Max method (Pu et al., 2011), after which the intensities of the bands at 930 and 1150 cm^{-1} were computed using the OPUS 7.0 software (Bruker, Madison, WI, USA).

5.3.5 Thermal analysis

The Differential Scanning Calorimeter (DSC) from Mettler Toledo (Columbus, OH, USA) was used to measure the gelatinization onset, peak and conclusion temperature, as well as the enthalpy of gelatinization of the starches based on methods described by Okyere et al. (2019) with slight modifications. This was done by heating one part starch (4 mg) in three parts (12 mg) deionized water in a hermetically sealed DSC pan from 25°C to 120°C at a heating rate of 5°C/min. Starches were equilibrated to room temperature for approximately 30 min prior to testing. The starches were then tested against an empty pan used as a reference. The results were analyzed using the STARe thermal analysis software version 11.00. Samples were run in duplicate.

5.3.6 X-ray photoelectron spectroscopy analysis of treated and untreated starches

The chemical surface analysis measurements were performed on a PHI 5000 Versa Probe III XPS system (ULVAC-PHI) (Chanhassen, MN, USA) using a monochromatic Al K_α X-ray source (1486.6 eV). The base pressure was 3.0 x 10^{-8} Pa. Starch samples were mounted on a piece of sticking tape on the sample holder. The sample was not conductive, and the charge neutralization was applied during the data collection. The measurements were conducted using an X-ray spot size of 0.1 x 0.1 mm^2 with a power of 25 W under 15 kV. The survey spectra were measured using 280 eV pass energy and 1.0 eV/step. The high-resolution spectra were collected using 55 eV pass energy and 0.1 eV/step. The atomic percentages were calculated from the survey spectra using the Multipak software provided with the XPS system. For the high-resolution data, the lowest binding energy C_{1s} peak (C-C and C-H) was set at 285.0 eV and used as the reference. The curve fitting used a combination of Gaussian/Lorentzian function with the Gaussian percentages being 80% or higher (Bie et al., 2016).

5.3.7 Hydration properties of starch

5.3.7.1 Swelling power and solubility

The solubility and swelling power of the starch samples were determined using the method by X. Han et al., (2022), with some modifications. Blended suspensions with 5% starch samples were heated at 85 °C for 30 min and then centrifuged at 3000 *g* for 10 min. The precipitates were weighed, and the supernatants dried at 135 °C for 2 h. The solubility (%) and swelling power (g/g) were expressed using the following equations:

$$Solubility\ (\%) = \frac{A}{W} \times 100 \qquad (2)$$

$$Swelling\ Power\ (g/g) = \frac{B}{W} \times (1 - S) \qquad (3)$$

Where A is the residual starch mass of supernatant after drying; W is the weight of starch sample; B is the precipitate weight after centrifugation; S is the solubility of the sample. The experiments were run in duplicate.

5.3.7.2 Water absorption capacity

The water absorption capacity of the starch samples was determined using the method by X. Han et al., (2022) , with some modifications. Approximately 6% starch solution was prepared with the samples and distilled water, and vortexed for 5 min to mix the solution well. The solutions were then placed at ambient temperature (~ 22 °C) for 30 min to allow sufficient absorption of water by the starch samples. Afterwards, the mixture was centrifuged at 3000 g for 10 min and the supernatant discarded. The precipitate was then weighed. The water absorption capacity was calculated using the following equation:

$$Water\ Absorption\ Capacity\ (\%) = \frac{M-W}{W} \times 100 \qquad (4)$$

Where M is the weight of the precipitate; and W is the weight of the starch sample. The analysis was done in duplicate.

5.3.8 Statistical analysis

All results were statistically analyzed by one-way ANOVA with Statgraphics Centurion XVI, version 16.1.0 (Stat Point, Warrenton, VA, U.S.A.). Duncan's multiple range test was used to determine statistical significance between means at $p < 0.05$.

5.4 Results and Discussion

5.4.1 Physicochemical properties of Plasma-activated water

The pH, Oxidative-Reductive Potential (ORP), and electrical conductivity of Double Distilled Water (DDW) and PAW are presented in Table 5-1. The pH of DDW significantly decreased from 6.5 to 2.6 after 30 min of APPJ treatment. The use of air as the discharge gas in PAW generation results in the formation of reactive species such as hydroxyls ($OH^{\cdot}$), nitrate (NO_3^-), and nitrites (NO_2^-) at the gas-water interface (Lukes et al., 2014). These species continue to undergo several reactions resulting in the formation of hydrogen peroxide (H_2O_2), nitric acid (HNO_3), and peroxynitrous acid in PAW, which makes the water acidic (Oehmigen et al., 2010). The conductivity measures the flow of ions and electric currents in water (Thirumdas et al., 2018). We observed an increase ($p < 0.05$) in the conductivity from 1.7 in DDW to 749 µS/cm in PAW which could be attributed to the generation of reactive oxygen species (ROS) and reactive nitrogen species (RNS) in PAW (Lukes et al., 2014). The ORP of PAW also increased significantly after treatment from 345.5 to 581 mV. The formation of ROS such as H_2O_2 accounts for the increase observed in ORP (Lukes et al., 2012).

Table 5-1: pH, ORP, and electric conductivity of plasma-activated water

Water	pH	Oxidative-Reductive Potential (ORP) (mV)	Conductivity (µS/cm)
DDW	6.5 ± 0.1^b	345.5 ± 0.7^a	1.7 ± 0.0^a
PAW	2.6 ± 0.1^a	581.0 ± 2.8^b	749.0 ± 1.4^b

DDW-Double Distilled Water, PAW-Plasma-Activated Water; Values are expressed as duplicate measurement of the mean ± standard deviation. The superscript on the means shows significant differences ($p < 0.05$) between the parameters measured for DDW and PAW

5.4.2 Thermal properties

Treatment of starches with plasma-activated water at 60°C significantly increased the gelatinization parameters (T_o, T_p, T_c, and ΔH) of the starches except for ΔH in waxy potato starch (PAW-WPS 60°C) (Table 5-2). Incubating the starches in PAW at 25°C, significantly increased the T_o (67.3°C), T_p (71.4°C), T_c (76.3°C) and ΔH (11.0 J/g) in high amylose potato starch. Also, incubating waxy maize starch in plasma-activated water at 25°C (PAW-WMS 25°C) increased ($p < 0.05$) the ΔH from 5.3 to 6.1 J/g. The higher gelatinization temperatures suggest that treating starches in PAW at 25°C (in the case of HAPS) and 60°C resulted in the reorganization of the double helices into a perfect crystalline structure (Vamadevan et al., 2013). In addition, plasma-activated water is rich in H^+ ions which could induce the formation of additional hydrogen bonds between the double helices due to the close alignment of the strands and strengthen the crystal structure (Bogracheva et al., 2001). This alignment hinders plasticization during heating and increases the gelatinization temperatures (Vamadevan et al., 2013).

The increases observed in ΔH indicate the presence of longer double helices formed by the organization of the unraveled ends of the external chains of the amylopectin (Qi et al., 2003). In the case of PAW-WPS 25°C and 60°C, the reactive species in plasma-activated water possibly distorted the crystal structure and decreased the ΔH (Noda et al., 2009). The temperature ranges (T_c-T_o) increased ($p < 0.05$) in the high amylose PAW starches incubated at 25°C and decreased ($p < 0.05$) in all starches incubated at 60°C, except for PAW-HAMS, in which it remained the same. The lower melting temperature ranges of the 60°C PAW starches suggest that increasing the temperature during PAW treatment of starches leads to the formation of homogenous amylopectin crystals that are

more stable (Ratnayake et al., 2001; Annor et al., 2014b). However, when the incubation temperature goes beyond the gelatinization temperatures of the starches, they become amorphous, as in the case of the PAW starches incubated at 80°C (Fig S1). We did not report on these gelatinization parameters since they were amorphized. Overall, the melting temperatures of the high amylose starches were higher than their respective waxy starches. This is because the gelatinization temperatures increase with increasing amylose content (Matveev et al., 2001).

Table 5-2: Thermal properties of PAW treated and untreated starches

Samples	T_o (°C)	T_p (°C)	T_c (°C)	T_c-T_o (°C)	ΔH J/g
WMS	65.1±0.4[a]	70.1±0.1[a]	76.5±0.2[a]	11.4±0.2[b]	5.3±0.1[a]
PAW-WMS 25°C	64.3±0.4[a]	69.8±0.3[a]	75.9±0.3[a]	11.6±0.1[b]	6.1±0.1[b]
PAW-WMS 60°C	70.3±0.4[b]	73.3±0.4[b]	77.9±0.1[b]	7.7±0.4[a]	7.8±0.1[c]
HAMS	69.3±0.1[a]	73.7±0.4[a]	81.2±0.1[a]	11.9±0.3[a]	1.8±0.1[a]
PAW-HAMS 25°C	68.6±0.0[a]	73.9±0.3[a]	81.9±0.3[a]	13.3±0.3[b]	1.8±0.0[a]
PAW-HAMS 60°C	72.2±0.4[b]	76.9±0.1[b]	84.1± 0.4[b]	11.9±0.0[a]	4.0±0.0[b]
WPS	63.3±0.0[a]	67.9±0.0[a]	72.6±0.0[a]	9.3±0.0[b]	12.5±0.0[b]
PAW-WPS 25°C	63.2±0.0[a]	67.8±0.1[a]	72.6±0.2[a]	9.4±0.2[b]	11.9±0.0[a]
PAW-WPS 60°C	70.0±0.4[b]	73.3±0.4[b]	77.1±0.3[b]	7.1±0.1[a]	11.9±0.2[a]
HAPS	66.7±0.1[a]	70.7±0.1[a]	75.1±0.1[a]	8.3±0.0[b]	10.4±0.0[a]
PAW-HAPS 25°C	67.3±0.0[b]	71.4±0.0[b]	76.3±0.0[b]	9.0±0.1[c]	11.0±0.0[b]
PAW-HAPS 60°C	74.8±0.2[c]	77.3±0.2[c]	80.8±0.3[c]	6.0±0.1[a]	13.7±0.0[c]

[a] Values are expressed as duplicate measurement of the mean ± standard deviation. Means with different superscript letters shows significant differences ($p < 0.05$) between treated and untreated starches of the same type; The different incubation temperatures for the starches are attached to the sample name.
WMS: Waxy Maize Starch, PAW-WMS 25°C : Plasma-Activated Water Waxy Maize Starch 25°C, PAW-WMS 60°C: Plasma-Activated Water Waxy Maize Starch 60°C, HAMS: High Amylose Maize Starch, PAW-HAMS 25°C: Plasma-Activated Water High Amylose Maize Starch 25°C, PAW-HAMS 60°C: Plasma-Activated Water High Amylose Maize Starch 60°C, WPS: Waxy Potato Starch, PAW-WPS 25°C: Plasma-Activated Water Waxy Potato Starch 25°C, PAW-WPS 60°C: Plasma-Activated Water Waxy Potato Starch 60°C , HAPS: High Amylose Potato Starch, PAW-HAPS 25°C: Plasma-Activated Water High Amylose Potato Starch 25°C , PAW-HAPS 60°C: Plasma-Activated Water High Amylose Potato Starch 60°C
T_o: onset temperature, T_p: peak temperature, T_c: conclusion temperature, ΔH: enthalpy of gelatinization, T_c-T_o: (conclusion temperature – onset temperature) Gelatinization temperature range

5.4.3 Swelling power and solubility

When compared to the control starches, a significant reduction in the swelling power (SP) of the starches was observed when treated with PAW irrespective of the temperature except for high amylose maize (Figure 5-1). Within the samples treated with PAW at different temperatures, the SP of HAMS and WPS were statistically similar when incubated at 25°C and 60°C but decreased ($p < 0.05$) at 80°C. In the case of WMS, reductions in SP were observed even at 60°C. HAPS was unique in the sense that increases in SP was observed with increases in the temperature of PAW and it is unclear why this was observed. The reductions observed in the swelling power suggest that the reactive species present in PAW induced the oxidation of lipids in the high amylose maize starch (Sarangapani et al., 2017). Thus, these lipids could form complexes with the starches, which would inhibit the swelling ability of the starches (Tester & Morrison, 1990; Eliasson & Ljunger, 1988). In the case of the other starches, PAW could induce the acid hydrolysis of the amorphous and crystalline structures decreasing their ability to bind water and swell (Yan et al., 2020).

The solubility of waxy maize and waxy potato starches incubated at 25°C (7.2%, 22.8%) and 60°C (42.0%, 29.1%), respectively, was higher than their untreated starches (Figure 5-2.). PAW-WMS and PAW-WPS incubated at 80°C possessed, however, considerably higher solubilities than after treatment at 25 or 60°C. This could be attributed to PAW and temperature damaging the double helical structure in amylopectin leading to more amylopectin leaching out and solubilizing (Y. Yan et al., 2020). In the case of the high amylose starches, we only observed a significant increase in the PAW starches incubated at 80°C. The high temperature combined with PAW could have facilitated the acid hydrolysis of the amorphous regions causing amylose to leach out and solubilize (Yan et al., 2020).

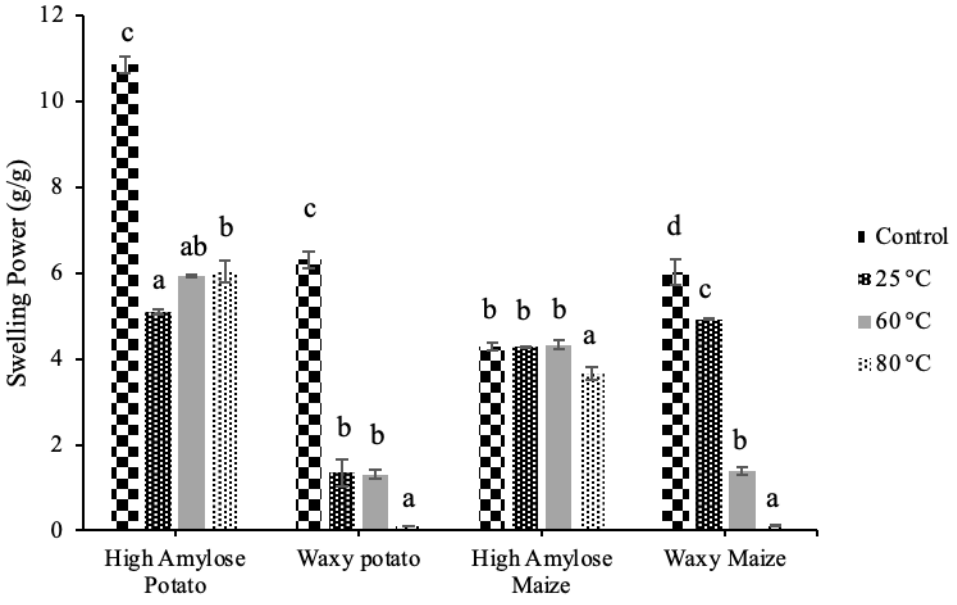

Figure 5-1: Swelling power of PAW treated and untreated starches

Lowercase letters show significant differences ($p < 0.05$) between treated and untreated starches of the same type; Control = untreated starches, 25°C = Plasma-activated water starch incubated at 25°C, 60°C = Plasma-activated water starch incubated at 60°C, 80°C = Plasma-activated water starch incubated at 80°C

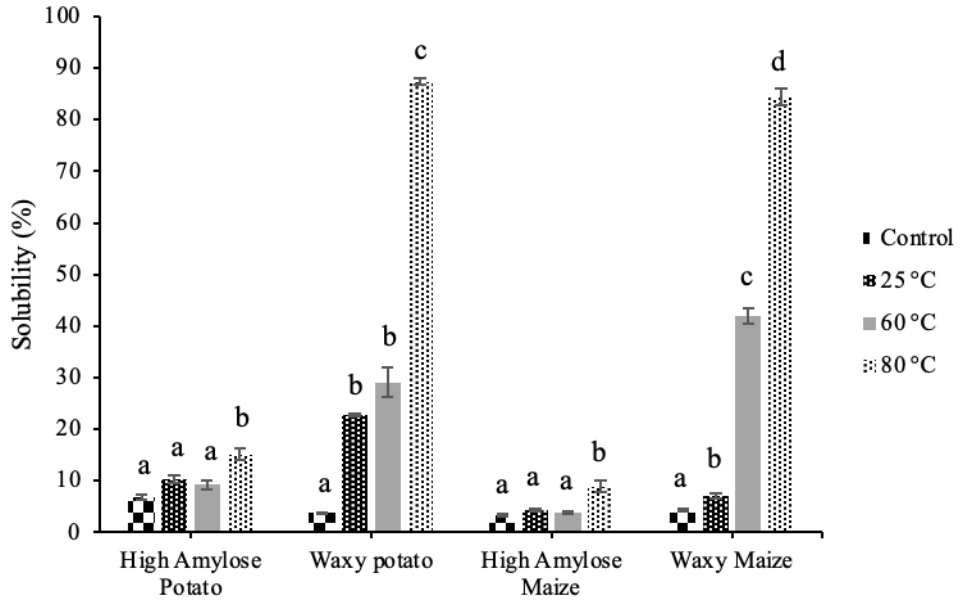

Figure 5-2: Solubility of PAW treated and untreated starches

Lowercase letters show significant differences ($p < 0.05$) between treated and untreated starches of the same type; Control = untreated starches, 25°C = Plasma-activated water starch incubated at 25°C, 60°C = Plasma-activated water starch incubated at 60°C, 80°C = Plasma-activated water starch incubated at 80°C

5.4.4 Water absorption capacity

There were no significant increases in the water absorption capacity (WAC) of the PAW starches incubated at 25°C compared to the control samples (Figure 5-3) except for high amylose potato (97.5%). This exception suggests that PAW induced a reorganization of the double helices, and thereby enabled the starch to absorb more water. This phenomenon could be explained by the backbone model of amylopectin, which suggests flexibility for rearrangement of the double helices (Bertoft, 2017). Similarly, significant

increases were observed in PAW-WPS (129.2%), and PAW-HAPS (114.2%) incubated at 60°C, whereas the maize starches were unaffected. However, all plasma-activated water starches incubated at 80°C possessed very high increase in WAC. At 80°C, the starches were completely gelatinized and damaged (Jane et al., 1999). Thus, they had completely lost their granule structure and crystallinity and can absorb more water compared to the control and PAW starches incubated at 25°C (Tester & Morrison, 1990). Incubation at 60°C also disrupts the crystalline sites and leads to the absorption of more water (Tester & Morrison, 1990; Pinkrová et al., 2011).

Correlations were performed to determine the relationships between the hydration properties of starches. Swelling power was negatively correlated with solubility ($r = -0.72$, $p = 0.002$), and water absorption capacity ($r = -0.56$, $p = 0.03$). Water absorption capacity was positively correlated with solubility ($r = 0.72$, $p = 0.002$). These correlations suggest that PAW treatment of starches at different temperatures enhanced the ability of these starches to hold water without necessarily swelling. On the other hand, starches modified with PAW at different temperatures would dissolve in solution relatively easily.

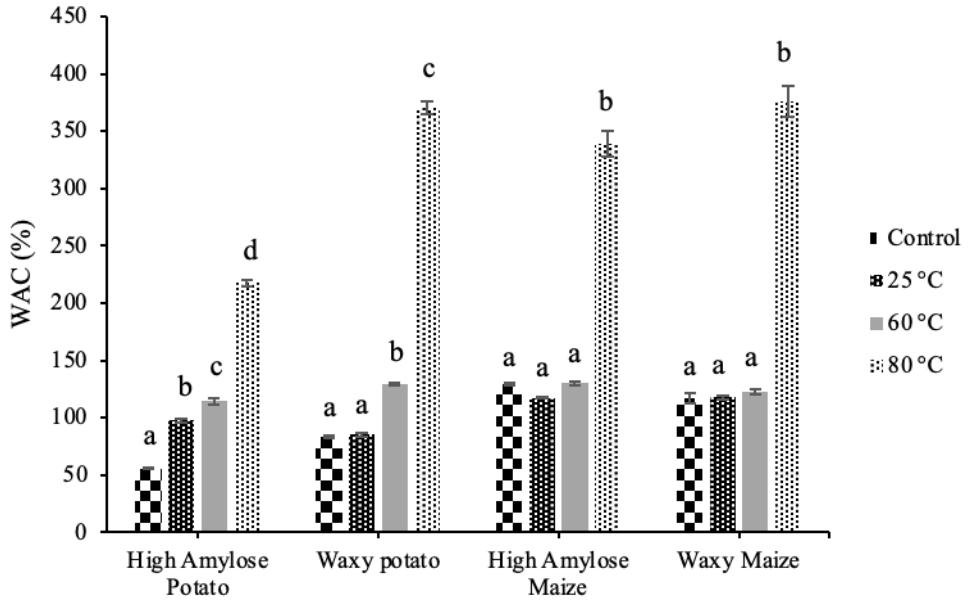

Figure 5-3: Water Absorption Capacity of PAW treated and untreated starches

Lowercase letters show significant differences ($p < 0.05$) between treated and untreated starches of the same type; Control = untreated starches, 25°C = Plasma-activated water starch incubated at 25°C, 60°C = Plasma-activated water starch incubated at 60°C, 80°C = Plasma-activated water starch incubated at 80°C.

5.4.5 Fourier transform infrared spectroscopy-attenuated total reflectance (FTIR-ATR) measurement of treated and untreated starches

The infrared spectra of the treated and untreated starches are shown in Figure 5-4. All the starches were characterized by bands at 765 cm^{-1} (C-C stretching), 860-866 cm^{-1} (C(1)-H, CH_2 deformation), 930-961 cm^{-1} (C-O-C skeletal mode of glycosidic linkage), 1018-1094 cm^{-1} (C-O-H bending), 1149-1162 cm^{-1} (C-O-C asymmetric stretching of the glycosidic bond), 1344-1348 cm^{-1} (C-O-H bending, CH_2 twisting), and 1415-1429 cm^{-1} (CH_2 bending, C-O-O stretch) (Kizil et al., 2002; Deeyai et al., 2013; Abdullah et al., 2018; Pozo et al., 2018). The band at 1640-1670 cm^{-1} shows the water adsorbed in the amorphous

part of starch, while the bands at 2900-3000 cm^{-1} and 3000-3600 cm^{-1} correspond to the CH, CH_2 stretching region and O-H stretching region, respectively (Kizil et al., 2002; Deeyai et al., 2013; Abdullah et al., 2018; Pozo et al., 2018). The absorption bands of the treated and untreated starches were mostly overlapping. However, we observed a distinct reduction in peak height of the O-H stretching region compared to the controls in both potato starches (PAW-HAPS and PAW-WPS) treated at 80°C and in PAW-HAMS at all temperatures. This suggests that treatment of starches in plasma-activated water at different temperatures did not induce the formation of any new hydroxyl functional groups (Thirumdas et al., 2017).

We also observed a slight increase in the peak height of the O-H stretching region in PAW-WMS 60°C and PAW-WMS 80°C, indicating the incorporation of new hydroxyl functional groups. We also observed distinct increases in the peak height of the C-OH bending region, CH_2 twisting region, CH_2 bending, C-O-O stretch, and CH, CH_2 stretching region in PAW-HAPS 80°C. Although there was an elevation in the peak height of C-O-C skeletal mode of glycosidic linkage in PAW-HAPS 80°C, this does not suggest the occurrence of cross-linking since there was no corresponding increase in the relative intensity (Table 3). However, treatment of starches with plasma-activated water at different temperatures induced the formation of cross-linking via ether linkages in PAW-WMS 80°C and PAW-HAPS 25°C (Zou, Liu, & Eliasson, 2004; Okyere et al., 2019).

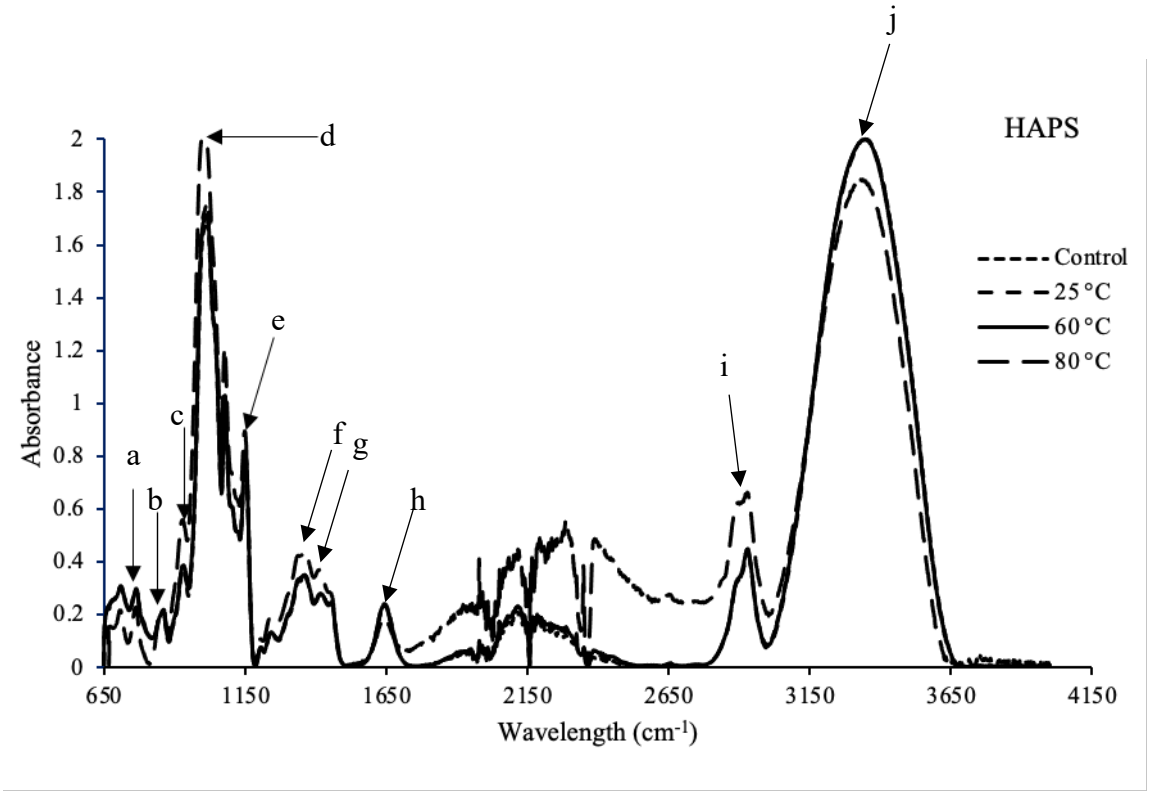
HAPS
Absorbance
Wavelength (cm-1)
Control
25 °C
60 °C
80 °C
a
b
c
d
e
f
g
h
i
j

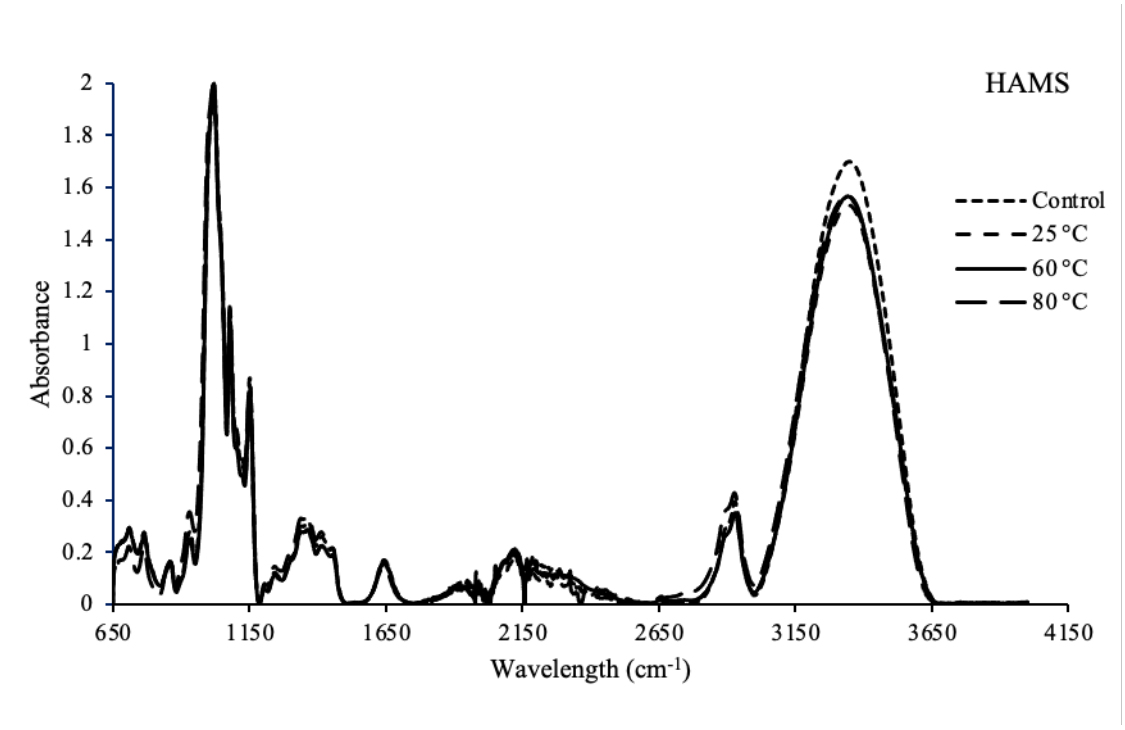
HAMS
Absorbance
Wavelength (cm-1)
Control
25 °C
60 °C
80 °C

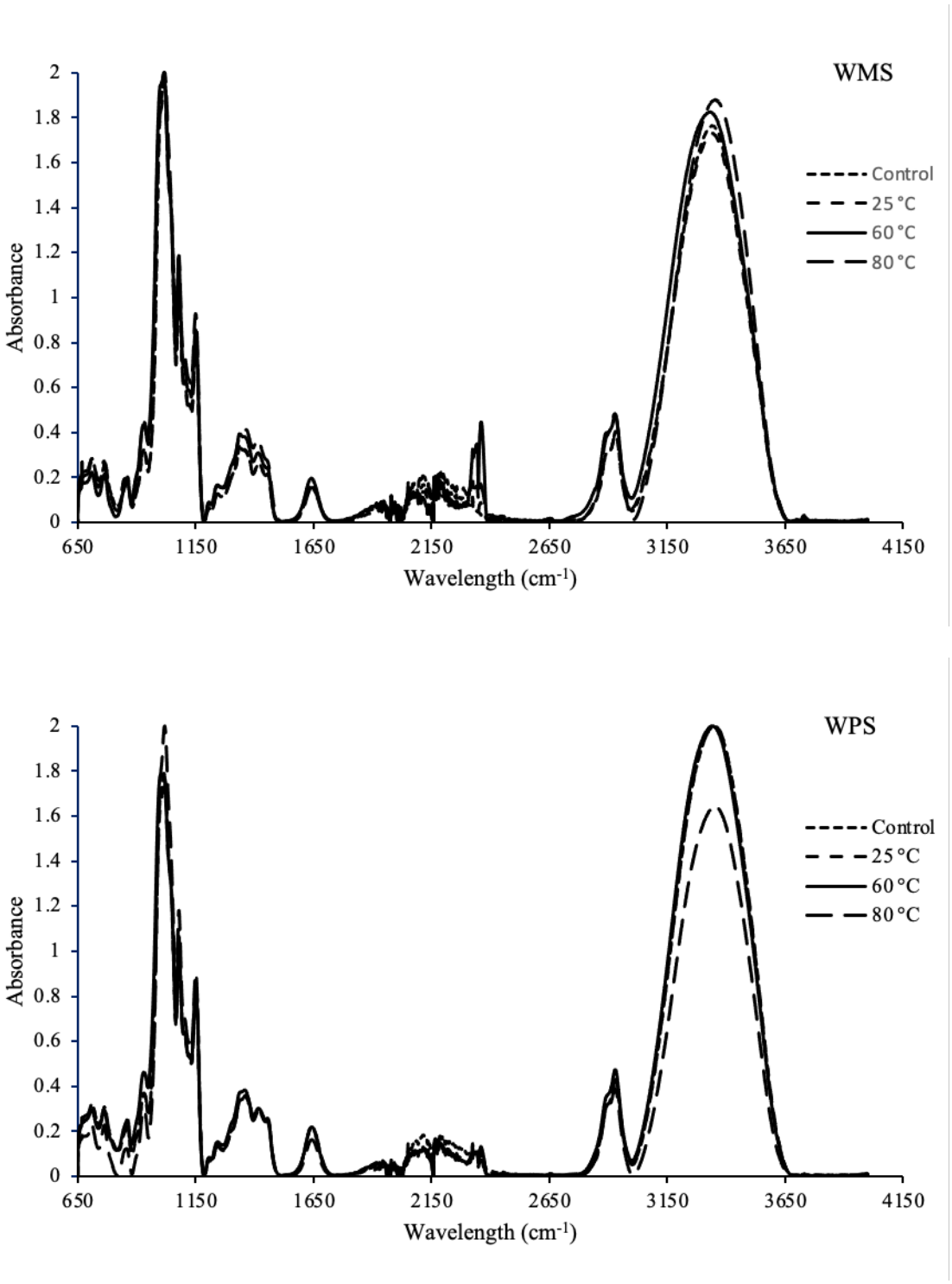

Figure 5-4: FTIR-ATR spectra of PAW treated and untreated starches

HAPS = High Amylose Potato Starches, HAMS = High Amylose Maize Starches, WMS = Waxy Maize Starches and WPS = Waxy Potato starches. In all the graphs, Control =

untreated Starches, 25°C = Plasma-activated water starch incubated at 25°C, 60°C = Plasma-activated water starch incubated at 60°C, 80°C = Plasma-activated water starch incubated at 80°C.

a = C-C stretching, b = C (1)-H, CH_2 deformation, c = C-O-C skeletal mode of glycosidic linkage, d = C-O-H bending, e = C-O-C asymmetric stretching of the glycosidic bond, f = C-O-H bending, CH_2 twisting, g = CH_2 bending, C-O-O stretch, h = water adsorbed in the amorphous part of starch, i = CH, CH_2 stretching region, and h = O-H stretching region.

Table 5-3: Relative Intensities of C-O-C Glycosidic Linkages after FTIR-ATR Analysis

Sample	Relative Intensities of C-O-C Glycosidic Linkages	
	930cm^{-1}	1150cm^{-1}
WMS	0.140	0.321
PAW-WMS 25°C	0.137	0.305
PAW-WMS 60°C	0.119	0.327
PAW-WMS 80°C	0.141	0.343
HAMS	0.139	0.390
PAW-HAMS 25°C	0.125	0.373
PAW-HAMS 60°C	0.128	0.360
PAW-HAMS 80°C	0.108	0.320
WPS	0.139	0.365
PAW-WPS 25°C	0.137	0.337
PAW-WPS 60°C	0.107	0.354
PAW-WPS 80°C	0.151	0.348
HAPS	0.142	0.354
PAW-HAPS 25°C	0.144	0.361
PAW-HAPS 60°C	0.139	0.359
PAW-HAPS 80°C	0.108	0.313

The different incubation temperatures for the starches are attached to the sample name.
WMS: Waxy Maize Starch, PAW-WMS 25°C : Plasma-Activated Water Waxy Maize Starch 25°C, PAW-WMS 60°C: Plasma-Activated Water Waxy Maize Starch 60°C, PAW-WMS 80°C: Plasma-Activated Water Waxy Maize Starch 80°C, HAMS: High Amylose Maize Starch, PAW-HAMS 25°C : Plasma-Activated Water High Amylose Maize Starch 25°C, PAW-HAMS 60°C: Plasma-Activated Water High Amylose Maize Starch 60°C, PAW-HAMS 80°C: Plasma-Activated Water High Amylose Maize Starch 80°C, WPS: Waxy Potato Starch, PAW-WPS 25°C: Plasma-Activated Water Waxy Potato Starch 25°C, PAW-WPS 60°C: Plasma-Activated Water Waxy Potato Starch 60°C, PAW-WPS 80°C: Plasma-Activated Water Waxy Potato Starch 80°C, HAPS: High Amylose Potato Starch, PAW-HAPS 25°C: Plasma-Activated Water High Amylose Potato Starch 25°C, PAW-HAPS 60°C: Plasma-Activated Water High Amylose Potato Starch 60°C, PAW-HAPS 80°C: Plasma-Activated Water High Amylose Potato Starch 80°C

5.4.6 X-ray photoelectron spectroscopy analysis of treated and untreated starches

The major elements present in the starches were carbon and oxygen as shown by the XPS survey scan (Table 5-4) (Figure D1). Minute quantities of nitrogen were detected in PAW-WMS 25°C, PAW-WMS 60°C, HAMS, PAW-HAMS 60°C, HAPS, PAW-HAPS 25°C, and PAW-HAPS 60°C, which indicates the presence of protein residues on the starch granule surface (Russell et al., 1987; Saad et al., 2011). Also, it could be an indication of plasma-activated water inducing the formation of reactive nitrogen species on the granule surface in the case of PAW-WMS 25°C and PAW-WMS 60°C since we did not detect any nitrogen in the untreated WMS (Thirumdas et al., 2018). Trace quantities of silicon (Si_{2p}) was also detected on the surface of PAW-WMS 80°C, PAW-WPS 60°C, PAW-HAPS 25°C, PAW-HAPS 60°C, and PAW-HAPS 80°C, which was due to contamination from the air (Russell et al., 1987; Saad et al., 2011). Starch has a theoretical O/C ratio of 0.83 based on the formula $(C_6H_{10}O_5)_n$ (Russell et al., 1987; Angellier et al., 2005). From our study, the experimental O/C ratio calculated using the sum of peak areas due to O-C-O (287.8) and C-O (286.5) as a measure of carbon content ranged from 0.66-0.90 in both treated and untreated starches. Except for WMS, all the experimental O/C ratio were either lower or higher than theoretical O/C ratio and thus indicates the presence of other surface components besides glucose polymers on the starch (Russell et al., 1987). These components could either be lipids or protein residues (Saad et al., 2011).

The C_{1s} core level spectrum was curve fitted to obtain four component peaks at 285 (C1), 286.5 (C2), 287.8 (C3), and 289.1 eV (C4) (Table 5-5)(Figure E1). The peak at 285 eV is characteristic of a carbon bonded to a carbon and/or a hydrogen atom. The peak at 286.5eV denotes carbon singly bonded to an oxygen atom, while the peak at 287.8eV

denotes carbon atoms bonded to two non-carbonyl oxygen atoms or to a single carbonyl oxygen atom. The final peak at 289.1eV is characteristic of carbon atoms bonded to a single oxygen atom and to a carbonyl oxygen (Russell et al., 1987; Angellier et al., 2005; Saad et al., 2011). The peaks observed at C-C/C-H and O-C=O further confirms the presence of lipids on the starch surface (Angellier et al., 2005; Wei et al., 2014). Treatment of starches in plasma-activated water at different temperatures successfully decreased the content of C1, C2 (except in PAW-HAMS 60°C), while increasing the content of C4 in PAW-WMS 60°C, PAW-WMS 80°C, PAW-HAMS 60°C and PAW-HAMS 80°C. This indicates that these structures were disrupted during heat treatment and oxidized by the reactive species in PAW into carboxyl groups (Bie et al., 2016). Contrarily, we observed increases in the content of C1, C2, and C3 in PAW-WMS 25°C (except C3), PAW-HAMS 25°C (except C2 and C3), PAW-WPS 25°C (except C2 and C3), PAW-WPS 60°C (C2 and C3), PAW-WPS 80°C (except C1), as well as PAW-HAPS 25°C, 60°C, and 80°C, which suggests some level of polymerization taking place in these starches (Zhu, 2017). Overall, the XPS data show that PAW treatment of starches at different temperatures successfully altered the surface molecular structure of these starches.

Table 5-4: Elemental surface composition (atomic %) and oxygen to carbon ratio of treated and untreated starches measured by XPS

Samples	O_{1s} (%)	C_{1s} (%)	O_{1s}/C_{1s}	N_{1s} (%)	Si_{2p} (%)
WMS	45.5	54.5	0.83	-	-
PAW-WMS 25°C	46.0	54.0	0.85	< 0.1	-
PAW-WMS 60°C	43.9	55.1	0.80	1.0	-
PAW-WMS 80°C	46.7	52.5	0.89	-	0.8
HAMS	41.5	57.8	0.72	0.6	-
PAW-HAMS 25°C	42.2	57.8	0.73	-	-
PAW-HAMS 60°C	43.1	55.3	0.78	1.5	-
PAW-HAMS 80°C	46.6	53.4	0.87	-	-
WPS	45.0	55.0	0.82	-	-
PAW-WPS 25°C	44.5	55.5	0.80	-	-
PAW-WPS 60°C	44.4	55.1	0.81	-	0.4
PAW-WPS 80°C	45.2	54.8	0.82	-	-
HAPS	37.6	57.4	0.66	5.0	-
PAW-HAPS 25°C	40.7	56.2	0.72	3.1	-
PAW-HAPS 60°C	39.7	56.8	0.70	3.1	0.4
PAW-HAPS 80°C	47.1	52.4	0.90	-	0.4

*The subscript on the elements denotes the orbital from which the electrons are displaced.

The different incubation temperatures for the starches are attached to the sample name.
WMS: Waxy Maize Starch, PAW-WMS 25°C : Plasma-Activated Water Waxy Maize Starch 25°C, PAW-WMS 60°C: Plasma-Activated Water Waxy Maize Starch 60°C, PAW-WMS 80°C: Plasma-Activated Water Waxy Maize Starch 80°C, HAMS: High Amylose Maize Starch, PAW-HAMS 25°C : Plasma-Activated Water High Amylose Maize Starch 25°C, PAW-HAMS 60°C: Plasma-Activated Water High Amylose Maize Starch 60°C, PAW-HAMS 80°C: Plasma-Activated Water High Amylose Maize Starch 80°C, WPS: Waxy

Potato Starch, PAW-WPS 25°C: Plasma-Activated Water Waxy Potato Starch 25°C, PAW-WPS 60°C: Plasma-Activated Water Waxy Potato Starch 60°C, PAW-WPS 80°C: Plasma-Activated Water Waxy Potato Starch 80°C, HAPS: High Amylose Potato Starch, PAW-HAPS 25°C: Plasma-Activated Water High Amylose Potato Starch 25°C, PAW-HAPS 60°C: Plasma-Activated Water High Amylose Potato Starch 60°C, PAW-HAPS 80°C: Plasma-Activated Water High Amylose Potato Starch 80°C

Table 5-5: Surface functional group composition obtained from curve fitting C1s XPS spectra of treated and untreated starches

Samples	C1 (%)	C2 (%)	C3 (%)	C4 (%)
	C-C/C-H	C-O	O-C-O/C=O	O-C=O-
Binding Energies (eV)	285.0±0.3	286.5±0.3	287.8±0.3	289.1±0.3
WMS	17.7	52.7	22.2	7.5
PAW-WMS 25°C	19.1	56.5	19.7	4.7
PAW-WMS 60°C	16.7	51.1	23.0	9.2
PAW-WMS 80°C	7.9	31.3	41.5	19.3
HAMS	20.5	53.3	19.5	6.8
PAW-HAMS 25°C	14.9	49.1	29.3	6.8
PAW-HAMS 60°C	12.1	53.8	25.3	8.9
PAW-HAMS 80°C	9.9	34.6	39.3	16.3
WPS	14.9	53.6	23.7	7.8
PAW-WPS 25°C	17.8	53.3	22.5	6.4
PAW-WPS 60°C	27.5	46.5	20.6	5.5
PAW-WPS 80°C	12.1	56.5	27.2	4.3
HAPS	6.8	17.2	18.0	58.0
PAW-HAPS 25°C	17.2	45.5	26.6	10.8
PAW-HAPS 60°C	19.2	44.5	27.0	9.3
PAW-HAPS 80°C	14.2	56.7	22.8	6.3

*The subscript on the elements denotes the orbital from which the electrons are displaced. The binding energy for the C_{1s} spectra is expressed as the mean ± standard deviation for each sample.

The different incubation temperatures for the starches are attached to the sample name.
WMS: Waxy Maize Starch, PAW-WMS 25°C : Plasma-Activated Water Waxy Maize Starch 25°C, PAW-WMS 60°C: Plasma-Activated Water Waxy Maize Starch 60°C, PAW-WMS 80°C: Plasma-Activated Water Waxy Maize Starch 80°C, HAMS: High Amylose Maize Starch, PAW-HAMS 25°C : Plasma-Activated Water High Amylose Maize Starch 25°C, PAW-HAMS 60°C: Plasma-Activated Water High Amylose Maize Starch 60°C, PAW-HAMS 80°C: Plasma-Activated Water High Amylose Maize Starch 80°C, WPS: Waxy Potato Starch, PAW-WPS 25°C: Plasma-Activated Water Waxy Potato Starch 25°C, PAW-WPS 60°C: Plasma-Activated Water Waxy Potato Starch 60°C, PAW-WPS 80°C: Plasma-Activated Water Waxy Potato Starch 80°C, HAPS: High Amylose Potato Starch, PAW-HAPS 25°C: Plasma-Activated Water High Amylose Potato Starch 25°C, PAW-HAPS 60°C: Plasma-Activated Water High Amylose Potato Starch 60°C, PAW-HAPS 80°C: Plasma-Activated Water High Amylose Potato Starch 80°C

5.5 Conclusion

Incubation of the starches at 60°C during plasma-activated water treatment increases the gelatinization parameters and induces the formation of stable amylopectin crystals. Plasma-activated water treatment at 80°C is effective in increasing the water absorption capacity and solubility, while decreasing the swelling power of cereal and tuber waxy and high amylose starches. FTIR-ATR data showed the occurrence of cross-linking in plasma-activated water waxy maize and high amylose potato starches incubated at 80°C and 25°C respectively. Chemical surface analysis showed carbon and oxygen as the dominant elements in the starches with trace quantities of nitrogen and silicon in some cases. Plasma-activated water and incubation of the starches at ≥ 60°C induced the oxidation of C-C/C-H and C-O in carboxyl groups. Overall, incubation of the starches at 60°C and 80°C during plasma-activated water treatment was more effective in altering the thermal and hydration properties, as well as the chemical surface of the starches.

5.6 Funding

This research did not receive any specific grant from funding agencies in the public, commercial, or non-profit sectors.

5.7 Acknowledgements

The authors are grateful to Professor Daniel D. Gallaher and Cynthia M. Gallaher (Department of Food Science and Nutrition, University of Minnesota) for their excellent assistance. Parts of this work was also carried out in the Characterization Facility, University of Minnesota, which receives partial support from NSF through the MRSEC program with the help of Dr. Bing Luo.

5.8 Conflict of interest

The authors declare no conflict of interest.

Chapter 6: Conclusions and recommendations

To investigate the effects of radio frequency cold plasma (RF) and plasma-activated water (PAW) on starch properties, this three-part study treated waxy and high amylose cereal and tuber starches with RF and PAW. For the first study, waxy maize, rice and potato starches were modified with a carbon dioxide-argon radio frequency cold plasma at 0 and 120 W of power. At 0 W of power the starches were treated with gases in the RF plasma chamber with no RF plasma power to determine the effect of just the gases on starch properties. Treatment of starches with cold plasma or gas did not affect the ability of the starches to form inclusion complexes with iodine. The λ_{max} and peak values of waxy potato increased ($p<0.05$) after plasma treatment suggesting the ability of RF plasma to remove some amylopectin branches and cause longer internal chain segments to react with iodine. Slight increases were observed in the internal chain length of waxy potato which confirms the above-mentioned statement. Plasma or gas treatment did not induce the formation of any new fissures or cavities in the starches as show by SEM data. Light optical microscopy images displayed characteristic angular shapes for maize and rice, and a characteristic oval shape for potato in both treated and untreated starches. Decreases ($p<0.05$) were observed in the crystallinity of waxy potato after plasma and gas treatment but not in rice and maize. Thus, the B-type crystalline starches are more susceptible to degradation than the A-type crystal starches. This is possibly because they hold more water molecules in their unit cells which could breakdown and react with the plasma reactive species and cause decreases in crystallinity. The enthalpy of gelatinization was higher after treatment indicating the presence of longer double helices in these starches. The breakdown values were much lower in maize and rice after plasma treatment indicating the stability of these starch pastes.

Lower setback and final viscosities also showed the ability of plasma to reduce the onset of retrogradation in waxy maize, rice, and potato. Solid state ^{13}C NMR analysis showed the formation of V-type single helices in maize and rice suggesting the formation of starch-lipid complexes. Plasma or gas treatment induced damages in the starch structure. Also, starches were more resistant to digestion after plasma or gas treatment.

In the second study, granular or non-granular waxy maize, rice and potato starches were treated with a carbon dioxide-argon radio frequency cold plasma at 120 W of power. Plasma treatment induced slight decreases in the carbohydrate concentration at the peak DP of the short chains at DP $\geq$ 12 in granular and non-granular waxy maize and rice. Subsequent increases were observed in the carbohydrate concentration of the long chains from DP $\geq$ 62 in granular and non-granular waxy rice and maize. Slight increases were observed in the internal chain length of granular waxy potato and rice after plasma treatment. *In vitro* digestion studies showed an increase ($p < 0.05$) in the amount of rapidly digestible starches in granular waxy maize. The amount of slowly digestible starches increased ($p < 0.05$) in non-granular waxy maize and rice starch. The content of resistant starches was much higher after plasma treatment in non-granular waxy maize and granular waxy potato after plasma treatment. In general, the ratio of SDS:TDS was much higher after plasma treatment showing that carbon dioxide-argon radio frequency cold plasma was successful in slowing down the rate of starch digestion. FTIR-ATR data confirmed the occurrence of cross-linking in non-granular waxy maize and rice, and in granular waxy rice and potato starch after plasma treatment. These cross-linked networks would stabilize the starch and afford starch the ability to withstand high temperature and pressure treatments.

Also, FTIR-ATR data confirmed the ability of plasma to incorporate hydroxyl functional groups in non-granular waxy maize and rice, and granular waxy rice.

Plasma-activated water (PAW) at different temperatures (25°C, 60°C, 80°C) was used to modify high amylose maize, high amylose potato, waxy maize and waxy potato. Plasma-activated water at 60°C significantly increased the gelatinization parameters (T_o, T_p, T_c, and ΔH) of all the starches except for waxy potato in which we observed a decrease in ΔH. The swelling power of all the starches reduced after treatment with PAW at different temperatures. However, marked increases were observed in the water absorption capacities and solubility. XPS analysis showed carbon and oxygen as the dominant elements in both treated and untreated starches with trace quantities of nitrogen or silicon in some of the starches. In addition, plasma-activated water at $\geq$ 60°C induced the oxidation of C-C/C-H and C-O into carboxyl groups in the starches. FTIR-ATR data showed the occurrence of cross-linking in waxy maize and high amylose potato starches treated with PAW at 80°C and 25°C respectively.

Overall, carbon dioxide-argon radio frequency cold plasma significantly altered most of the starch properties studied. This makes RF an environmentally friendly alternative for starch modification. Similar conclusions can be made for PAW. The changes observed however did not occur at the molecular level of the starches. It would be interesting for future studies to explore an in-depth comparative study on the different cold plasma setups or types and their effect on the various botanical starches. This would help in identifying which cold plasma type is best suited for modifying a particular botanical starch. In addition, a detailed study on the toxicity of starches modified with carbon dioxide-argon radio frequency cold plasma and plasma-activated water would help in the

adoption of these starches in food use. A consumer research study on foods in which cold plasma modified starches have been used can help in determining the acceptability of cold plasma modified starches.

Comprehensive Bibliography

Abdullah, A. H. D., Chalimah, S., Primadona, I., & Hanantyo, M. H. G. (2018). Physical and chemical properties of corn, cassava, and potato starchs. *IOP Conference Series: Earth and Environmental Science*, *160*, 012003. https://doi.org/10.1088/1755-1315/160/1/012003

Abidin, N., Rukunudin, I., & Zaaba, S. (2018). Atmospheric pressure cold plasma (ACP) treatment a new technique to improve microstructure and textural properties of healthy noodles fortified with mango flour. J*ournal of Telecommunication Electronic and Computer Engineering, 10.*

Abou-Ghazala, A., Katsuki, S., Schoenbach, K. H., Dobbs, F. C., & Moreira, K. R. (2002). Bacterial decontamination of water by means of pulsed-corona discharges. *IEEE Transactions on Plasma Science,* 30, 1449–1453. https://doi.org/10.1109/TPS.2002.804193.

Abuzairi, T., Ramadhanty, S., Puspohadiningrum, D. F., Ratnasari, A., Poespawati, N. R., & Purnamaningsih, R. W. (2018). Investigation on physicochemical properties of plasma-activated water for the application of medical device sterilization. Presented at the 2nd biomedical engineering's recent progress in biomaterials, drugs development, and medical devices: Proceedings of the International Symposium of Biomedical Engineering (ISBE) 2017, Bali, Indonesia, p. 040017. https://doi.org/10.1063/1.5023987.

Adhikari, B., Adhikari, M., Ghimire, B., Park, G., & Choi, E. H. (2019). Cold Atmospheric Plasma-Activated Water Irrigation Induces Defense Hormone and

Gene expression in Tomato seedlings. *Scientific Reports*, *9*(1), 16080. https://doi.org/10.1038/s41598-019-52646-z

Aditya, S., Gnanasekaran, S., Stephen, J., & Radhakrishnan, M. (2020). Enhancing the properties of eggshell powder by cold plasma for improved calcium fortification in black coffee. *Journal of Food Processing Engineering*, 43, e13450. https://doi.org/10.1111/jfpe.13450

Ai, Y., & Jane, J. (2018). Understanding Starch Structure and Functionality. In *Starch in Food* (pp. 151–178). Elsevier. https://doi.org/10.1016/B978-0-08-100868-3.00003-2

Akasapu, K., Ojah, N., Gupta, A. K., Choudhury, A. J., & Mishra, P. (2020). An innovative approach for iron fortification of rice using cold plasma. *Food Research International*, 136, 109599. https://doi.org/10.1016/j.foodres.2020.109599.

Alimi, B.A., & Workneh, T.S. (2018). Structural and physicochemical properties of heat moisture treated and citric acid modified acha and iburu starches. *Food Hydrocolloids*, 81, 449–455. https://doi.org/10.1016/j.foodhyd.2018.03.027.

Amini, M., & Ghoranneviss, M. (2016). Effects of cold plasma treatment on antioxidants activity, phenolic contents and shelf life of fresh and dried walnut (Juglans regia L.) cultivars during storage. *LWT,* 73, 178–184. https://doi.org/10.1016/j.lwt.2016.06.014.

Andrade, C. T., Simão, R. A., Thiré, R. M. S. M., & Achete, C. A. (2005). Surface modification of maize starch films by low-pressure glow 1-butene plasma.

Carbohydrate Polymers, *61*(4), 407–413. https://doi.org/10.1016/j.carbpol.2005.05.001

Angellier, H., Molina-Boisseau, S., Belgacem, M. N., & Dufresne, A. (2005). Surface Chemical Modification of Waxy Maize Starch Nanocrystals. *Langmuir*, *21*(6), 2425–2433. https://doi.org/10.1021/la047530j

Annor, G. A., Marcone, M., Bertoft, E., & Seetharaman, K. (2014a). Unit and Internal Chain Profile of Millet Amylopectin. *Cereal Chemistry Journal*, *91*(1), 29–34. https://doi.org/10.1094/CCHEM-08-13-0156-R

Annor, G. A., Marcone, M., Bertoft, E., & Seetharaman, K. (2014b). Physical and Molecular Characterization of Millet Starches. *Cereal Chemistry Journal*, *91*(3), 286–292. https://doi.org/10.1094/CCHEM-08-13-0155-R

Bailey, J. M., & Whelan, W. J. (1961). Physical Properties of Starch. *Journal of Biological Chemistry*, *236*(4), 969–973. https://doi.org/10.1016/S0021-9258(18)64226-7

Banura, S., Thirumdas, R., Kaur, A., Deshmukh, R. R., & Annapure, U. S. (2018). Modification of starch using low pressure radio frequency air plasma. *LWT*, *89*, 719–724. https://doi.org/10.1016/j.lwt.2017.11.056

Bello-Pérez, L.A., Ottenhof, M.-A., Agama-Acevedo, E., & Farhat, I.A. (2005). Effect of Storage Time on the Retrogradation of Banana Starch Extrudate. *Journal of Agricultural and Food Chemistry*, 53, 1081–1086. https://doi.org/10.1021/jf048858l

Bemiller, J. N. (1997). Starch Modification: Challenges and Prospects. *Starch - Stärke*, *49*(4), 127–131. https://doi.org/10.1002/star.19970490402

BeMiller, J. N., & Whistler, R. L. (2009). Starch: chemistry and technology. *Oxford: Academic Press.*

Bertoft, E. (1989). Partial characterisation of amylopectin alpha-dextrins. *Carbohydrate Research, 189, 181–193.* https://doi.org/10.1016/0008-6215(89)84096-0

Bertoft, E. (2004). On the nature of categories of chains in amylopectin and their connection to the super helix model. *Carbohydrate Polymers*, *57*(2), 211–224. https://doi.org/10.1016/j.carbpol.2004.04.015

Bertoft, E. (2017). Understanding Starch Structure: Recent Progress. *Agronomy*, *7*(3), 56. https://doi.org/10.3390/agronomy7030056

Bertoft, E., Annor, G. A., Shen, X., Rumpagaporn, P., Seetharaman, K., & Hamaker, B. R. (2016). Small differences in amylopectin fine structure may explain large functional differences of starch. *Carbohydrate Polymers*, *140*, 113–121. https://doi.org/10.1016/j.carbpol.2015.12.025

Bertoft, E., Piyachomkwan, K., Chatakanonda, P., & Sriroth, K. (2008). Internal unit chain composition in amylopectins. *Carbohydrate Polymers*, *74*(3), 527–543. https://doi.org/10.1016/j.carbpol.2008.04.011

Bethke, P. C., & Jansky, S. H. (2008). The Effects of Boiling and Leaching on the Content of Potassium and Other Minerals in Potatoes. *Journal of Food Science*, *73*(5), H80–H85. https://doi.org/10.1111/j.1750-3841.2008.00782.x

Bie, P., Li, X., Xie, F., Chen, L., Zhang, B., & Li, L. (2016). Supramolecular structure and thermal behavior of cassava starch treated by oxygen and helium glow-

plasmas. *Innovative Food Science & Emerging Technologies*, *34*, 336–343. https://doi.org/10.1016/j.ifset.2016.03.005

Bie, P., Pu, H., Zhang, B., Su, J., Chen, L., & Li, X. (2016). *Structural characteristics and rheological properties of plasma-treated starch*. 10.

Bogaerts, A., Neyts, E., Gijbels, R., & van der Mullen, J. (2002). Gas discharge plasmas and their applications. *Spectrochimica Acta Part B: Atomic Spectroscopy*, *57*(4), 609–658. https://doi.org/10.1016/S0584-8547(01)00406-2

Bogracheva, T. Ya., Wang, Y. L., & Hedley, C. L. (2001). The effect of water content on the ordered/disordered structures in starches. *Biopolymers*, *58*(3), 247–259. https://doi.org/10.1002/1097-0282(200103)58:3<247::AID-BIP1002>3.0.CO;2-L

Brandenburg, R. (2018). Corrigendum: Dielectric barrier discharges: progress on plasma sources and on the understanding of regimes and single filaments (2017 Plasma Sources Sci. Technol. 26 053001. *Plasma Sources Science & Technology,* 27, 079501. https://doi.org/10.1088/1361-6595/aaced9.

Bu, F., Nayak, G., Bruggeman, P., Annor, G., & Ismail, B. P. (2022). Impact of plasma reactive species on the structure and functionality of pea protein isolate. *Food Chemistry*, *371*, 131135. https://doi.org/10.1016/j.foodchem.2021.131135

Buléon, A., Gérard, C., Riekel, C., Vuong, R., & Chanzy, H. (1998). Details of the Crystalline Ultrastructure of C-Starch Granules Revealed by Synchrotron Microfocus Mapping. *Macromolecules*, *31*(19), 6605–6610. https://doi.org/10.1021/ma980739h

Bursać Kovačević, D., Gajdoš Kljusurić, J., Putnik, P., Vukušić, T., Herceg, Z., & Dragović-Uzelac, V. (2016a). Stability of polyphenols in chokeberry juice treated

with gas phase plasma. *Food Chemistry*, 212, 323–331. https://doi.org/10.1016/j.foodchem.2016.05.192.

Bursać Kovačević, D., Putnik, P., Dragović-Uzelac, V., Pedisić, S., Režek Jambrak, A., & Herceg, Z. (2016b). Effects of cold atmospheric gas phase plasma on anthocyanins and color in pomegranate juice. *Food Chemistry*, 190, 317–323. https://doi.org/10.1016/j.foodchem.2015.05.099

Carvalho, A. P. M. G., Barros, D. R., da Silva, L. S., Sanches, E. A., Pinto, C. da C., de Souza, S. M., Clerici, M. T. P. S., Rodrigues, S., Fernandes, F. A. N., & Campelo, P. H. (2021). Dielectric barrier atmospheric cold plasma applied to the modification of Ariá (Goeppertia allouia) starch: Effect of plasma generation voltage. *International Journal of Biological Macromolecules*, *182*, 1618–1627. https://doi.org/10.1016/j.ijbiomac.2021.05.165

Casper, J. L., & Atwell, W. A. (2014). Gluten-free baked product. In American Associate of Cereal Chemists International (Pp. 23-47). AACC International Press.

Chaiwat, W., Wongsagonsup, R., Tangpanichyanon, N., Jariyaporn, T., Deeyai, P., Suphantharika, M., Fuongfuchat, A., Nisoa, M., & Dangtip, S. (2016). Argon Plasma Treatment of Tapioca Starch Using a Semi-continuous Downer Reactor. *Food and Bioprocess Technology*, *9*(7), 1125–1134. https://doi.org/10.1007/s11947-016-1701-6

Chang, E. H., Bae, Y. S., Shin, I. S., Choi, H. J., Lee, J. H., & Choi, J. W. 2018). Microbial decontamination of onion by corona discharge air plasma during cold storage. *Journal of Food Quality*, 3481806. https://doi.org/10.1155/2018/3481806.

Charoux, Clémentine M.G., Free, L., Hinds, L.M., Vijayaraghavan, R.K., Daniels, S., O'Donnell, C.P., & Tiwari, B.K. (2020). Effect of non-thermal plasma technology on microbial inactivation and total phenolic content of a model liquid food system and black pepper grains. *LWT,* 118, 108716. https://doi.org/10.1016/j.lwt.2019.108716.

Chauhan, F., & Seetharaman, K. (2013). On the organization of chains in amylopectin. *Starch - Stärke*, *65*(3–4), 191–199. https://doi.org/10.1002/star.201200132

Chen, L., Ma, R., Zhang, Z., Huang, M., Cai, C., Zhang, R., McClements, D. J., Tian, Y., & Jin, Z. (2019). Comprehensive investigation and comparison of surface microstructure of fractionated potato starches. *Food Hydrocolloids*, *89*, 11–19. https://doi.org/10.1016/j.foodhyd.2018.10.017

Chen, Y.-F., Kaur, L., & Singh, J. (2018). Chemical Modification of Starch. In *Starch in Food* (pp. 283–321). Elsevier. https://doi.org/10.1016/B978-0-08-100868-3.00007-X

Chizoba Ekezie, F.-G., Sun, D.-W., & Cheng, J.-H. (2017). A review on recent advances in cold plasma technology for the food industry: Current applications and future trends. *Trends in Food Science and Technology*, 69, 46–58. https://doi.org/10.1016/j.tifs.2017.08.007.

Chrastil, J. (1987). Improved colorimetric determination of amylose in starches or flours. *Carbohydrate Research, 159*(1), 154-158. https://doi.org/10.1016/S0008-6215(00)90013-2

Collart, E. J. H., Baggerman, J. A. G., & Visser, R. J. (1991). Excitation mechanisms of oxygen atoms in a low pressure O 2 radio-frequency plasma. *Journal of Applied Physics*, *70*(10), 5278–5281. https://doi.org/10.1063/1.350237

Conrads, H., & Schmidt, M. (2000). Plasma generation and plasma sources. *Plasma Sources Science and Technology*, *9*(4), 441–454. https://doi.org/10.1088/0963-0252/9/4/301

Crookes, W. (1879). On radiant matter. A lecture to the British association for the advancement of science, in Sheffield, UK on Friday, 22nd August 1879.

Crookes, W. (1881). Radiant matter: a resume of the principal lectures and papers of Prof. William Crookes, on the 'fourth state of matter'. Philadelphia, PA: James W. Queen & Co.

Dai, Y., van Spronsen, J., Witkamp, G. J., Verpoorte, R., & Choi, Y. H. (2013). Natural deep eutectic solvents as new potential media for green technology. *Analytica Chimica Acta*, 766, 61–68.

Dasan, B.G., Boyaci, I.H., & Mutlu, M. (2017). Nonthermal plasma treatment of Aspergillus spp. spores on hazelnuts in an atmospheric pressure fluidized bed plasma system: Impact of process parameters and surveillance of the residual viability of spores. *Journal of Food Engineering*, 196, 139–149. https://doi.org/10.1016/j.jfoodeng.2016.09.028.

de Albuquerque, M. D. F., Bastos, D. C., & Simão, R. A. (2014). Surface Modification of Starch Films by Plasma. *Macromolecular Symposia*, *343*(1), 96–101. https://doi.org/10.1002/masy.201300199

Debet, M. R., & Gidley, M. J. (2006). Three classes of starch granule swelling: Influence of surface proteins and lipids. *Carbohydrate Polymers*, *64*(3), 452–465. https://doi.org/10.1016/j.carbpol.2005.12.011

Deeyai, P., Suphantharika, M., Wongsagonsup, R., & Dangtip, S. (2013). Characterization of Modified Tapioca Starch in Atmospheric Argon Plasma under Diverse Humidity by FTIR Spectroscopy. *Chinese Physics Letters*, *30*(1), 018103. https://doi.org/10.1088/0256-307X/30/1/018103

Desmet, T., Morent, R., De Geyter, N., Leys, C., Schacht, E., & Dubruel, P. (2009). Nonthermal Plasma Technology as a Versatile Strategy for Polymeric Biomaterials Surface Modification: A Review. *Biomacromolecules*, *10*(9), 2351–2378. https://doi.org/10.1021/bm900186s

Duan, J., & Kasper, D. L. (2011). Oxidative depolymerization of polysaccharides by reactive oxygen/nitrogen species. *Glycobiology*, *21*(4), 401–409. https://doi.org/10.1093/glycob/cwq171

DuBois, Michel., Gilles, K. A., Hamilton, J. K., Rebers, P. A., & Smith, Fred. (1956). Colorimetric Method for Determination of Sugars and Related Substances. *Analytical Chemistry*, *28*(3), 350–356. https://doi.org/10.1021/ac60111a017

Ebnesajjad, S. (2014). Plasma Treatment of Polymeric Materials. In *Surface Treatment of Materials for Adhesive Bonding* (pp. 227–269). Elsevier. https://doi.org/10.1016/B978-0-323-26435-8.00009-5

Elez Garofulić, I., Režek Jambrak, A., Milošević, S., Dragović-Uzelac, V., Zorić, Z., & Herceg, Z. (2015). The effect of gas phase plasma treatment on the anthocyanin and phenolic acid content of sour cherry Marasca (Prunus cerasus var. Marasca)

juice. *LWT - Food Science and Technology*, *62*(1), 894–900. https://doi.org/10.1016/j.lwt.2014.08.036

Eliasson, A.-C., & Ljunger, G. (1988). Interactions between amylopectin and lipid additives during retrogradation in a model system. *Journal of the Science of Food and Agriculture*, *44*(4), 353–361. https://doi.org/10.1002/jsfa.2740440408

Englyst, H. N., Kingman, S. M. & Cummings, J. H. (1992). Classification and measurement of nutritionally important starch fractions. *Eur. J. Clin. Nutr*., *46 (Suppl. 2), S33-S50.*

Fan, Y., & Picchioni, F., (2020). Modification of starch: A review on the application of "green" solvents and controlled functionalization. Carbohydrate Polymers, 241, 116350. https://doi.org/10.1016/j.carbpol.2020.116350

Fannon, J. E., Hauber, R. J., & BeMiller, J. N. (1992). Surface pores of starch granules. *Cereal Chemistry, 69, 284-288.*

French, D. (1972). Fine Structure of Starch and its Relationship to the Organization of Starch Granules. *Journal of the Japanese Society of Starch Science*, *19*(1), 8–25. https://doi.org/10.5458/jag1972.19.8

Fridman, G., Friedman, G., Gutsol, A., Shekhter, A. B., Vasilets, V. N., & Fridman, A. (2008). Applied Plasma Medicine. *Plasma Processes and Polymers*, *5*(6), 503–533. https://doi.org/10.1002/ppap.200700154

Frost, G., & Dornhorst, A. (2000). The relevance of the glycaemic index to our understanding of dietary carbohydrates. *Diabetic Medicine*, *17*(5), 336–345. https://doi.org/10.1046/j.1464-5491.2000.00266.x

Gallant, D. J., Bouchet, B., & Baldwin, P. M. (1997). Microscopy of starch: Evidence of a new level of granule organization. *Carbohydrate Polymers*, *32*(3–4), 177–191. https://doi.org/10.1016/S0144-8617(97)00008-8

Gao, S., Liu, H., Sun, L., Liu, N., Wang, J., Huang, Y., Wang, F., Cao, J., Fan, R., Zhang, X., & Wang, M. (2019). The effects of dielectric barrier discharge plasma on physicochemical and digestion properties of starch. *International Journal of Biological Macromolecules*, *138*, 819–830. https://doi.org/10.1016/j.ijbiomac.2019.07.147

Ge, X., Shen, H., Su, C., Zhang, B., Zhang, Q., Jiang, H., & Li, W. (2021). The improving effects of cold plasma on multi-scale structure, physicochemical and digestive properties of dry heated red adzuki bean starch. *Food Chemistry,* 349, 129159. https://doi.org/10.1016/j.foodchem.2021.129159

Ge, X., Shen, H., Su, C., Zhang, B., Zhang, Q., Jiang, H., Yuan, L., Yu, X., & Li, W. (2021b). Pullulanase modification of granular sweet potato starch: Assistant effect of dielectric barrier discharge plasma on multi-scale structure, physicochemical properties. *Carbohydrate Polymers*, *272*, 118481. https://doi.org/10.1016/j.carbpol.2021.118481

Gessler, K., Uson, I., Takaha, T., Krauss, N., Smith, S. M., Okada, S., Sheldrick, G. M., & Saenger, W. (1999). V-Amylose at atomic resolution: X-ray structure of a cycloamylose with 26 glucose residues (cyclomaltohexaicosaose). *Proceedings of the National Academy of Sciences*, *96*(8), 4246–4251. https://doi.org/10.1073/pnas.96.8.4246

Gibson, T. S., Al Qalla, H., & McCleary, B. V. (1992). An improved enzymic method for the measurement of starch damage in wheat flour. *Journal of Cereal Science*, *15*(1), 15–27. https://doi.org/10.1016/S0733-5210(09)80053-2

Gidley, M. J., & Bociek, S. M. (1985). Molecular organization in starches: A carbon 13 CP/MAS NMR study. *Journal of the American Chemical Society*, *107*(24), 7040–7044. https://doi.org/10.1021/ja00310a047

Giri, S., Banerji, A., Lele, S. S., & Ananthanarayan, L. (2017). Starch digestibility and glycaemic index of selected Indian traditional foods: Effects of added ingredients. *International Journal of Food Properties*, *20*(sup1), S290–S305. https://doi.org/10.1080/10942912.2017.1295387

Glittenberg, D. (2012). Starch-Based Biopolymers in Paper, Corrugating, and Other Industrial Applications. In *Polymer Science: A Comprehensive Reference* (pp. 165–193). Elsevier. https://doi.org/10.1016/B978-0-444-53349-4.00258-2

Go, S.-M., Park, M.-R., Kim, H.-S., Choi, W.S., & Jeong, R.-D. (2019). Antifungal effect of non-thermal atmospheric plasma and its application for control of postharvest Fusarium oxysporum decay of paprika. *Food Control,* 98, 245–252. https://doi.org/10.1016/j.foodcont.2018.11.028.

Goldstein, A., Annor, G., Vamadevan, V., Tetlow, I., Kirkensgaard, J. J. K., Mortensen, K., Blennow, A., Hebelstrup, K. H., & Bertoft, E. (2017). Influence of diurnal photosynthetic activity on the morphology, structure, and thermal properties of normal and waxy barley starch. *International Journal of Biological Macromolecules*, *98*, 188–200. https://doi.org/10.1016/j.ijbiomac.2017.01.118

Grzegorzewski, F., Ehlbeck, J., Schlüter, O., Kroh, L.W., & Rohn, S. (2011). Treating lamb's lettuce with a cold plasma – Influence of atmospheric pressure Ar plasma immanent species on the phenolic profile of *Valerianella locusta*. *LWT*, 44, 2285–2289. https://doi.org/10.1016/j.lwt.2011.05.004.

Guo, P., Yu, J., Copeland, L., Wang, S., & Wang, S. (2018). Mechanisms of starch gelatinization during heating of wheat flour and its effect on in vitro starch digestibility. *Food Hydrocolloids*, *82*, 370–378. https://doi.org/10.1016/j.foodhyd.2018.04.012

Guo, Z., Gou, Q., Yang, L., Yu, Q., & Han, L. (2022). Dielectric barrier discharge plasma: A green method to change structure of potato starch and improve physicochemical properties of potato starch films. *Food Chemistry*, *370*, 130992. https://doi.org/10.1016/j.foodchem.2021.130992

Hagenimana, A., & Ding, X. (2005). A Comparative Study on Pasting and Hydration Properties of Native Rice Starches and Their Mixtures. *Cereal Chemistry Journal*, *82*(1), 70–76. https://doi.org/10.1094/CC-82-0070

Hall, D. M., & Sayre, J. G. (1971). *A Scanning Electron-Microscope Study of Starches*. Part II: Cereal starches. *Textile Research Journal*, 39, 1044-1052.

Han, S. H., Suh, H. J., Hong, K. B., Kim, S. Y., & Min, S. C. (2016). Oral Toxicity of Cold Plasma-Treated Edible Films for Food Coating: Cold plasma-treated edible film toxicity…. *Journal of Food Science*, *81*(12), T3052–T3057. https://doi.org/10.1111/1750-3841.13551

Han, X., Wen, H., Luo, Y., Yang, J., Xiao, W., & Xie, J. (2022). Effects of chitosan modification, cross-linking, and oxidation on the structure, thermal stability, and

adsorption properties of porous maize starch. *Food Hydrocolloids*, *124*, 107288. https://doi.org/10.1016/j.foodhyd.2021.107288

Han, X.-Z., & Hamaker, B. R. (2001). Amylopectin Fine Structure and Rice Starch Paste Breakdown. *Journal of Cereal Science*, *34*(3), 279–284. https://doi.org/10.1006/jcrs.2001.0374

Herceg, Z., Kovačević, D.B., Kljusurić, J.G., Jambrak, A.R., Zorić, Z., & Dragović-Uzelac, V. (2016). Gas phase plasma impact on phenolic compounds in pomegranate juice. *Food Chemistry*, 190, 665–672. https://doi.org/10.1016/j.foodchem.2015.05.135.

Hizukuri, S. (1985). Relationship between the distribution of the chain length of amylopectin and the crystalline structure of starch granules. *Carbohydrate Research*, *141*(2), 295–306. https://doi.org/10.1016/S0008-6215(00)90461-0

Hizukuri, S., Kaneko, T., & Takeda, Y. (1983). Measurement of the chain length of amylopectin and its relevance to the origin of crystalline polymorphism of starch granules. *Biochimica et Biophysica Acta (BBA) - General Subjects*, *760*(1), 188–191. https://doi.org/10.1016/0304-4165(83)90142-3

Hizukuri, S., Takeda, Y., Yasuda, M., & Suzuki, A. (1981). Multi-branched nature of amylose and the action of debranching enzymes. *Carbohydrate Research*, *94*(2), 205–213. https://doi.org/10.1016/S0008-6215(00)80718-1

Hong Y., & Liu X. (2018). Pre-gelatinized Modification of Starch. In: Sui Z., Kong X. (eds) Physical Modifications of Starch. Springer, Singapore. https://doi.org/10.1007/978- 981-13-0725-6_4.

Huber, K. C., & BeMiller, J. N. (2000). Channels of maize and sorghum starch granules. *Carbohydrate Polymers*, *41*(3), 269–276. https://doi.org/10.1016/S0144-8617(99)00145-9

I, Y.-P., Liu, Y.-C., Han, K.-Y., & She, T.-C. (2004). Construction of a Low-Pressure Microwave Plasma Reactor and Its Application in the Treatment of Volatile Organic Compounds. *Environmental Science & Technology*, *38*(13), 3785–3791. https://doi.org/10.1021/es034697a

Imberty, A., Buléon, A., Tran, V., & Péerez, S. (1991). Recent Advances in Knowledge of Starch Structure. *Starch - Stärke*, *43*(10), 375–384. https://doi.org/10.1002/star.19910431002

Imberty, A., & Pérez, S. (1989). Conformational analysis and molecular modelling of the branching point of amylopectin. *International Journal of Biological Macromolecules*, *11*(3), 177–185. https://doi.org/10.1016/0141-8130(89)90065-2

Iqdiam, B.M., Abuagela, M.O., Boz, Z., Marshall, S.M., Goodrich-Schneider, R., Sims, C.A., Marshall, M.R., MacIntosh, A.J., Welt, B.A., 2020. Effects of atmospheric pressure plasma jet treatment on aflatoxin level, physiochemical quality, and sensory attributes of peanuts. J*ournal of Food Processing and Preservation,* 44, e14305. https://doi.org/10.1111/jfpp.14305.

Jackson, D.S. (2003). Starch| structure, properties, and determination. *Encyclopedia of Food Sciences and Nutrition, 9, 5561- 5572.*

Jane, J., Chen, Y. Y., Lee, L. F., McPherson, A. E., Wong, K. S., Radosavljevic, M., & Kasemsuwan, T. (1999). Effects of Amylopectin Branch Chain Length and Amylose Content on the Gelatinization and Pasting Properties of Starch. *Cereal Chemistry Journal*, *76*(5), 629–637. https://doi.org/10.1094/CCHEM.1999.76.5.629

Jayakody, L., & Hoover, R. (2008). Effect of annealing on the molecular structure and physicochemical properties of starches from different botanical origins – A review. *Carbohydrate Polymers*, *74*(3), 691–703. https://doi.org/10.1016/j.carbpol.2008.04.032

Judée, F., Simon, S., Bailly, C., & Dufour, T. (2018). Plasma-activation of tap water using DBD for agronomy applications: Identification and quantification of long lifetime chemical species and production/consumption mechanisms. *Water Research*, *133*, 47–59. https://doi.org/10.1016/j.watres.2017.12.035

Kalaivendan, R. G. T., Mishra, A., Eazhumalai, G., & Annapure, U. S. (2022). Effect of atmospheric pressure non-thermal pin to plate plasma on the functional, rheological, thermal, and morphological properties of mango seed kernel starch. *International Journal of Biological Macromolecules*, *196*, 63–71. https://doi.org/10.1016/j.ijbiomac.2021.12.013

Kanazawa, T., Atsumi, M., Mineo, H., Fukushima, M., Nishimura, N., Noda, T., & Chiji, H. (2008). Ingestion of Gelatinized Potato Starch Containing a High Level of Phosphorus Decreases Serum and Liver Lipids in Rats. *Journal of Oleo Science*, *57*(6), 335–343. https://doi.org/10.5650/jos.57.335

Kaur, A., Singh, N., Ezekiel, R., & Guraya, H.S. (2007). Physicochemical, thermal and pasting properties of starches separated from different potato cultivars grown at different locations. *Food Chemistry*, 101, 643–651. https://doi.org/10.1016/j.foodchem.2006.01.054.

Kaur, B., Ariffin, F., Bhat, R., & Karim, A. A. (2012). Progress in starch modification in the last decade. *Food Hydrocolloids*, *26*(2), 398–404. https://doi.org/10.1016/j.foodhyd.2011.02.016

Kim, S. J., Chung, T. H., Bae, S. H., Leem, S. H., 2009. Characterization of atmospheric pressure microplasma jet source and its application to bacterial inactivation. *Plasma Processes and Polymers,* 6, 676–685.

Kizil, R., Irudayaraj, J., & Seetharaman, K. (2002). Characterization of Irradiated Starches by Using FT-Raman and FTIR Spectroscopy. *Journal of Agricultural and Food Chemistry*, *50*(14), 3912–3918. https://doi.org/10.1021/jf011652p

Koch, K., Andersson, R., & Åman, P. (1998). Quantitative analysis of amylopectin unit chains by means of high-performance anion-exchange chromatography with pulsed amperometric detection. *Journal of Chromatography A*, *800*(2), 199–206. https://doi.org/10.1016/S0021-9673(97)01151-5

Kohyama, K., Matsuki, J., Yasui, T., & Sasaki, T. (2004). A differential thermal analysis of the gelatinization and retrogradation of wheat starches with different amylopectin chain lengths. *Carbohydrate Polymers*, *58*(1), 71–77. https://doi.org/10.1016/j.carbpol.2004.06.032

Korachi, M., Gurol, C., & Aslan, N. (2010). Atmospheric plasma discharge sterilization effects on whole cell fatty acid profiles of *Escherichia coli* and *Staphylococcus*

aureus. Journal of Electrostatics, 68, 508–512. https://doi.org/10.1016/j.elstat.2010.06.014.

Krystyjan, M., Ciesielski, W., Gumul, D., Buksa, K., Ziobro, R., & Sikora, M. (2017). Physico-chemical and rheological properties of gelatinized/freeze-dried cereal starches. *International Agrophysics*, *31*(3), 357–365. https://doi.org/10.1515/intag-2016-0058

Kumar, R., & Khatkar, B. S. (2017). Thermal, pasting and morphological properties of starch granules of wheat (Triticum aestivum L.) varieties. *Journal of Food Science and Technology*, *54*(8), 2403–2410. https://doi.org/10.1007/s13197-017-2681-x

Laovachirasuwan, P., Peerapattana, J., Srijesdaruk, V., Chitropas, P., & Otsuka, M. (2010). The physicochemical properties of a spray dried glutinous rice starch biopolymer. *Colloids and Surfaces B: Biointerfaces*, *78*(1), 30–35. https://doi.org/10.1016/j.colsurfb.2010.02.004

Laroque, D. A., Seó, S. T., Valencia, G. A., Laurindo, J. B., & Carciofi, B. A. M. (2022). Cold plasma in food processing: Design, mechanisms, and application. *Journal of Food Engineering*, *312*, 110748. https://doi.org/10.1016/j.jfoodeng.2021.110748

Lee, H.-C. (2018). Review of inductively coupled plasmas: Nano-applications and bistable hysteresis physics. *Applied Physics Reviews*, *5*(1), 011108. https://doi.org/10.1063/1.5012001

Li, H., Gidley, M. J., & Dhital, S. (2019). High-Amylose Starches to Bridge the "Fiber Gap": Development, Structure, and Nutritional Functionality: High-amylose

starch to bridge “fiber gap” . . . *Comprehensive Reviews in Food Science and Food Safety*, *18*(2), 362–379. https://doi.org/10.1111/1541-4337.12416

Liao, X., Cullen, P. J., Muhammad, A. I., Jiang, Z., Ye, X., Liu, D., & Ding, T. (2020). Cold Plasma–Based Hurdle Interventions: New Strategies for Improving Food Safety. *Food Engineering Reviews*, *12*(3), 321–332. https://doi.org/10.1007/s12393-020-09222-3

Lii, C., Liao, C., Stobinski, L., & Tomasik, P. (2002a). Exposure of granular starches to low-pressure glow ethylene plasma. *European Polymer Journal*, *38*(8), 1601–1606. https://doi.org/10.1016/S0014-3057(02)00022-8

Lii, C., Liao, C., Stobinski, L., & Tomasik, P. (2002b). Behaviour of granular starches in low-pressure glow plasma. *Carbohydrate Polymers*, *49*(4), 499–507. https://doi.org/10.1016/S0144-8617(01)00365-4

Limpisut, P., & Jindal, V. K. (2002). Comparison of Rice Flour Pasting Properties using Brabender Viscoamylograph and Rapid Visco Analyser for Evaluating Cooked Rice Texture. *Starch - Stärke*, *54*(8), 350–357. https://doi.org/10.1002/1521-379X(200208)54:8<350::AID-STAR350>3.0.CO;2-R

Lin, C.-M., Hsiao, C.-P., Lin, H.-S., Liou, J. S., Hsieh, C.-W., Wu, J.-S., & Hou, C.-Y. (2020). The Antibacterial Efficacy and Mechanism of Plasma-Activated Water Against Salmonella Enteritidis (ATCC 13076) on Shell Eggs. *Foods*, *9*(10), 1491. https://doi.org/10.3390/foods9101491

Lippens, P. (2007). Low-pressure cold plasma processing technology. Europlasma N.V., Belgium. Shishoo, R. Plasma technologies for textiles. Woodhead publishing series in textiles.

Lopez-Rubio, A., Flanagan, B. M., Gilbert, E. P., & Gidley, M. J. (2008). A novel approach for calculating starch crystallinity and its correlation with double helix content: A combined XRD and NMR study. *Biopolymers*, *89*(9), 761–768. https://doi.org/10.1002/bip.21005

Los, A., Ziuzina, D., Van Cleynenbreugel, R., Boehm, D., & Bourke, P. (2020). Assessing the Biological Safety of Atmospheric Cold Plasma Treated Wheat Using Cell and Insect Models. *Foods*, *9*(7), 898. https://doi.org/10.3390/foods9070898

Lu, P., Boehm, D., Bourke, P., & Cullen, P. J. (2017). Achieving reactive species specificity within plasma-activated water through selective generation using air spark and glow discharges. *Plasma Processes and Polymers*, *14*(8), 1600207. https://doi.org/10.1002/ppap.201600207

Lukes, P., Clupek, M., Babicky, V., & Sunka, P. (2008). Ultraviolet radiation from the pulsed corona discharge in water. *Plasma Sources Science and Technology*, *17*(2), 024012. https://doi.org/10.1088/0963-0252/17/2/024012

Lukes, P., Dolezalova, E., Sisrova, I., & Clupek, M. (2014). Aqueous-phase chemistry and bactericidal effects from an air discharge plasma in contact with water: Evidence for the formation of peroxynitrite through a pseudo-second-order post-discharge reaction of H_2O_2 and HNO_2. *Plasma Sources Science Technology*, *23*(1), 015019. https://doi.org/10.1088/0963-0252/23/1/015019

Lukes, P., Locke, B. R., & Brisset, J.-L. (2012). Aqueous-Phase Chemistry of Electrical Discharge Plasma in Water and in Gas–Liquid Environments. In V. I. Parvulescu,

M. Magureanu, & P. Lukes (Eds.), *Plasma Chemistry and Catalysis in Gases and Liquids* (pp. 243–308). WILEY-VCH Verlag GmBH & Co. KGaA.

Mahdavian Mehr, H., Koocheki, A., 2020. Effect of atmospheric cold plasma on structure, interfacial and emulsifying properties of Grass pea (Lathyrus sativus L.) protein isolate. *Food Hydrocolloids*, 106, 105899. https://doi.org/10.1016/j.foodhyd.2020.105899.

Manners, D. J. (1989). Recent developments in our understanding of amylopectin structure. *Carbohydrate Polymers*, *11*(2), 87–112. https://doi.org/10.1016/0144-8617(89)90018-0

Mason, W. R. (2009). Starch Use in Foods. In *Starch* (pp. 745–795). Elsevier. https://doi.org/10.1016/B978-0-12-746275-2.00020-3

Matveev, Y. I., van Soest, J. J. G., Nieman, C., Wasserman, L. A., Protserov, V. A., Ezernitskaja, M., & Yuryev, V. P. (2001). The relationship between thermodynamic and structural properties of low and high amylose maize starches. *Carbohydrate Polymers*, *44*(2), 151–160. https://doi.org/10.1016/S0144-8617(00)00211-3

McMahon, K. A. (2004). Practical botany – The Maltese cross. In Tested studies for laboratory teaching (pp. 352-357), Volume 25 (M. A. O'Donnell, Editor). Proceedings of the 25th Workshop/Conference of the Association for Biology Laboratory Education (ABLE).

Mihhalevski, A., Heinmaa, I., Traksmaa, R., Pehk, T., Mere, A., & Paalme, T. (2012). Structural Changes of Starch during Baking and Staling of Rye Bread. *Journal of*

Agricultural and Food Chemistry, *60*(34), 8492–8500. https://doi.org/10.1021/jf3021877

Milella, A., & Palumbo, F. (2014). Cold Plasma. In E. Drioli & L. Giorno (Eds.), *Encyclopedia of Membranes* (pp. 1–2). Springer Berlin Heidelberg. https://doi.org/10.1007/978-3-642-40872-4_1107-1

Misra, N. N., Pankaj, S. K., Segat, A., & Ishikawa, K. (2016). Cold plasma interactions with enzymes in foods and model systems. *Trends in Food Science & Technology*, *55*, 39–47. https://doi.org/10.1016/j.tifs.2016.07.001

Moiseev, T., Misra, N.N., Patil, S., Cullen, P.J., Bourke, P., Keener, K.M., & Mosnier, J.P. (2014). Post-discharge gas composition of a large-gap DBD in humid air by UV–Vis absorption spectroscopy. *Plasma Sources Science and Technology*, 23, 065033. https://doi.org/10.1088/0963-0252/23/6/065033.

Moreau, M., Orange, N., & Feuilloley, M. G. J. (2008). Non-thermal plasma technologies: New tools for bio-decontamination. *Biotechnology Advances*, *26*(6), 610–617. https://doi.org/10.1016/j.biotechadv.2008.08.001

Morent, R., De Geyter, N., Desmet, T., Dubruel, P., & Leys, C. (2011). Plasma Surface Modification of Biodegradable Polymers: A Review: Plasma Surface Modification of Biodegradable Polymers: A Review. *Plasma Processes and Polymers*, *8*(3), 171–190. https://doi.org/10.1002/ppap.201000153

Niemira, B.A. (2012). Cold plasma decontamination of foods. *Annual Review of Food Science and Technology*, 3, 125–142. https://doi.org/10.1146/annurev-food-022811-101132.

Noda, T., Isono, N., Krivandin, A. V., Shatalova, O. V., Błaszczak, W., & Yuryev, V. P. (2009). Origin of defects in assembled supramolecular structures of sweet potato starches with different amylopectin chain-length distribution. *Carbohydrate Polymers*, *76*(3), 400–409. https://doi.org/10.1016/j.carbpol.2008.10.029

Oehmigen, K., Hähnel, M., Brandenburg, R., Wilke, Ch., Weltmann, K.-D., & von Woedtke, Th. (2010). The Role of Acidification for Antimicrobial Activity of Atmospheric Pressure Plasma in Liquids: The Role of Acidification for Antimicrobial …. *Plasma Processes and Polymers*, *7*(3–4), 250–257. https://doi.org/10.1002/ppap.200900077

Oh, J.-S., Kakuta, M., Furuta, H., Akatsuka, H., & Hatta, A. (2016). Effect of plasma jet diameter on the efficiency of reactive oxygen and nitrogen species generation in water. *Japanese Journal of Applied Physics*, *55*(6S2), 06HD01. https://doi.org/10.7567/JJAP.55.06HD01

Okyere, A. Y., Bertoft, E., & Annor, G. A. (2019). Modification of cereal and tuber waxy starches with radio frequency cold plasma and its effects on waxy starch properties. *Carbohydrate Polymers*, *223*, 115075. https://doi.org/10.1016/j.carbpol.2019.115075

Okyere, A. Y., Boakye, P. G., Bertoft, E., & Annor, G. A. (2022). Structural characterization and enzymatic hydrolysis of radio frequency cold plasma treated starches. *Journal of Food Science*, 1750-3841.16037. https://doi.org/10.1111/1750-3841.16037

Pankaj, S. K., Wan, Z., De León, J. E., Mosher, C., Colonna, W., & Keener, K. M. (2017). High-voltage atmospheric cold plasma treatment of different types of

starch films: Cold plasma treatment of starch films. *Starch - Stärke*, *69*(11–12), 1700009. https://doi.org/10.1002/star.201700009

Pankaj, S., Wan, Z., & Keener, K. (2018). Effects of Cold Plasma on Food Quality: A Review. *Foods*, *7*(1), 4. https://doi.org/10.3390/foods7010004

Park, H., Puligundla, P., & Mok, C. (2020). Cold plasma decontamination of brown rice grains: Impact on biochemical and sensory qualities of their corresponding seedlings and aqueous tea infusions. *LWT*, 131, 109508. https://doi.org/10.1016/j.lwt.2020.109508

Park, S. H., Na, Y., Kim, J., Kang, S. D., & Park, K.-H. (2017). Properties and applications of starch modifying enzymes for use in the baking industry. *Food Science and Biotechnology*. https://doi.org/10.1007/s10068-017-0261-5

Peat, S., Whelan, W., & Thomas, G. J. (1952). Evidence of multiple branching in waxy maize starch. *Journal of the Chemical Society, 4546–4548.*

Pérez, S., & Bertoft, E. (2010). The molecular structures of starch components and their contribution to the architecture of starch granules: A comprehensive review. *Starch - Stärke*, *62*(8), 389–420. https://doi.org/10.1002/star.201000013

Pignata, C., D'angelo, D., Fea, E., & Gilli, G. (2017). A review on microbiological decontamination of fresh produce with nonthermal plasma. *Journal of Applied Microbiology*, 122, 1438–1455.

Pinkrová, J., Hubáčková, B., Kadlec, P., Příhoda, J., & Bubník, Z. (2011). Changes of starch during microwave treatment of rice. *Czech Journal of Food Sciences*, *21*(No. 5), 176–184. https://doi.org/10.17221/3496-CJFS

Popov, D., Buléon, A., Burghammer, M., Chanzy, H., Montesanti, N., Putaux, J.-L., Potocki-Véronèse, G., & Riekel, C. (2009). Crystal Structure of A-amylose: A Revisit from Synchrotron Microdiffraction Analysis of Single Crystals. *Macromolecules*, *42*(4), 1167–1174. https://doi.org/10.1021/ma801789j

Pozo, C., Rodríguez-Llamazares, S., Bouza, R., Barral, L., Castaño, J., Müller, N., & Restrepo, I. (2018). Study of the structural order of native starch granules using combined FTIR and XRD analysis. *Journal of Polymer Research*, *25*(12), 266. https://doi.org/10.1007/s10965-018-1651-y

Pu, H., Chen, L., Li, X., Xie, F., Yu, L., & Li, L. (2011). An Oral Colon-Targeting Controlled Release System Based on Resistant Starch Acetate: Synthetization, Characterization, and Preparation of Film-Coating Pellets. *Journal of Agricultural and Food Chemistry*, *59*(10), 5738–5745. https://doi.org/10.1021/jf2005468

Puspitowati, S., & Driscoll, R. H. (2007). Effect of Degree of Gelatinisation on the Rheology and Rehydration Kinetics of Instant Rice Produced by Freeze Drying. *International Journal of Food Properties*, *10*(3), 445–453. https://doi.org/10.1080/10942910600871289

Qi, X., Tester, R. F., Snape, C. E., & Ansell, R. (2003). Molecular Basis of the Gelatinisation and Swelling Characteristics of Waxy Rice Starches Grown in the Same Location During the Same Season. *Journal of Cereal Science*, *37*(3), 363–376. https://doi.org/10.1006/jcrs.2002.0508

Raizer, Y. P., & Allen, J. E. (1997). Gas discharge physics (Vol. 2). Springer Berlin.

Ratnayake, W. S., Hoover, R., Shahidi, F., Perera, C., & Jane, J. (2001). Composition, molecular structure, and physicochemical properties of starches from four field

pea (Pisum sativum L.) cultivars. *Food Chemistry*, *74*(2), 189–202. https://doi.org/10.1016/S0308-8146(01)00124-8

Ratnayake, W. S., & Jackson, D. S. (2006). Gelatinization and Solubility of Corn Starch during Heating in Excess Water: New Insights. *Journal of Agricultural and Food Chemistry*, *54*(10), 3712–3716. https://doi.org/10.1021/jf0529114

Rohan, (2016). Industrial Starch Market worth 106.64 billion USD by 2022 https://www.prnewswire.com/news-releases/industrial-starch-market-worth-us-10664- billion-by-2022-602981256.html. (Accessed 28 October 2021).

Rombo, G. O., Taylor, J. R., & Minnaar, A. (2004). Irradiation of maize and bean flours: Effects on starch physicochemical properties. *Journal of the Science of Food and Agriculture*, *84*(4), 350–356. https://doi.org/10.1002/jsfa.1663

Rossi, F. (2012). Sterilization and decontamination of surfaces by plasma discharges. In Simmons, A. (Eds) Sterilisation of biomaterials and medical devices. ProQuest Ebook Central https://ebookcentral.proquest.com.

Roy Choudhury, A. K. (2017). Various ecofriendly finishes. In *Principles of Textile Finishing* (pp. 467–525). Elsevier. https://doi.org/10.1016/B978-0-08-100646-7.00014-X

Russell, P. L., Gough, B. M., Greenwell, P., Fowler, A., & Munro, H. S. (1987). A study by ESCA of the surface of native and chlorine-treated wheat starch granules: The effects of various surface treatments. *Journal of Cereal Science*, *5*(1), 83–100. https://doi.org/10.1016/S0733-5210(87)80013-9

Saad, M., Gaiani, C., Mullet, M., Scher, J., & Cuq, B. (2011). X-ray Photoelectron Spectroscopy for Wheat Powders: Measurement of Surface Chemical

Composition. *Journal of Agricultural and Food Chemistry*, *59*(5), 1527–1540. https://doi.org/10.1021/jf102315h

Sarangapani, C., Ryan Keogh, D., Dunne, J., Bourke, P., & Cullen, P. J. (2017). Characterisation of cold plasma treated beef and dairy lipids using spectroscopic and chromatographic methods. *Food Chemistry*, *235*, 324–333. https://doi.org/10.1016/j.foodchem.2017.05.016

Saunders, J., Izydorczyk, M., & B., D. (2011). Limitations and Challenges for Wheat-Based Bioethanol Production. In M. A. Dos Santos Bernardes (Ed.), *Economic Effects of Biofuel Production*. InTech. https://doi.org/10.5772/20258

Scholtz, V., Pazlarova, J., Souskova, H., Khun, J., & Julak, J. (2015). Nonthermal plasma—A tool for decontamination and disinfection. *Biotechnology Advances*, *33*(6), 1108–1119. https://doi.org/10.1016/j.biotechadv.2015.01.002

Sheikhi, Z., Hosseini, S. M., Khani, M. R., Farhoodi, M., Abdolmaleki, K., Shokri, B., Shojaee-Aliabadi, S., & Mirmoghtadaie, L. (2020). Treatment of starch films with a glow discharge plasma in air and O_2 at low pressure. *Food Science and Technology International*, 108201322094864. https://doi.org/10.1177/1082013220948641

Sifuentes-Nieves, I., Mendez-Montealvo, G., Flores-Silva, P. C., Nieto-Pérez, M., Neira-Velazquez, G., Rodriguez-Fernandez, O., Hernández-Hernández, E., & Velazquez, G. (2021). Dielectric barrier discharge and radio-frequency plasma effect on structural properties of starches with different amylose content. *Innovative Food Science & Emerging Technologies*, *68*, 102630. https://doi.org/10.1016/j.ifset.2021.102630

Singh, J., Kaur, L., & McCarthy, O. J. (2009). *Chapter 10—Potato Starch and its Modification*. 46.

Snoeckx, R., & Bogaerts, A. (2017). Plasma technology – a novel solution for CO_2 conversion? *Chemical Society Reviews*, *46*(19), 5805–5863. https://doi.org/10.1039/C6CS00066E

Song, J., Jiang, B., Wu, Y., Chen, S., Li, S., Sun, H., & Li, X. (2019). Effects on Surface and Physicochemical Properties of Dielectric Barrier Discharge Plasma-Treated Whey Protein Concentrate/Wheat Cross-Linked Starch Composite Film. *Journal of Food Science*, 84, 268–275. https://doi.org/10.1111/1750-3841.14387.

Spencer, L. F., & Gallimore, A. D. (2011). Efficiency of CO2 Dissociation in a Radio-Frequency Discharge. *Plasma Chemistry and Plasma Processing*, *31*(1), 79–89. https://doi.org/10.1007/s11090-010-9273-0

Sudheesh, C., Sunooj, K. V., Sinha, S. K., George, J., Kumar, S., Murugesan, P., Arumugam, S., Ashwath Kumar, K., & Sajeev Kumar, V. A. (2019). Impact of energetic neutral nitrogen atoms created by glow discharge air plasma on the physico-chemical and rheological properties of kithul starch. *Food Chemistry*, *294*, 194–202. https://doi.org/10.1016/j.foodchem.2019.05.067

Sujka, M., & Jamroz, J. (2007). *Starch granule porosity and its changes by means of amylolysis*. 7.

Sun, X., Saleh, A. S. M., Sun, Z., Ge, X., Shen, H., Zhang, Q., Yu, X., Yuan, L., & Li, W. (2022). Modification of multi-scale structure, physicochemical properties, and digestibility of rice starch via microwave and cold plasma treatments. *LWT*, *153*, 112483. https://doi.org/10.1016/j.lwt.2021.112483

Surowsky, B., Fröhling, A., Gottschalk, N., Schlüter, O., & Knorr, D. (2014). Impact of cold plasma on Citrobacter freundii in apple juice: Inactivation kinetics and mechanisms. *International Journal of Food Microbiology,* 174, 63–71. https://doi.org/10.1016/j.ijfoodmicro.2013.12.031

Tamura, M., Singh, J., Kaur, L., & Ogawa, Y. (2016). Impact of the degree of cooking on starch digestibility of rice – An in vitro study. *Food Chemistry*, *191*, 98–104. https://doi.org/10.1016/j.foodchem.2015.03.127

Tan, I., Flanagan, B. M., Halley, P. J., Whittaker, A. K., & Gidley, M. J. (2007). A Method for Estimating the Nature and Relative Proportions of Amorphous, Single, and Double-Helical Components in Starch Granules by ^{13} C CP/MAS NMR. *Biomacromolecules*, *8*(3), 885–891. https://doi.org/10.1021/bm060988a

Tester, R. F., & Morrison, W. R. (1990). Swelling and Gelatinization of Cereal Starches. I. Effects of Amylopectin, Amylose, and Lipids'. *Cereal Chemistry Journal*, *67*(6), 551–557.

Thirumdas, R., Kadam, D., & Annapure, U. S. (2017a). Cold Plasma: An Alternative Technology for the Starch Modification. *Food Biophysics*, *12*(1), 129–139. https://doi.org/10.1007/s11483-017-9468-5

Thirumdas, R., Kothakota, A., Annapure, U., Siliveru, K., Blundell, R., Gatt, R., & Valdramidis, V. P. (2018). Plasma activated water (PAW): Chemistry, physico-chemical properties, applications in food and agriculture. *Trends in Food Science & Technology*, *77*, 21–31. https://doi.org/10.1016/j.tifs.2018.05.007

Thirumdas, R., Saragapani, C., Ajinkya, M. T., Deshmukh, R. R., & Annapure, U. S. (2016). Influence of low pressure cold plasma on cooking and textural properties

of brown rice. *Innovative Food Science & Emerging Technologies*, *37*, 53–60. https://doi.org/10.1016/j.ifset.2016.08.009

Thirumdas, R., Trimukhe, A., Deshmukh, R. R., & Annapure, U. S. (2017b). Functional and rheological properties of cold plasma treated rice starch. *Carbohydrate Polymers*, *157*, 1723–1731. https://doi.org/10.1016/j.carbpol.2016.11.050

Thomas, M., & Mittal, K.L., (2013). Atmospheric Pressure Plasma Treatment of Polymers: Relevance to Adhesion, Atmospheric Pressure Plasma Treatment of Polymers: Relevance to Adhesion. Wiley, Salem.

Thornhill, W. (2007). "The Z-Pinch Morphology of Supernova 1987A and Electric Stars, "in *IEEE Transactions on Plasma Science*, 35, 834-844 doi:10.1109/TPS.2007.895423

Timoshkin, I. V., Maclean, M., Wilson, M. P., Given, M. J., MacGregor, S. J., Wang, T., & Anderson, J. G. (2012). Bactericidal effect of corona discharges in atmospheric air. *IEEE Transactions on Plasma Science,* 40, 2322–2333.

Trinh, K. S. (2018). Formation of boiling-stable resistant cassava starch using the atmospheric argon-plasma treatmen. *Journal of Bioenergy and Food Science*, *5*(3), 97–105. https://doi.org/10.18067/jbfs.v5i3.224

Turner, M. (2016). Chapter 2—Physics of Cold Plasma. In N. N. Misra, O. Schlüter, and P. J. Cullen (Eds.), Cold plasma in food and agriculture (pp. 17–51). *Academic Press.* https://doi.org/10.1016/B978-0-12-801365-6.00002-0.

Vaideki, K. (2016). Plasma technology for antimicrobial textiles. In *Antimicrobial Textiles* (pp. 73–86). Elsevier. https://doi.org/10.1016/B978-0-08-100576-7.00005-5

Vamadevan, V., & Bertoft, E. (2015). Structure-function relationships of starch components. *Starch - Stärke*, *67*(1–2), 55–68. https://doi.org/10.1002/star.201400188

Vamadevan, V., Bertoft, E., & Seetharaman, K. (2013). On the importance of organization of glucan chains on thermal properties of starch. *Carbohydrate Polymers*, *92*(2), 1653–1659. https://doi.org/10.1016/j.carbpol.2012.11.003

Vamadevan, V., Bertoft, E., Soldatov, D. V., & Seetharaman, K. (2013). Impact on molecular organization of amylopectin in starch granules upon annealing. *Carbohydrate Polymers*, *98*(1), 1045–1055. https://doi.org/10.1016/j.carbpol.2013.07.006

Varatharajan, V., Hoover, R., Li, J., Vasanthan, T., Nantanga, K. K. M., Seetharaman, K., Liu, Q., Donner, E., Jaiswal, S., & Chibbar, R. N. (2011). Impact of structural changes due to heat-moisture treatment at different temperatures on the susceptibility of normal and waxy potato starches towards hydrolysis by porcine pancreatic alpha amylase. *Food Research International*, *44*(9), 2594–2606. https://doi.org/10.1016/j.foodres.2011.04.050

Wang, R. X., Nian, W. F., Wu, H. Y., Feng, H. Q., Zhang, K., Zhang, J., Zhu, W. D., Becker, K. H., & Fang, J. (2012). Atmospheric-pressure cold plasma treatment of contaminated fresh fruit and vegetable slices: Inactivation and physiochemical properties evaluation. *The European Physical Journal D*, *66*(10), 276. https://doi.org/10.1140/epjd/e2012-30053-1

Warren, F. J., Gidley, M. J., & Flanagan, B. M. (2016). Infrared spectroscopy as a tool to characterise starch ordered structure—A joint FTIR–ATR, NMR, XRD and DSC

study. *Carbohydrate Polymers*, *139*, 35–42. https://doi.org/10.1016/j.carbpol.2015.11.066

Waterschoot, J., Gomand, S. V., Fierens, E., & Delcour, J. A. (2015). Production, structure, physicochemical and functional properties of maize, cassava, wheat, potato and rice starches. *Starch - Stärke*, *67*(1–2), 14–29. https://doi.org/10.1002/star.201300238

Wei, B., Xu, X., Jin, Z., & Tian, Y. (2014). Surface Chemical Compositions and Dispersity of Starch Nanocrystals Formed by Sulfuric and Hydrochloric Acid Hydrolysis. *PLoS ONE*, *9*(2), e86024. https://doi.org/10.1371/journal.pone.0086024

Weltmann, K.-D., Kindel, E., Brandenburg, R., Meyer, C., Bussiahn, R., Wilke, C., & von Woedtke, T. (2009). Atmospheric pressure plasma jet for medical therapy: plasma parameters and risk estimation. *Contributions to Plasma Physics*, 49, 631–640. https://doi.org/10.1002/ctpp.200910067.

Whistler, R. L., & Turner, E. S. (1955). Fine structure of starch granule sections. *Journal of Polymer Science*, *18*(87), 153–156. https://doi.org/10.1002/pol.1955.120188716

Wiesenborn, D.P., Orr, P.H., Casper, H.H., & Tacke, B.K. (1994). Potato Starch Paste Behavior as Related to Some Physical/Chemical Properties. *Journal of Food Science*, 59, 644–648. https://doi.org/10.1111/j.1365-2621.1994.tb05583.x.

Wilczek, S., Schulze, J., Brinkmann, R. P., Donkó, Z., Trieschmann, J., & Mussenbrock, T. (2020). Electron dynamics in low pressure capacitively coupled radio

frequency discharges. *Journal of Applied Physics*, *127*(18), 181101. https://doi.org/10.1063/5.0003114

Wongsagonsup, R., Deeyai, P., Chaiwat, W., Horrungsiwat, S., Leejariensuk, K., Suphantharika, M., Fuongfuchat, A., & Dangtip, S. (2014). Modification of tapioca starch by non-chemical route using jet atmospheric argon plasma. *Carbohydrate Polymers*, *102*, 790–798. https://doi.org/10.1016/j.carbpol.2013.10.089

Wrobel, A. M., Lamontagne, B., & Wertheimer, M. R. (1988). Large-area microwave and radiofrequency plasma etching of polymers. *Plasma Chemistry and Plasma Processing*, *8*(3), 315–329. https://doi.org/10.1007/BF01020409

Wu, T.-Y., Chang, C.-R., Chang, T.-J., Chang, Y.-J., Liew, Y., & Chau, C.-F. (2019). Changes in physicochemical properties of corn starch upon modifications by atmospheric pressure plasma jet. *Food Chemistry*, *283*, 46–51. https://doi.org/10.1016/j.foodchem.2019.01.043

Wu, T.-Y., Sun, N.-N., & Chau, C.-F. (2018). Application of corona electrical discharge plasma on modifying the physicochemical properties of banana starch indigenous to Taiwan. *Journal of Food and Drug Analysis*, 26, 244–251. https://doi.org/10.1016/j.jfda.2017.03.005.

Wu, X., Zhao, R., Wang, D., Bean, S. R., Seib, P. A., Tuinstra, M. R., Campbell, M., & O'Brien, A. (2006). Effects of Amylose, Corn Protein, and Corn Fiber Contents on Production of Ethanol from Starch-Rich Media. *Cereal Chemistry Journal*, *83*(5), 569–575. https://doi.org/10.1094/CC-83-0569

Yan, S., Chen, G., Hou, Y., & Chen, Y. (2020). Improved solubility of banana starch by dielectric barrier discharge plasma treatment. *International Journal of Food Science & Technology*, *55*(2), 641–648. https://doi.org/10.1111/ijfs.14318

Yan, Y., Feng, L., Shi, M., Cui, C., & Liu, Y. (2020). Effect of plasma-activated water on the structure and in vitro digestibility of waxy and normal maize starches during heat-moisture treatment. *Food Chemistry*, *306*, 125589. https://doi.org/10.1016/j.foodchem.2019.125589

Yan, Y., Zhou, Y., Shi, M., Liu, H., & Liu, Y. (2019). Influence of atmospheric pressure plasma jet on the structure of microcrystalline starch with different relative crystallinity. *International Journal of Food Science & Technology*, *54*(2), 567–575. https://doi.org/10.1111/ijfs.13973

Yeh, A., & Yeh, S. (1993). Some characteristics of hydroxypropylated and cross-linked rice starch. *Cereal Chemistry, 70 596–596.*

Zhang, B., Chen, L., Li, X., Li, L., & Zhang, H. (2015). Understanding the multi-scale structure and functional properties of starch modulated by glow-plasma: A structure-functionality relationship. *Food Hydrocolloids*, *50*, 228–236. https://doi.org/10.1016/j.foodhyd.2015.05.002

Zhang, B., Xiong, S., Li, X., Li, L., Xie, F., & Chen, L. (2014). Effect of oxygen glow plasma on supramolecular and molecular structures of starch and related mechanism. *Food Hydrocolloids*, *37*, 69–76. https://doi.org/10.1016/j.foodhyd.2013.10.034

Zhao, Y., Patange, A., Sun, D., & Tiwari, B. (2020). Plasma-activated water: Physicochemical properties, microbial inactivation mechanisms, factors

influencing antimicrobial effectiveness, and applications in the food industry. *Comprehensive Reviews in Food Science and Food Safety*, *19*(6), 3951–3979. https://doi.org/10.1111/1541-4337.12644

Zhou, Y., Yan, Y., Shi, M., & Liu, Y. (2019). *Effect of an Atmospheric Pressure Plasma Jet on the Structure and Physicochemical Properties of Waxy and Normal Maize Starch*. 15.

Zhu, F. (2017). Plasma modification of starch. *Food Chemistry*, *232*, 476–486. https://doi.org/10.1016/j.foodchem.2017.04.024

Zia-ud-Din, Xiong, H., & Fei, P. (2017). Physical and chemical modification of starches: A review. *Critical Reviews in Food Science and Nutrition*, *57*(12), 2691–2705. https://doi.org/10.1080/10408398.2015.1087379

Zou, J.-J., Liu, C.-J., & Eliasson, B. (2004). Modification of starch by glow discharge plasma. *Carbohydrate Polymers*, *55*(1), 23–26. https://doi.org/10.1016/j.carbpol.2003.06.001

Appendices

Appendix A: Solid-state ^{13}C Nuclear Magnetic Resonance (NMR) Spectra of radio frequency plasma treated and untreated starches

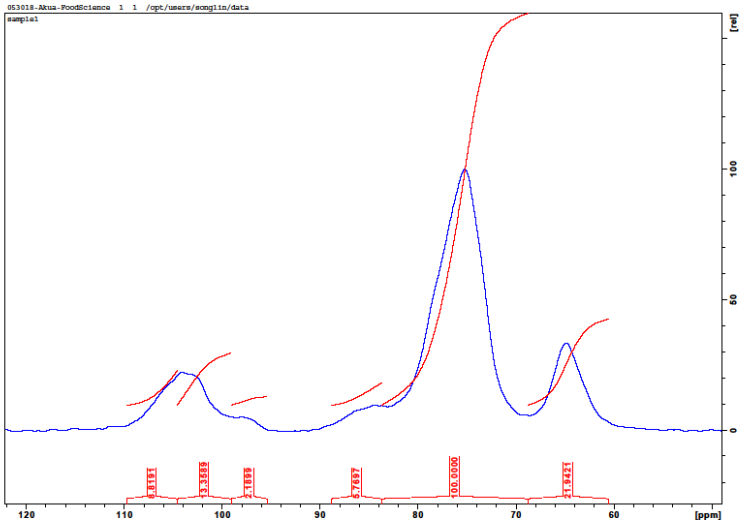

Plasma treated waxy rice NMR spectrum

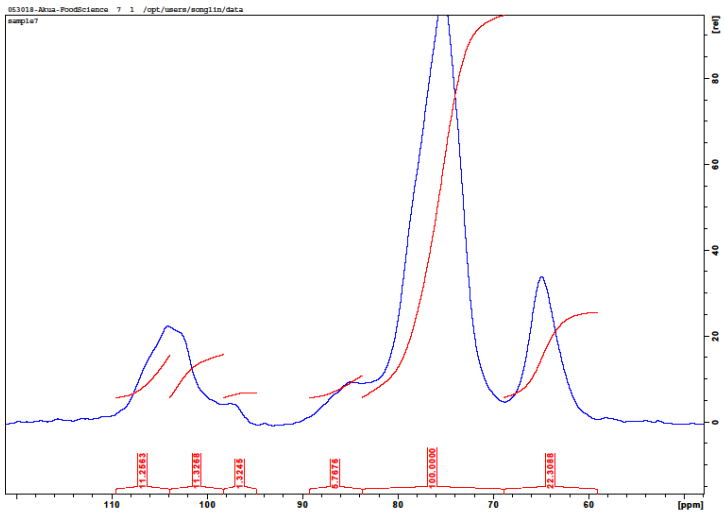

Gas treated waxy rice NMR spectrum

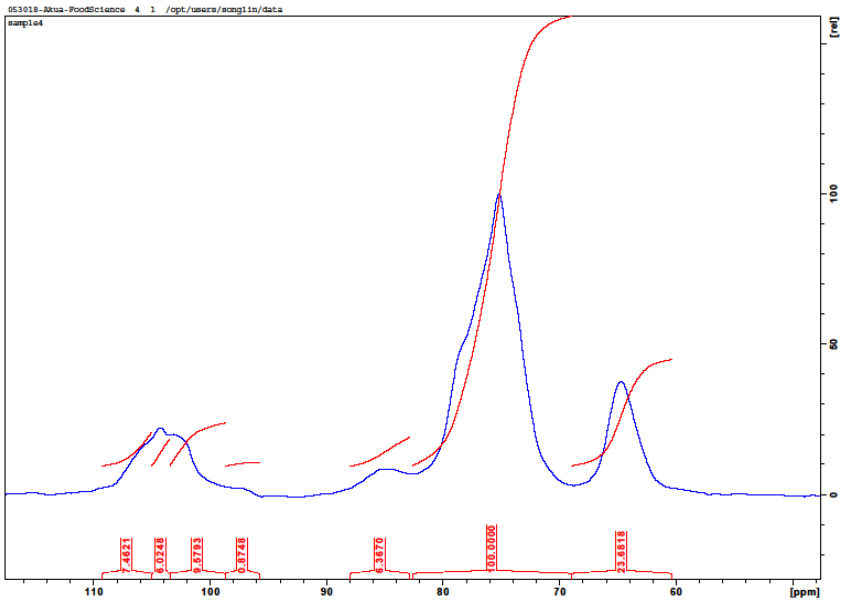

Waxy rice NMR spectrum

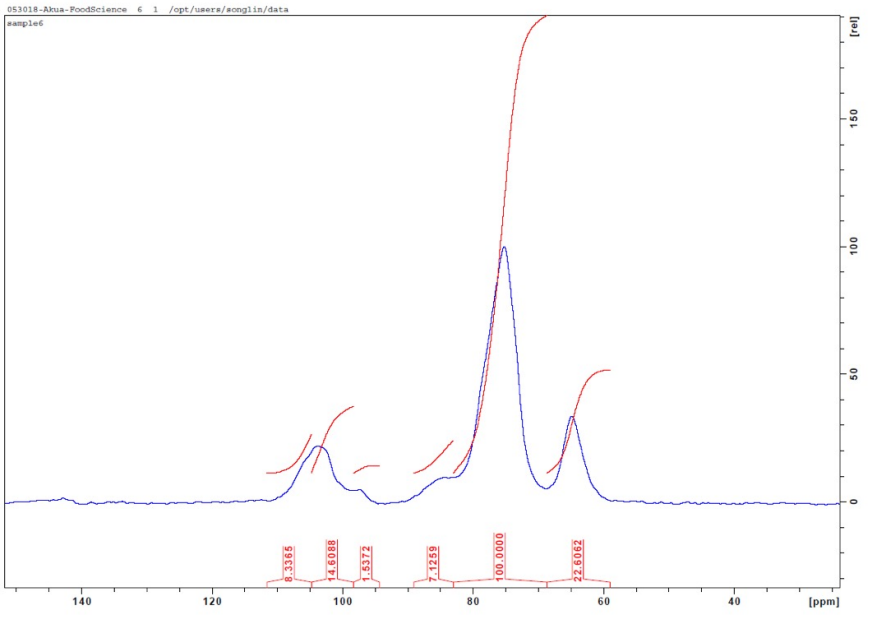

Plasma treated waxy maize NMR spectrum

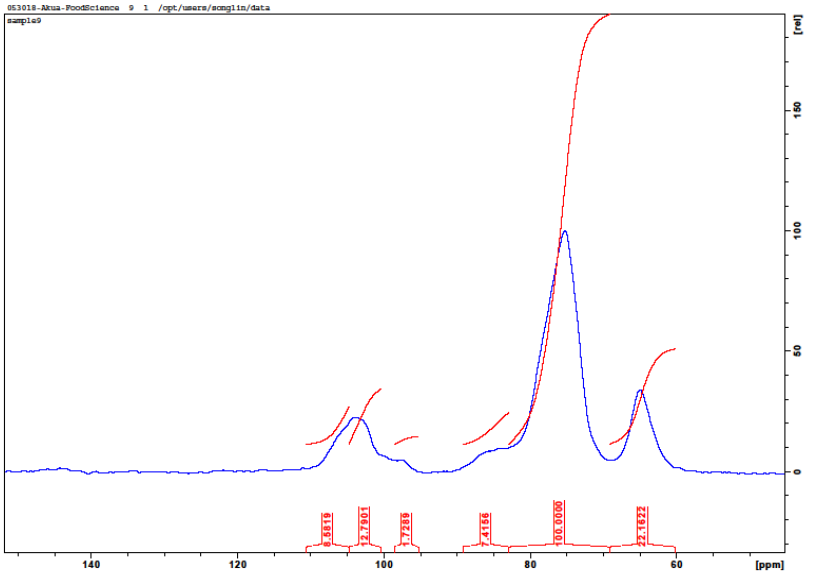

Gas treated waxy maize NMR spectrum

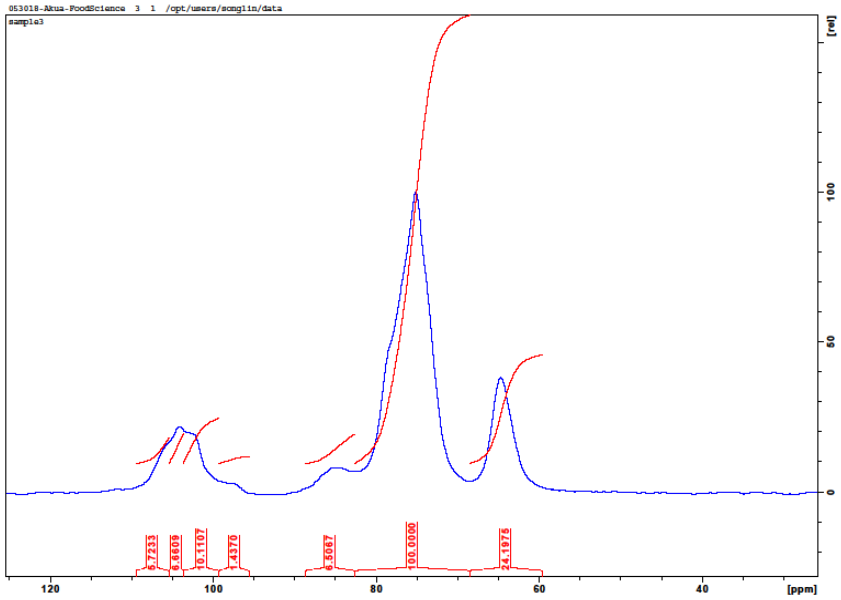

Waxy maize NMR spectrum

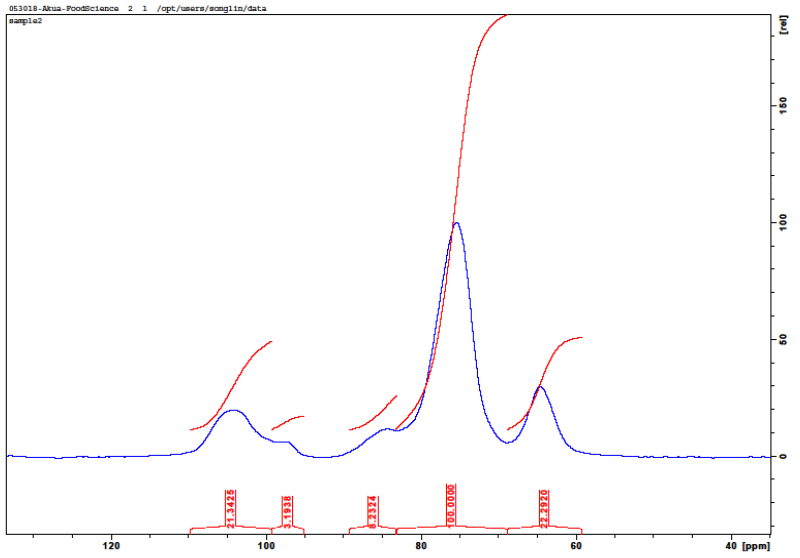

Plasma treated waxy potato NMR spectrum

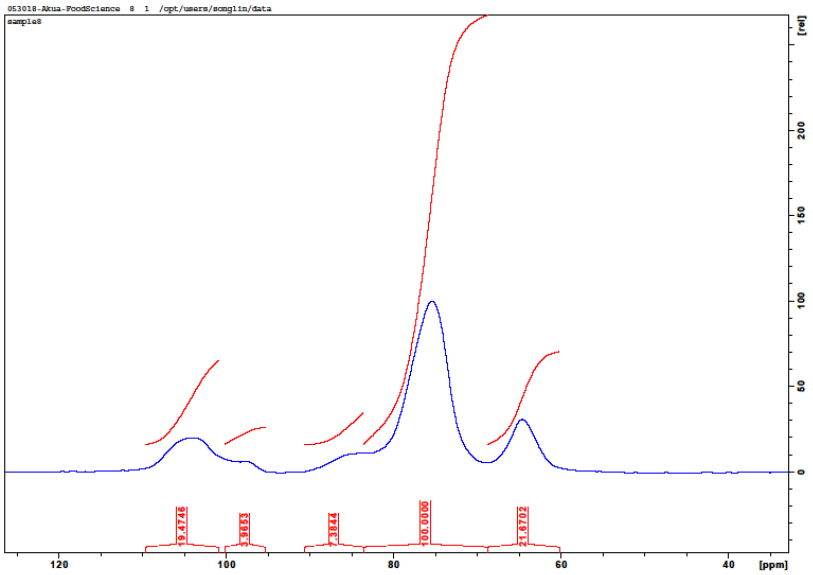

Gas treated waxy potato NMR spectrum

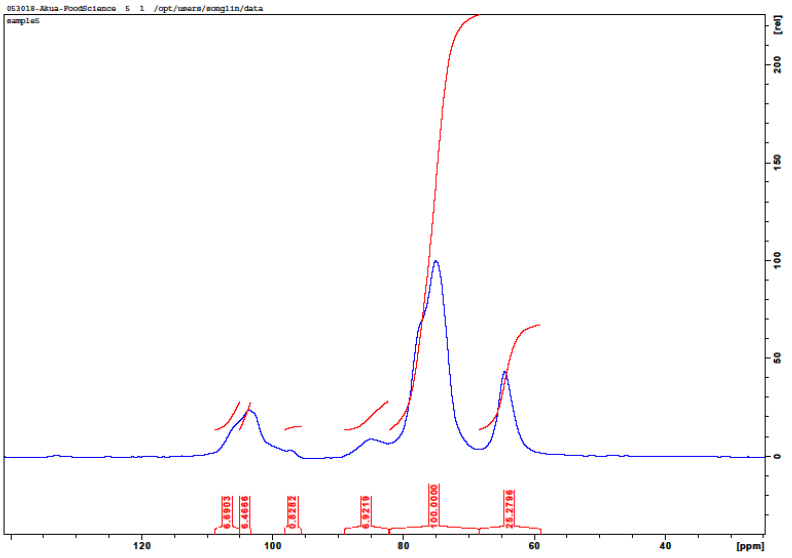

Waxy potato NMR spectrum

Figure A1: Supplementary data showing the NMR Spectra of starches

Appendix B: Unit and internal chain data of radio of radio frequency plasma treated and untreated starches

Table B1 Average chain lengths (CLs) of different chain categories and the β-Limit values of waxy maize, rice and potato starch

Sample	CL_a	SCL_a	LCL_a	ECL_a	ICL_a	$TICL_a$	β-limit $value_a$	$CL_{LD\ a}$
WMS G	18.8±0.2	15.7±0.0	52.9±0.7	12.4±0.2	5.4±0.0	14.5±0.1	55.4±0.4	8.4±0.0
PTWMS G	18.9±0.1	15.8±0.1	52.0±0.0	12.4±0.1	5.5±0.0	14.6±0.1	55.2±0.1	8.7±0.0
WMS NG	18.2±0.0	15.7±0.0	50.4±0.1	12.1±0.1	5.1±0.1	14.1±0.1	55.4±0.5	8.1±0.1
PTWMS NG	18.7±0.3	15.8±0.1	52.2±1.3	12.4±0.3	5.3±0.1	14.0±0.0	55.8±0.5	8.3±0.1
WRS G	17.4±0.0	14.8±0.0	50.9±0.6	11.6±0.1	4.8±0.1	14.1±0.0	55.1±0.5	7.8±0.1
PTWRS G	17.5±0.0	14.8±0.0	51.4±0.2	11.6±0.2	4.9±0.2	14.2±0.2	54.9±1.1	7.9±0.2
WRS NG	17.0±0.0	14.7±0.0	49.4±0.1	11.3±0.5	4.7±0.4	13.8±0.1	54.5±2.7	7.7±0.4
PTWRS NG	17.7±0.0	14.9±0.0	51.5±0.1	12.1±0.1	4.6±0.1	13.8±0.1	57.0±0.4	7.6±0.1
WPS G	21.0±0.1	15.7±0.0	56.2±0.2	13.3±0.0	6.7±0.1	19.6±0.1	53.7±0.2	9.7±0.1
PTWPS G	20.9±0.1	15.7±0.0	56.1±0.2	13.0±0.1	6.9±0.1	19.7±0.1	52.8±0.5	9.9±0.1
WPS NG	20.8±0.1	15.7±0.0	56.2±0.1	14.0±0.1	5.9±0.1	18.6±0.1	57.5±0.6	8.9±0.1
PTWPS NG	20.8±0.0	15.7±0.0	56.0±0.0	13.8±0.2	6.0±0.2	19.0±0.1	56.9±0.9	9.0±0.2

The subscript ($_a$) on the title of each column shows no significant differences (p-value < 0.05) between treated and untreated granular and non-granular waxy starches of the same botanical type and form; WMS G: Waxy Maize Starch Granular, PTWMS G: Plasma Treated Waxy Maize Starch Granular, WMS NG: Waxy Maize Starch Non-Granular, PTWMS NG: Plasma Treated Waxy Maize Starch Non-Granular, WRS G: Waxy Rice Starch Granular, PTWRS G: Plasma Treated Waxy Rice Starch Granular, WRS NG: Waxy Rice Starch Non-Granular, PTWRS NG: Plasma Treated Waxy Rice Starch Non-Granular; WPS G: Waxy Potato Starch Granular, PTWPS G: Plasma Treated Waxy Potato Starch Granular, WPS NG: Waxy Potato Starch Non-Granular, PTWPS NG: Plasma Treated Waxy Potato Starch Non-Granular.

[a] CL=chain length; SCL = CL of short chains; LCL = CL of long chains; ECL (external CL) = CL × (β -limit value/100) + 2; ICL (internal CL) = CL – ECL – 1; TICL (total internal CL) = B-CL_{LD} – 1 (B-CL_{LD}=CL_{LD} of B-chains); β-limit value was calculated from the difference in CL of amylopectin and its β-limit dextrin; CL_{LD} = average CL of β-limit dextrin

Table B2 Relative molar amounts (%) of chain categories in waxy maize, rice and potato starches

Sample	A-chains[p] [a]	A_{fp}[q] [a]	$A_{crystal}$[r] [a]	B-chains[s] [a]	BS [a]	BL [a]	B_{fp}[u] [a]	BS_{major}[v] [a]	B2[w] [a]	B3[x] [a]
WMS G	54.8±0.2	7.1±0.0	47.7±0.2	45.3±0.2	38.3±0.2	7.0±0.0	13.7±0.1	24.6±0.1	5.6±0.0	1.4±0.0
PTWMS G	54.3±0.0	7.1±0.0	47.2±0.0	45.8±0.0	38.7±0.0	7.0±0.0	13.8±0.0	24.9±0.0	5.7±0.0	1.4±0.0
WMS NG	55.4±1.9	7.1±0.0	48.3±1.9	44.6±1.9	37.7±1.7	6.9±0.2	13.9±0.8	23.8±0.9	5.7±0.1	1.2±0.0
PTWMS NG	53.9±0.8	7.1±0.0	46.8±0.8	46.0±0.8	39.1±0.7	6.9±0.1	14.4±0.2	24.8±0.5	5.8±0.1	1.2±0.0
WRS G	57.6±0.7	7.3±0.0	50.3±0.7	42.4±0.7	35.2±0.6	7.3±0.1	13.7±0.2	21.4±0.4	6.3±0.1	1.2±0.0
PTWRS G	57.5±0.6	7.3±0.0	50.2±0.6	42.5±0.6	35.1±0.3	7.3±0.2	13.7±0.1	21.5±0.3	6.2±0.1	1.2±0.1
WRS NG	57.4±3.9	7.4±0.0	50.1±3.9	42.6±3.9	35.6±3.3	7.0±0.6	14.4±1.3	21.2±1.9	5.9±0.6	1.1±0.1
PTWRS NG	58.6±0.3	7.4±0.0	51.2±0.3	41.5±0.3	34.6±0.2	6.9±0.1	13.7±0.1	20.9±0.3	5.8±0.0	1.0±0.0
WPS G	60.1±0.1	6.9±0.0	53.2±0.1	39.9±0.1	26.9±0.0	13.1±0.1	9.3±0.1	17.6±0.0	10.1±0.1	3.0±0.1
PTWPS G	60.0±0.2	6.9±0.0	52.7±0.2	40.4±0.2	27.7±0.1	12.8±0.1	9.5±0.0	18.2±0.1	9.7±0.1	3.1±0.0
WPS NG	62.9±0.3	6.8±0.0	56.1±0.3	37.1±0.3	26.4±0.1	10.7±0.2	9.1±0.0	17.3±0.1	8.3±0.1	2.4±0.1
PTWPS NG	63.2±0.7	6.8±0.0	56.3±0.7	36.9±0.7	25.6±0.4	11.3±0.3	8.9±0.0	16.6±0.4	8.2±0.3	2.6±0.1

The subscript ($_a$) on the title of each column shows no significant differences (p-value < 0.05) between treated and untreated granular and non-granular waxy starches of the same botanical type and form; WMS G: Waxy Maize Starch Granular, PTWMS G: Plasma Treated Waxy Maize Starch Granular, WMS NG: Waxy Maize Starch Non-Granular, PTWMS NG: Plasma Treated Waxy Maize Starch Non-Granular, WRS G: Waxy Rice Starch Granular, PTWRS G: Plasma Treated Waxy Rice Starch Granular, WRS NG: Waxy Rice Starch Non-Granular, PTWRS NG: Plasma Treated Waxy Rice Starch Non-Granular, WPS G: Waxy Potato Starch Granular, PTWPS G: Plasma Treated Waxy Potato Starch Granular, WPS NG: Waxy Potato Starch Non-Granular, PTWPS NG: Plasma Treated Waxy Potato Starch Non-Granular.

[p] Detected as maltose after debranching of β -limit dextrins ; [q]"Fingerprint" A-chains at DP 6–8 in the original amylopectin sample; [r] $A_{crystal}$-chains calculated as all A-chains – A_{fp}; [s] B-chains correspond to DP > 3 in β-limit dextrins and were divided into short (BS) and long (BL) chains at between DP 22–25 depending on the sample; [u]"Fingerprint" B-chains at DP 4–7 in β-limit dextrins; [v]The major group of short B-chains at DP 8 to 22–24, depending on the sample. [x] Long chains between DP 22 or 25 and 50, depending on the sample; [y] Long chains at DP > 50.

Appendix C: DSC thermogram of treated and untreated starches

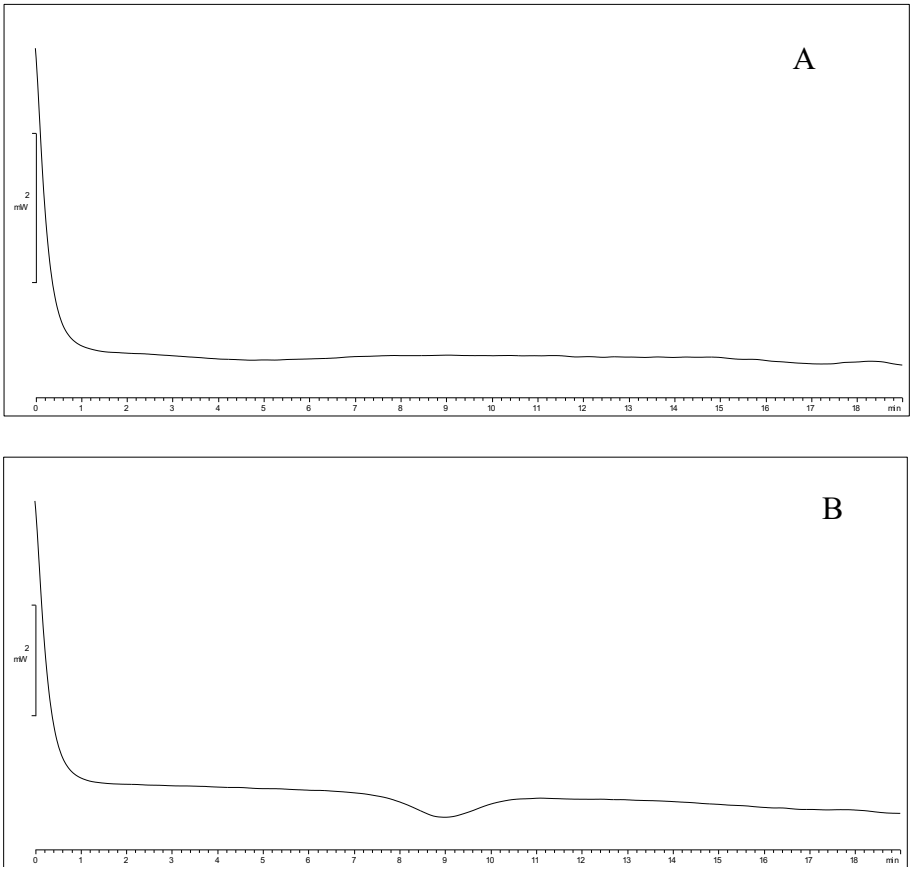

Figure C1. Representative DSC thermogram of treated and untreated starches. A = plasma-activated water starches incubated at 80°C; B = native starches and plasma-activated water starches incubated at 25°C and 60°C

Appendix D: Survey scans obtained from XPS analysis of treated and untreated starches

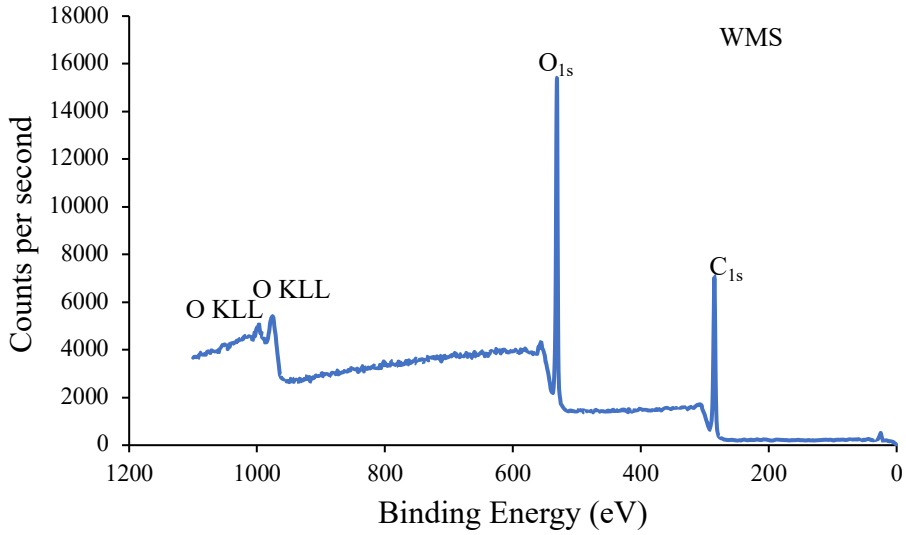

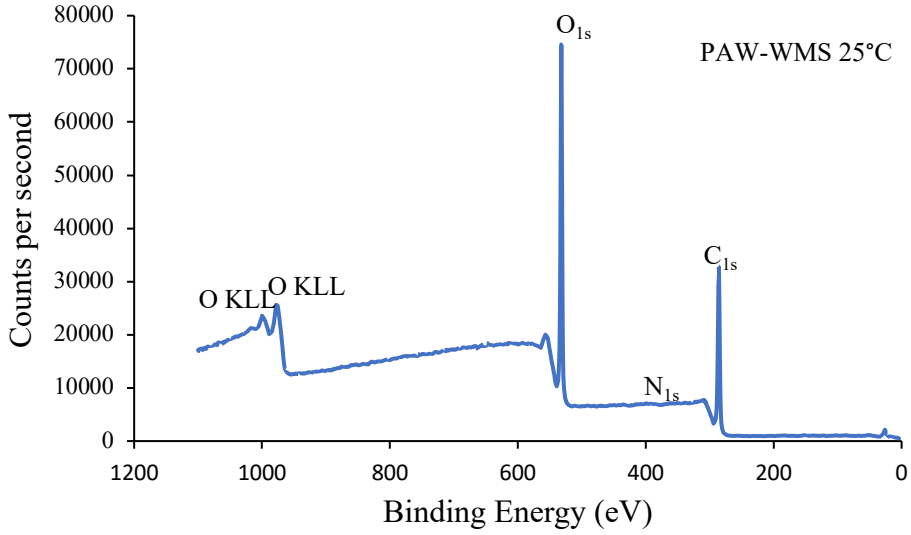

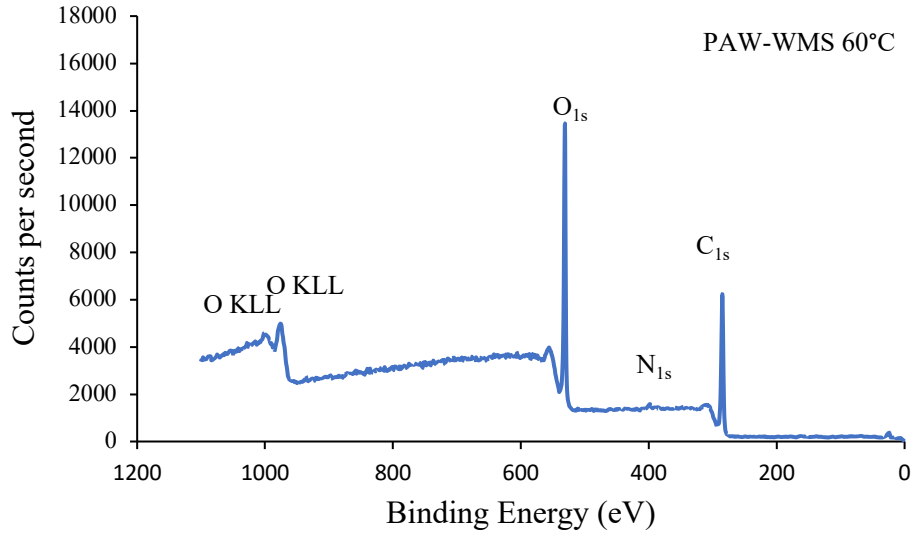
PAW-WMS 60°C
Counts per second
Binding Energy (eV)
O KLL
O KLL
O1s
N1s
C1s
18000
16000
14000
12000
10000
8000
6000
4000
2000
0
1200
1000
800
600
400
200
0

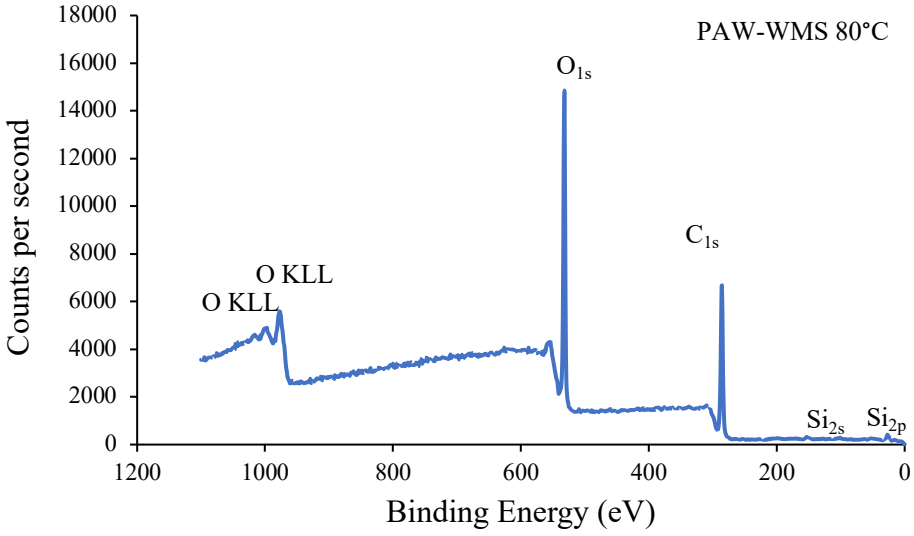
PAW-WMS 80°C
Counts per second
Binding Energy (eV)
O KLL
O KLL
O1s
C1s
Si2s
Si2p
18000
16000
14000
12000
10000
8000
6000
4000
2000
0
1200
1000
800
600
400
200
0

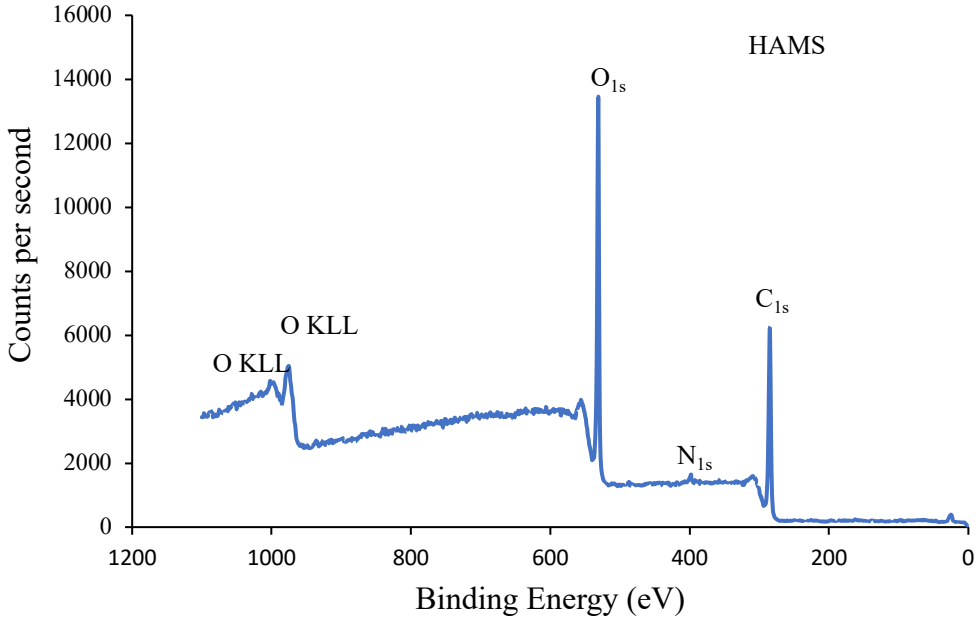
HAMS
Counts per second
Binding Energy (eV)
O KLL
O KLL
O1s
N1s
C1s
16000
14000
12000
10000
8000
6000
4000
2000
0
1200
1000
800
600
400
200
0

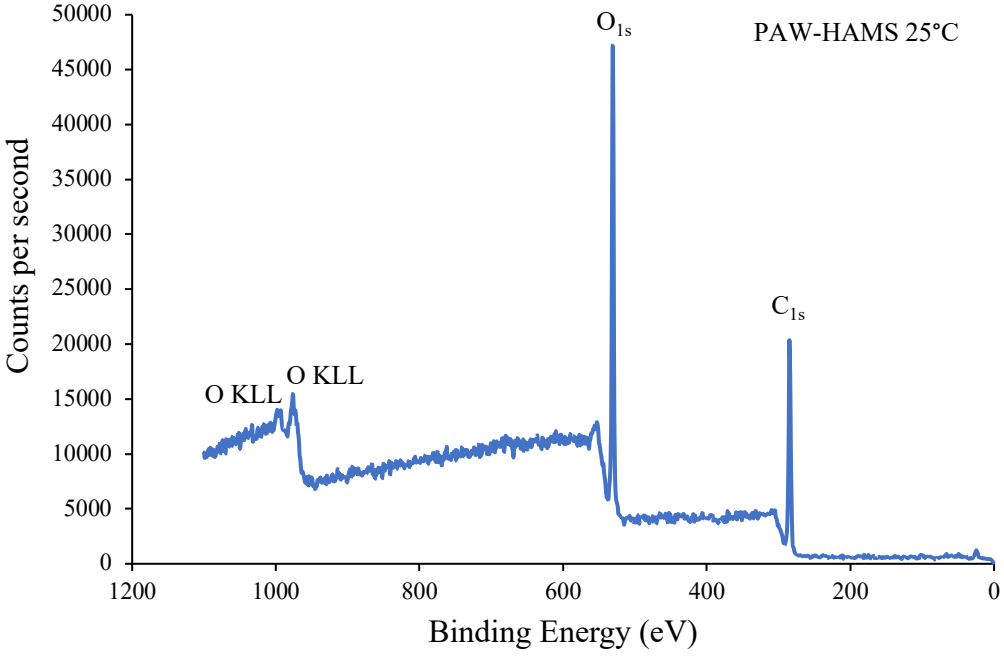
PAW-HAMS 25°C
Counts per second
Binding Energy (eV)
O KLL
O KLL
O1s
C1s
50000
45000
40000
35000
30000
25000
20000
15000
10000
5000
0
1200
1000
800
600
400
200
0

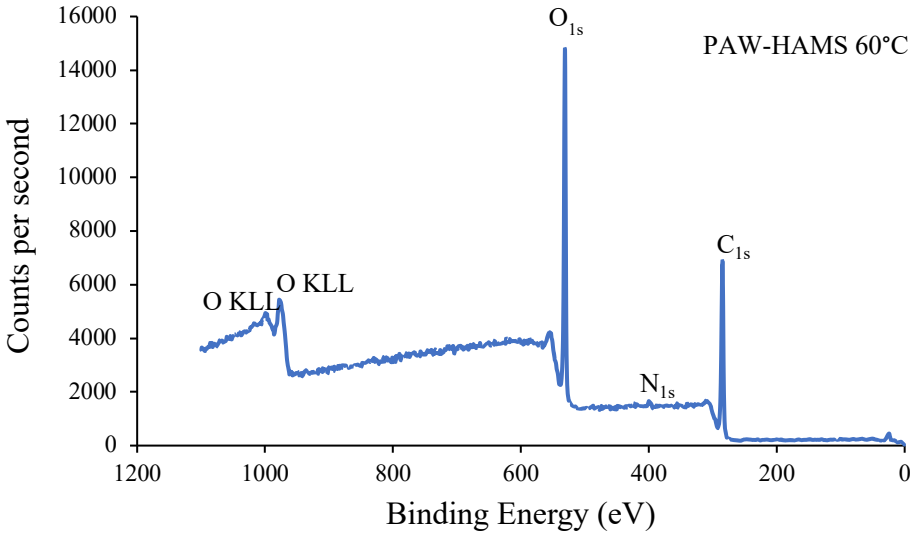
PAW-HAMS 60°C
Counts per second
Binding Energy (eV)
O KLL
O KLL
O1s
N1s
C1s
16000
14000
12000
10000
8000
6000
4000
2000
0
1200
1000
800
600
400
200
0

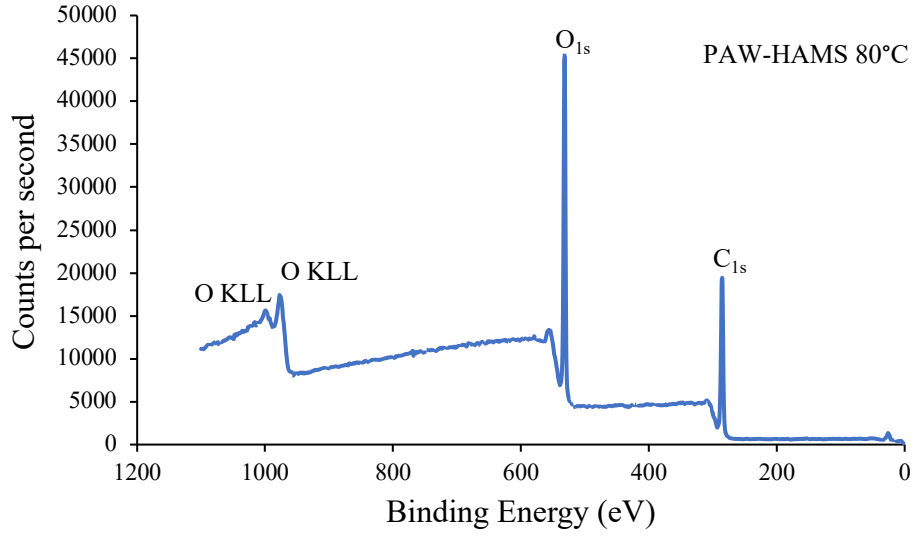
PAW-HAMS 80°C
Counts per second
Binding Energy (eV)
O KLL
O KLL
O1s
C1s
50000
45000
40000
35000
30000
25000
20000
15000
10000
5000
0
1200
1000
800
600
400
200
0

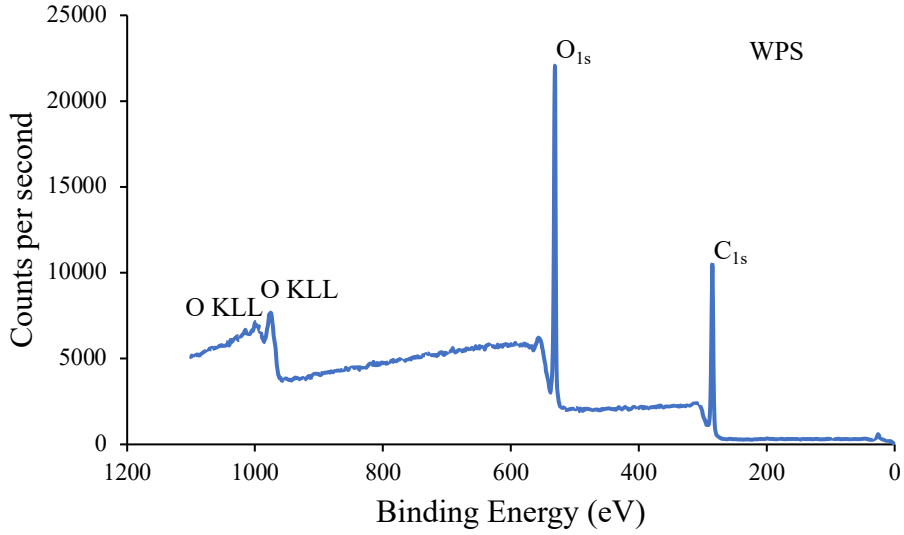
25000
20000
15000
10000
5000
0
Counts per second
1200
1000
800
600
400
200
0
Binding Energy (eV)
O1s
WPS
C1s
O KLL
O KLL

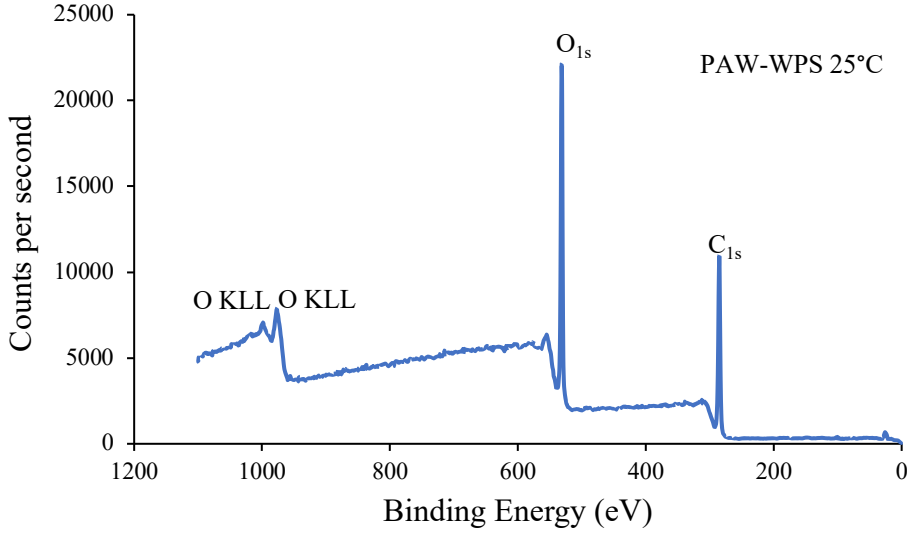
25000
20000
15000
10000
5000
0
Counts per second
1200
1000
800
600
400
200
0
Binding Energy (eV)
O1s
PAW-WPS 25°C
C1s
O KLL
O KLL

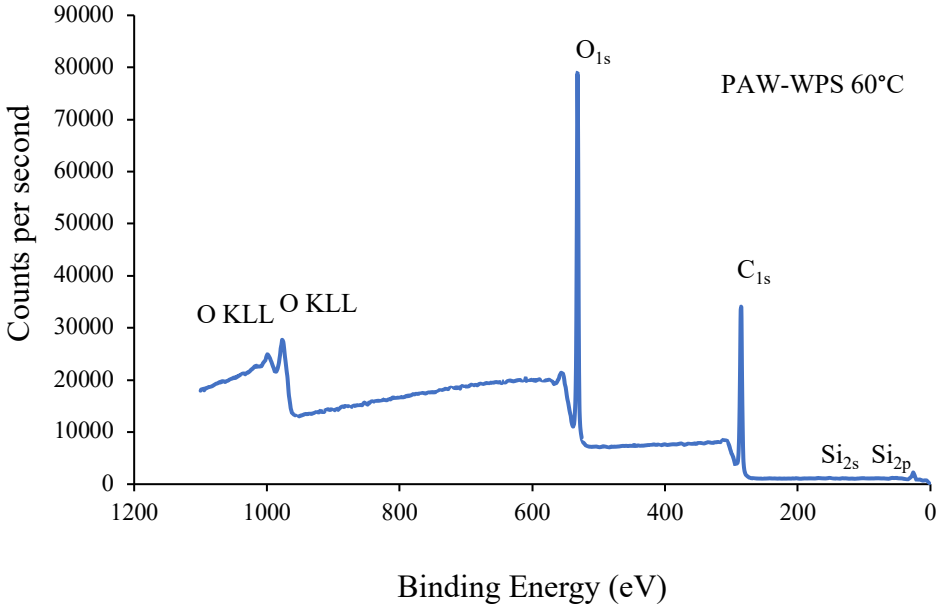
90000
80000
70000
60000
50000
40000
30000
20000
10000
0
Counts per second
1200
1000
800
600
400
200
0
Binding Energy (eV)
O1s
PAW-WPS 60°C
C1s
O KLL
O KLL
Si2s
Si2p

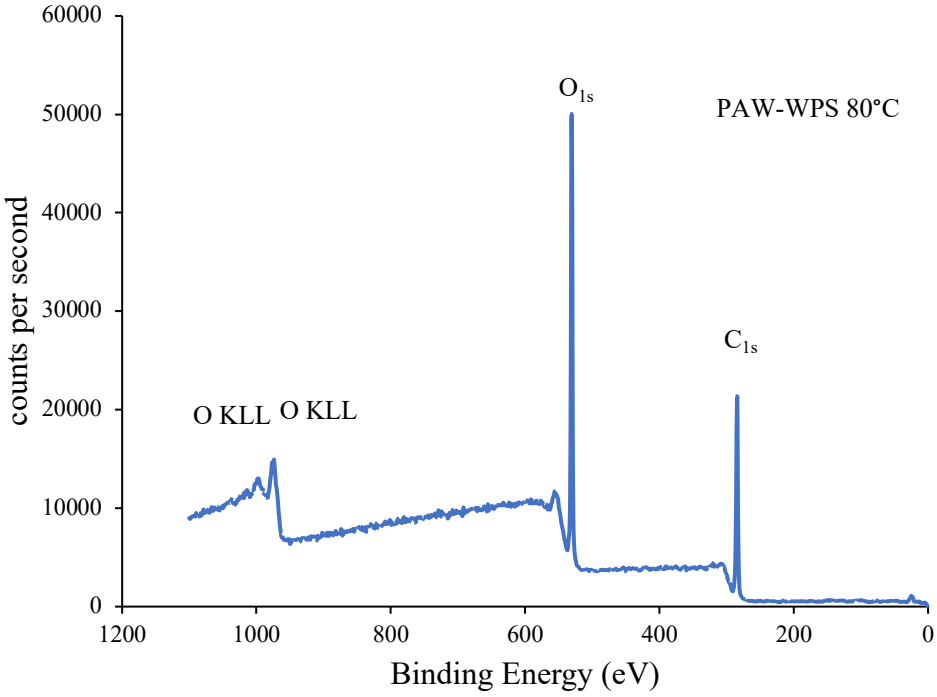
60000
50000
40000
30000
20000
10000
0
counts per second
1200
1000
800
600
400
200
0
Binding Energy (eV)
O1s
PAW-WPS 80°C
C1s
O KLL
O KLL

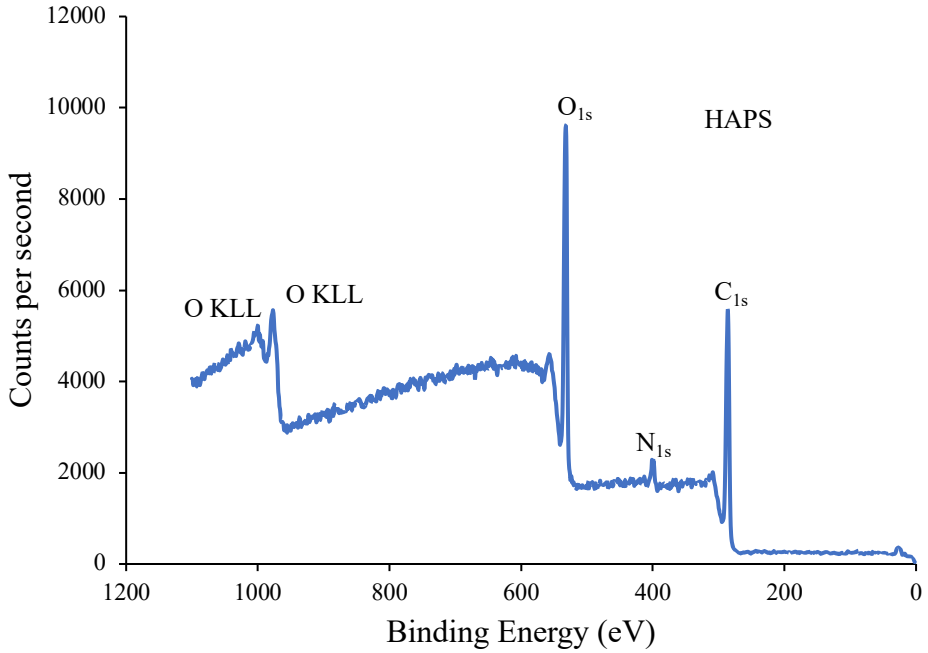
12000
10000
8000
6000
4000
2000
0
Counts per second
O KLL
O KLL
O1s
N1s
C1s
HAPS
1200
1000
800
600
400
200
0
Binding Energy (eV)

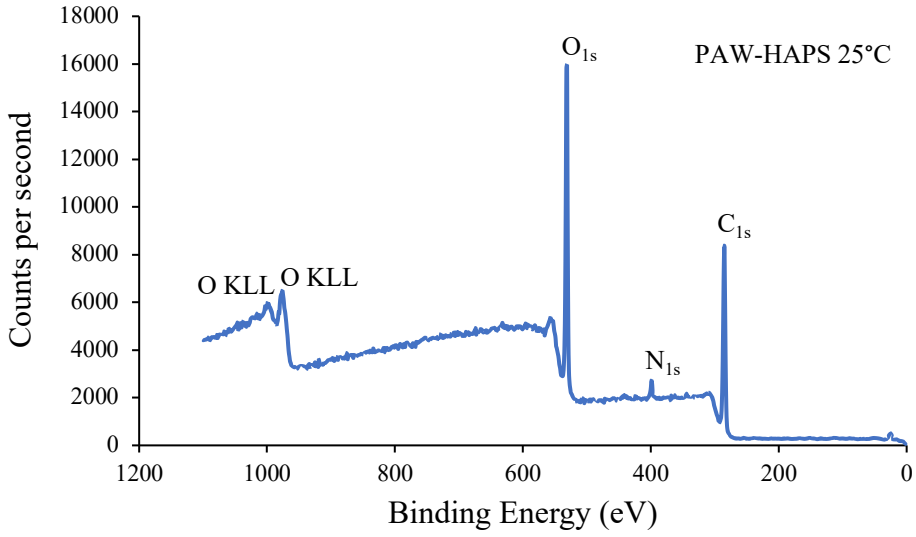
18000
16000
14000
12000
10000
8000
6000
4000
2000
0
Counts per second
O KLL
O KLL
O1s
N1s
C1s
PAW-HAPS 25°C
1200
1000
800
600
400
200
0
Binding Energy (eV)

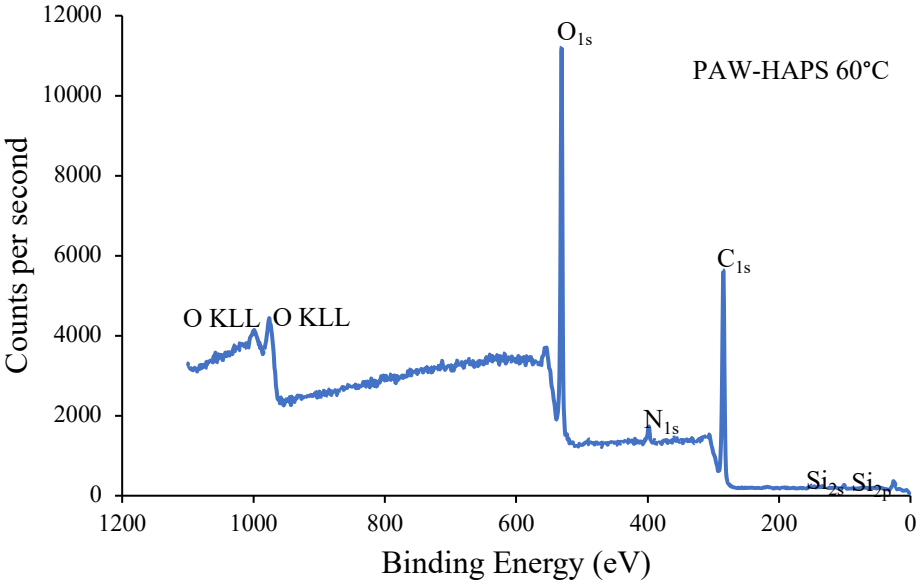
12000
10000
8000
6000
4000
2000
0
Counts per second
1200
1000
800
600
400
200
0
Binding Energy (eV)
O1s
PAW-HAPS 60°C
C1s
O KLL
O KLL
N1s
Si2s
Si2p

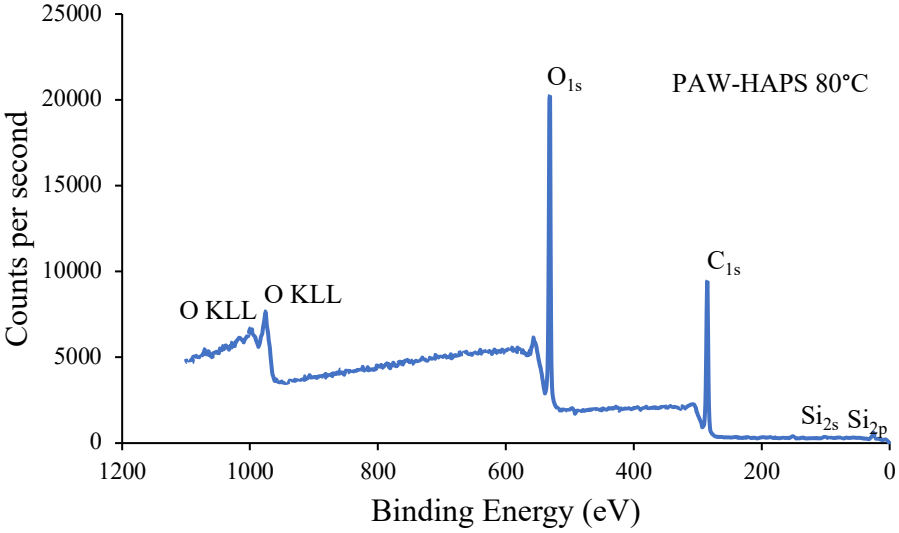
25000
20000
15000
10000
5000
0
Counts per second
1200
1000
800
600
400
200
0
Binding Energy (eV)
O1s
PAW-HAPS 80°C
C1s
O KLL
O KLL
Si2s
Si2p

Figure D1. Survey scans obtained from XPS analysis of treated and untreated starches. The different incubation temperatures for the starches are attached to the sample name. WMS: Waxy Maize Starch, PAW-WMS 25°C : Plasma-Activated Water Waxy Maize Starch 25°C, PAW-WMS 60°C: Plasma-Activated Water Waxy Maize Starch 60°C, PAW-WMS 80°C: Plasma-Activated Water Waxy Maize Starch 80°C, HAMS: High Amylose Maize Starch, PAW-HAMS 25°C : Plasma-Activated Water High Amylose Maize Starch 25°C, PAW-HAMS 60°C: Plasma-Activated Water High Amylose Maize Starch 60°C, PAW-HAMS 80°C: Plasma-Activated Water High Amylose Maize Starch 80°C, WPS: Waxy Potato Starch, PAW-WPS 25°C: Plasma-Activated Water Waxy Potato Starch 25°C, PAW-WPS 60°C: Plasma-Activated Water Waxy Potato Starch 60°C, PAW-WPS 80°C: Plasma-Activated Water Waxy Potato Starch 80°C, HAPS: High Amylose Potato Starch, PAW-HAPS 25°C: Plasma-Activated Water High Amylose Potato Starch 25°C, PAW-HAPS 60°C: Plasma-Activated Water High Amylose Potato Starch 60°C, PAW-HAPS 80°C: Plasma-Activated Water High Amylose Potato Starch 80°C

Appendix E: Curve fitted C1s XPS spectra of treated and untreated starches

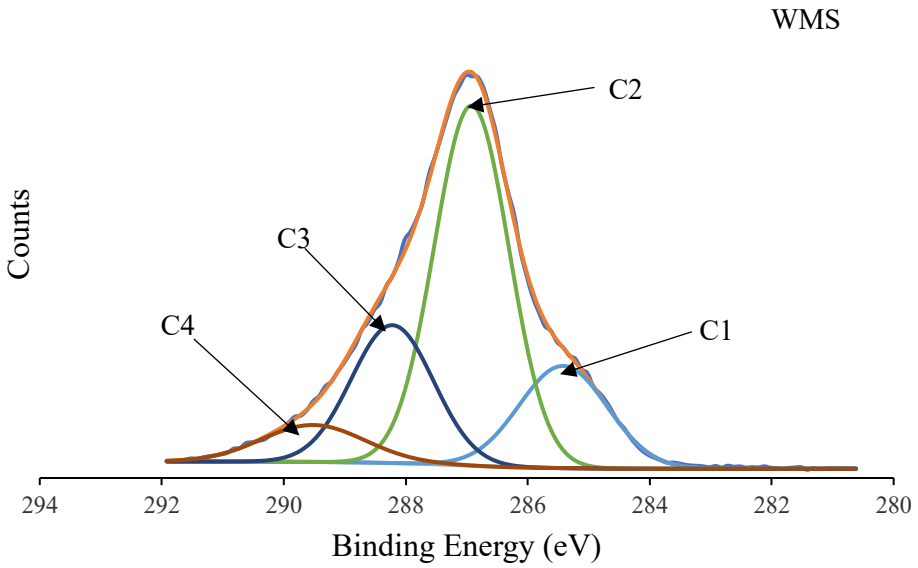

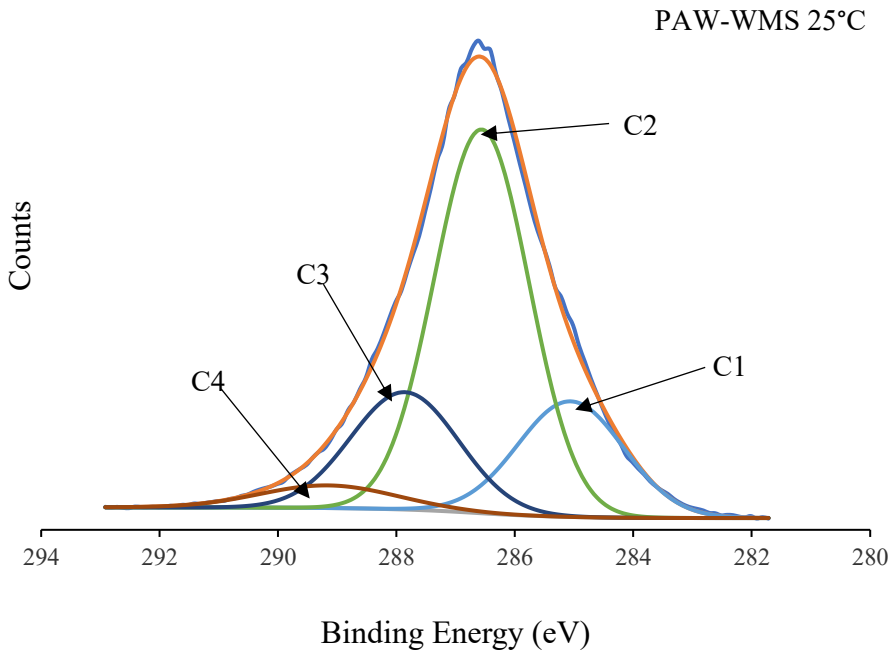

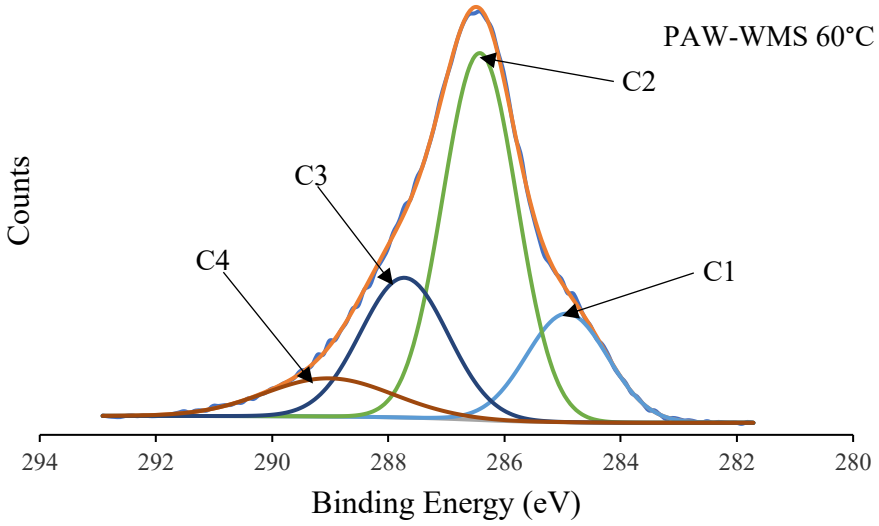
PAW-WMS 60°C
C2
C3
C4
C1
Counts
294
292
290
288
286
284
282
280
Binding Energy (eV)

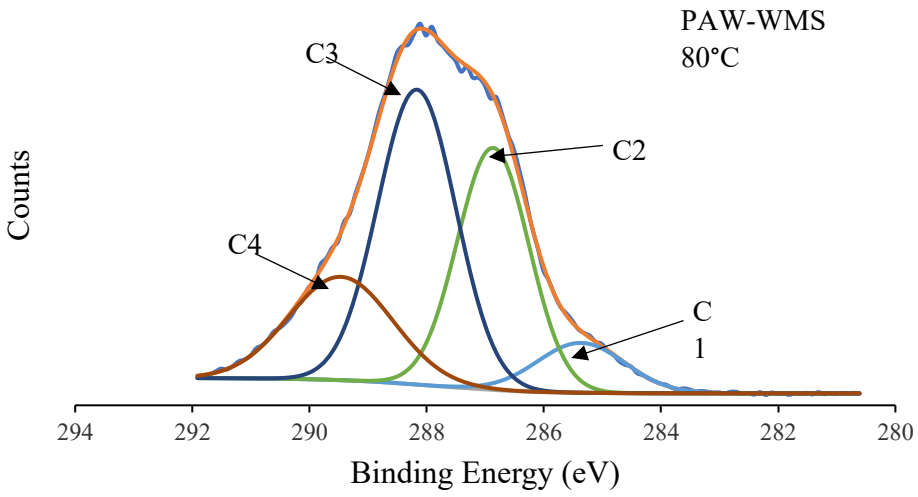
PAW-WMS
80°C
C3
C2
C4
C
1
Counts
294
292
290
288
286
284
282
280
Binding Energy (eV)

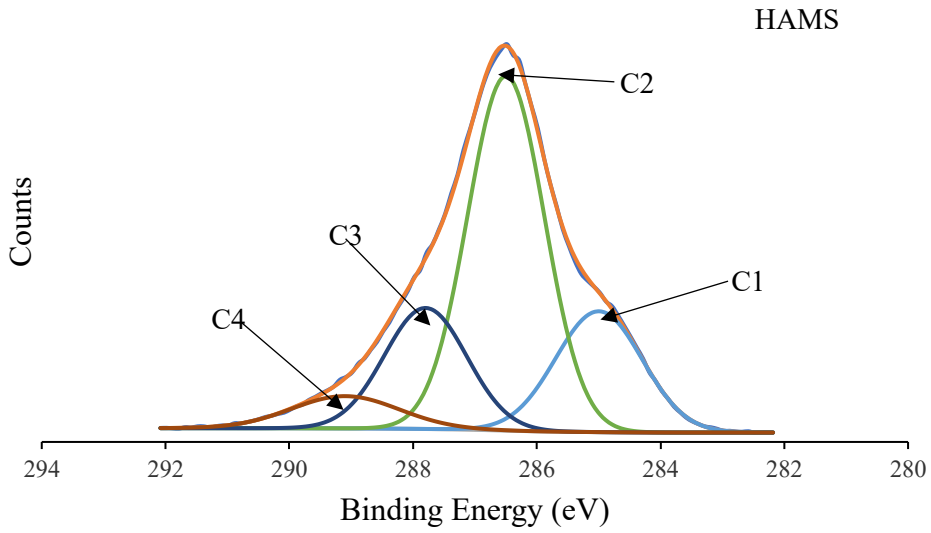
HAMS
C2
C3
C1
C4
Counts
294
292
290
288
286
284
282
280
Binding Energy (eV)

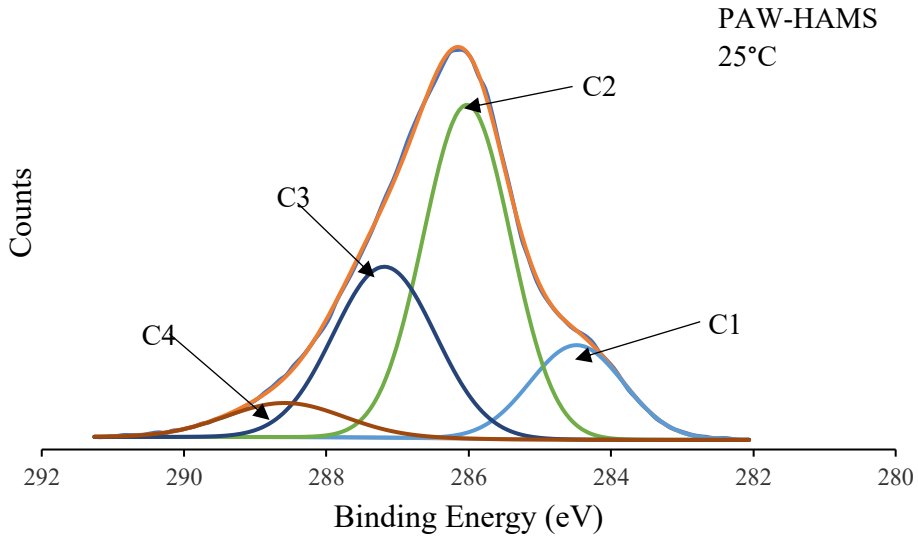
PAW-HAMS
25°C
C2
C3
C1
C4
Counts
292
290
288
286
284
282
280
Binding Energy (eV)

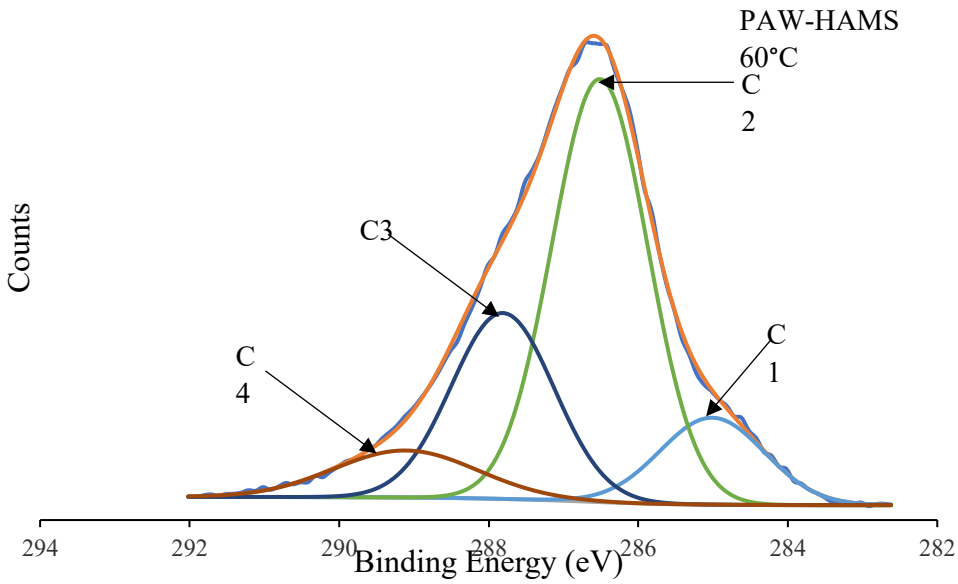
PAW-HAMS
60°C
C
2
C3
C
4
C
1
Counts
294
292
290
288
286
284
282
Binding Energy (eV)

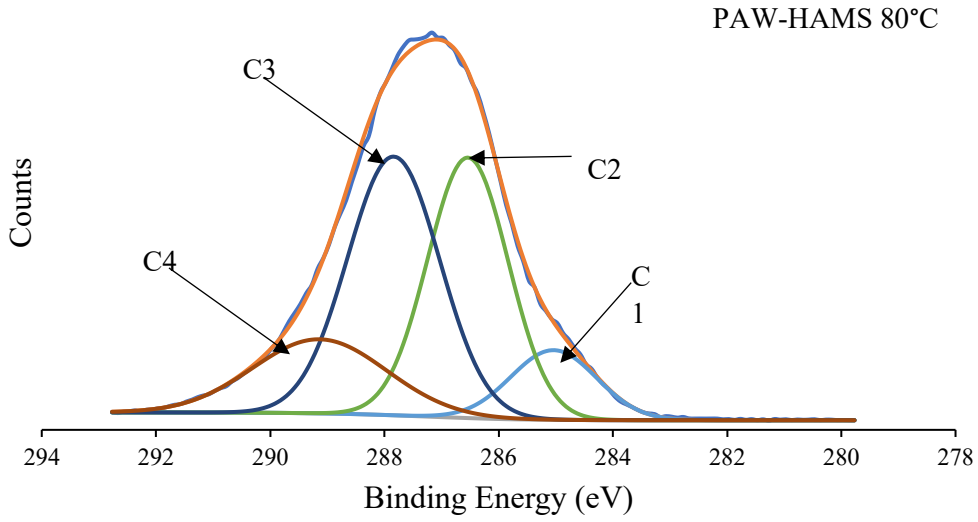
PAW-HAMS 80°C
C3
C2
C4
C
1
Counts
294
292
290
288
286
284
282
280
278
Binding Energy (eV)

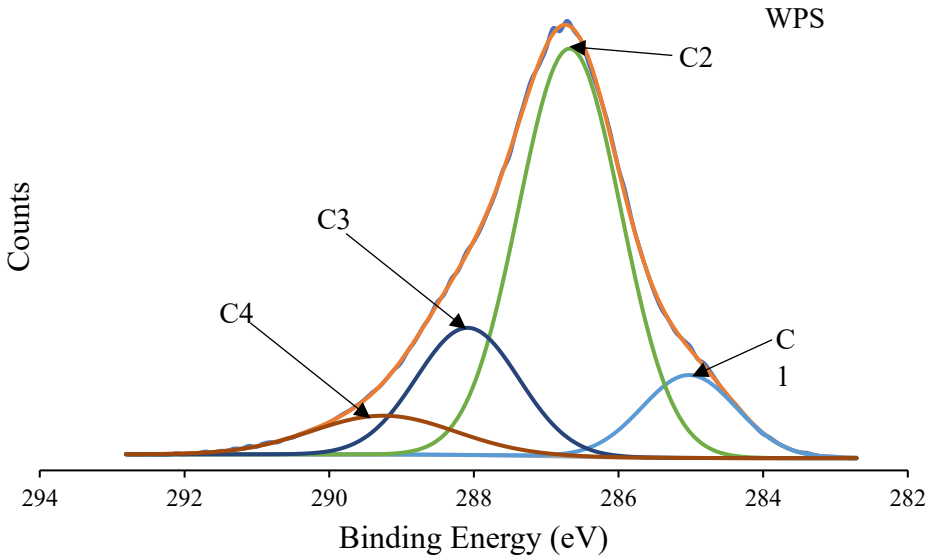
WPS
C2
C3
C4
C
1
Counts
294
292
290
288
286
284
282
Binding Energy (eV)

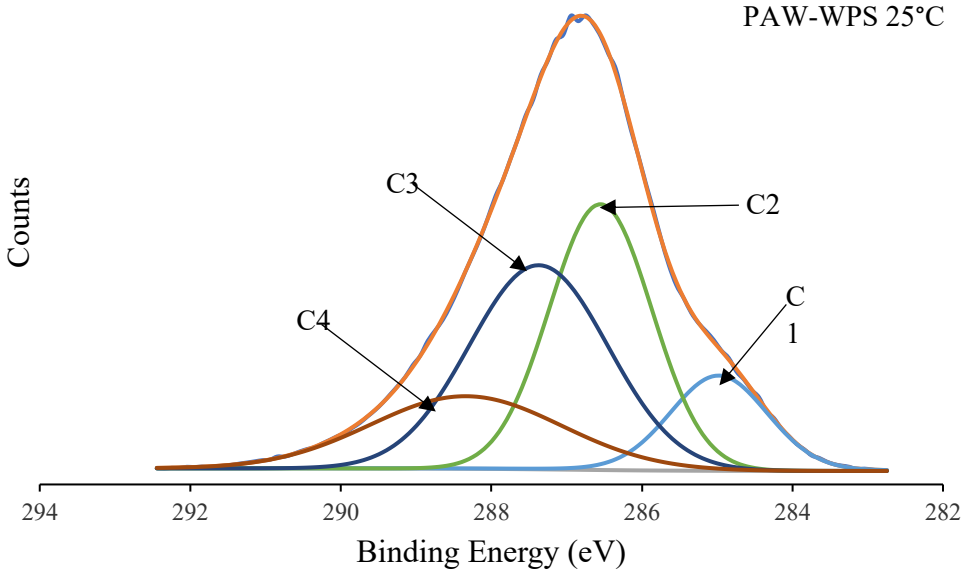
PAW-WPS 25°C
C3
C2
C4
C
1
Counts
294
292
290
288
286
284
282
Binding Energy (eV)

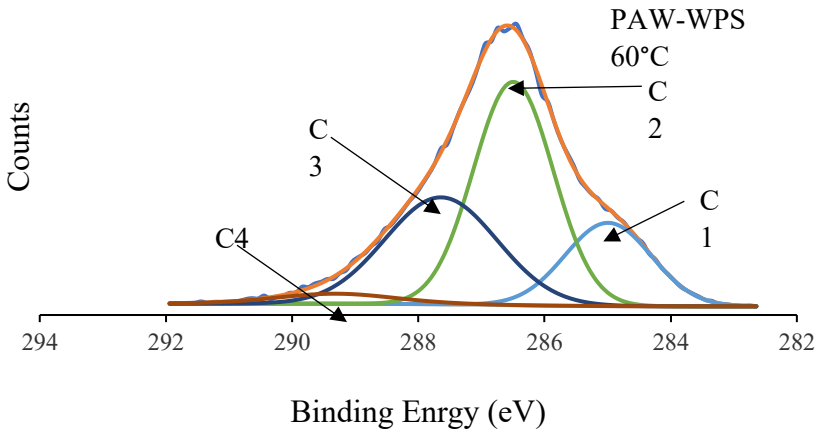
PAW-WPS
60°C
C
2
C
3
C
1
C4
Counts
294
292
290
288
286
284
282
Binding Enrgy (eV)

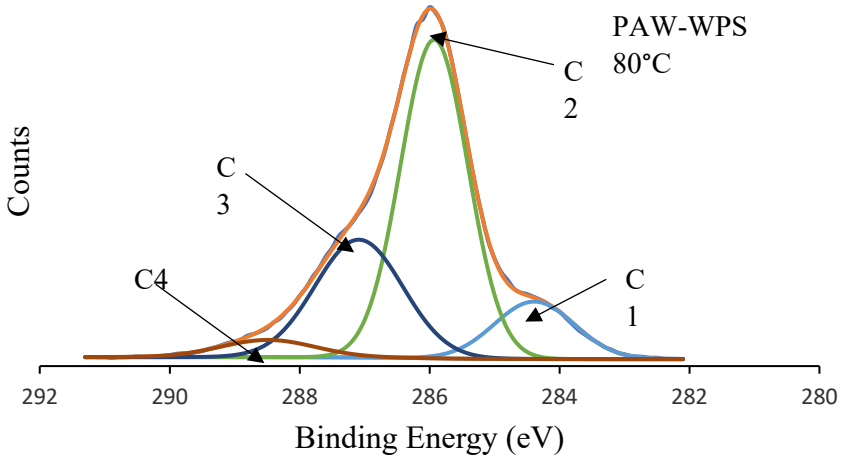
PAW-WPS
80°C
C
2
C
3
C
1
C4
Counts
292
290
288
286
284
282
280
Binding Energy (eV)

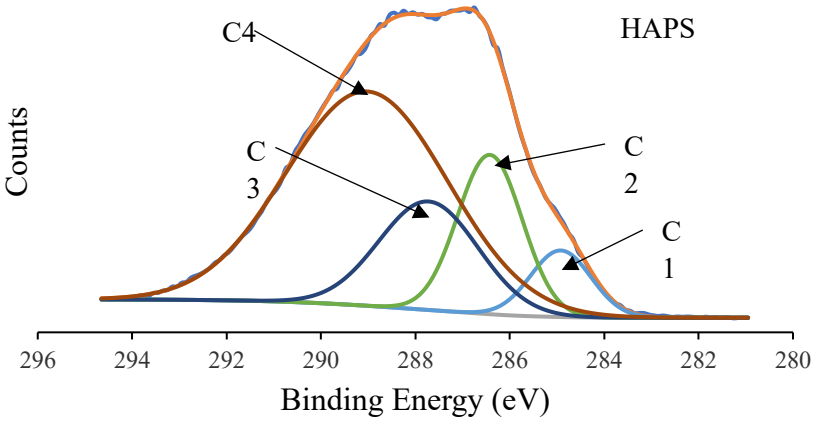
HAPS
C4
C
3
C
2
C
1
Counts
296
294
292
290
288
286
284
282
280
Binding Energy (eV)

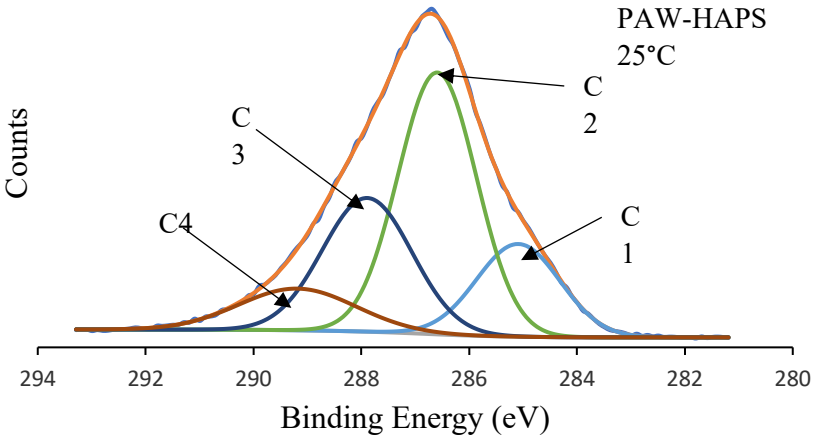
PAW-HAPS
25°C
C
2
C
3
C4
C
1
Counts
294
292
290
288
286
284
282
280
Binding Energy (eV)

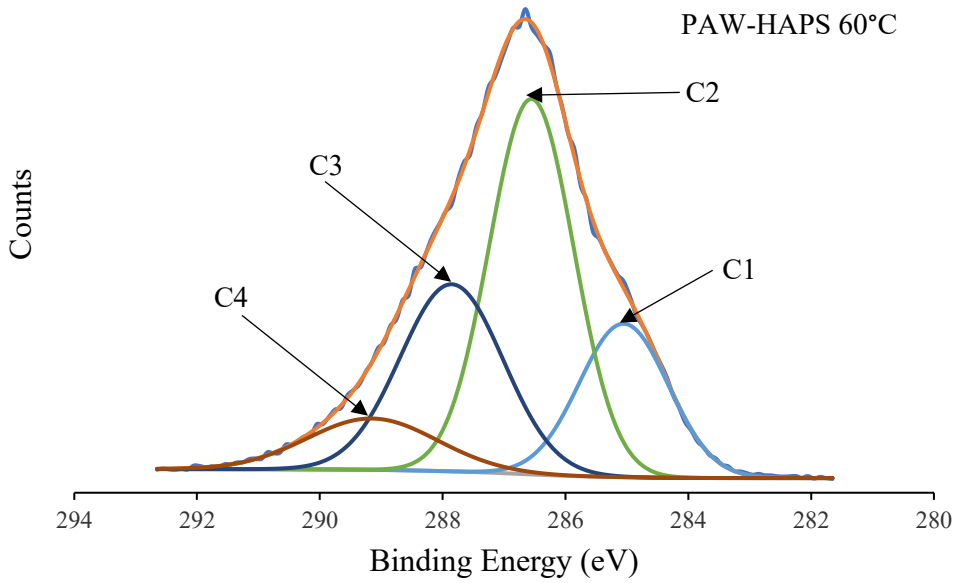
PAW-HAPS 60°C
C2
C3
C1
C4
Counts
294
292
290
288
286
284
282
280
Binding Energy (eV)

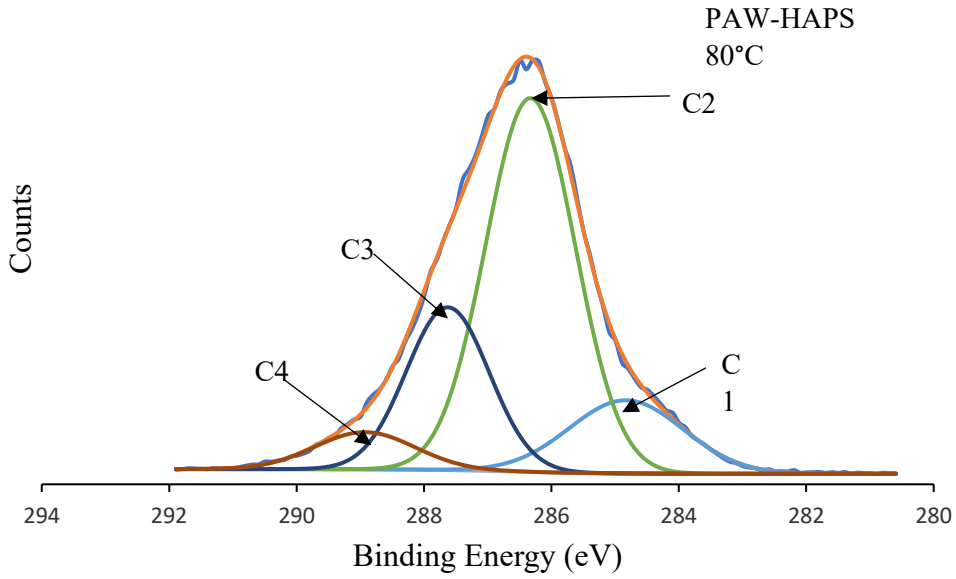
PAW-HAPS
80°C
C2
C3
C4
C
1
Counts
294
292
290
288
286
284
282
280
Binding Energy (eV)

Figure E1. Curve fitted C_{1s} XPS spectra of treated and untreated starches. The different incubation temperatures for the starches are attached to the sample name. WMS: Waxy Maize Starch, PAW-WMS 25°C : Plasma-Activated Water Waxy Maize Starch 25°C, PAW-WMS 60°C: Plasma-Activated Water Waxy Maize Starch 60°C, PAW-WMS 80°C: Plasma-Activated Water Waxy Maize Starch 80°C, HAMS: High Amylose Maize Starch, PAW-HAMS 25°C : Plasma-Activated Water High Amylose Maize Starch 25°C, PAW-HAMS 60°C: Plasma-Activated Water High Amylose Maize Starch 60°C, PAW-HAMS 80°C: Plasma-Activated Water High Amylose Maize Starch 80°C, WPS: Waxy Potato Starch, PAW-WPS 25°C: Plasma-Activated Water Waxy Potato Starch 25°C, PAW-WPS 60°C: Plasma-Activated Water Waxy Potato Starch 60°C, PAW-WPS 80°C: Plasma-Activated Water Waxy Potato Starch 80°C, HAPS: High Amylose Potato Starch, PAW-HAPS 25°C: Plasma-Activated Water High Amylose Potato Starch 25°C, PAW-HAPS 60°C: Plasma-Activated Water High Amylose Potato Starch 60°C, PAW-HAPS 80°C: Plasma-Activated Water High Amylose Potato Starch 80°C. C1 = C-C/C-H, C2 = C-O, C3 = O-C-O/C=O, C4 = O-C=O-